University of Bergamo
Faculty of Engineering
Department of Industrial Engineering

PhD in Energy and Environmental Technologies
XXI Cycle

Trigeneration Systems Assisted by Solar Energy
Design Criteria and Off Design Simulations

Supervisor:
Prof. Antonio Perdichizzi

Author:
Assunta Napolitano

In collaboration with:

EURAC research

Supported by: Stiftung Südtiroler Sparkasse

ACKNOWLEDGEMENTS

I really would like to thank everybody who accompanied me during the last three years, but if I mentioned all the names, the acknowledgments would be longer than the thesis itself. So, I strongly hope to include all of them in one page.

I would like to express my sincere gratitude to Prof. Antonio Perdichizzi for having been my guide and having trusted me.

I am warmly grateful to Prof. Giuseppe Franchini for having been the light in the dark moments of this research work.

My heartfelt gratitude is addressed to Mr. Dipl.-Ing. Wolfram Sparber for the chances he gives me to gain experience in the renewable energy field.

My affectionate thanks go to my past and present nice colleagues at EURAC, for the scientific collaboration but above all for the coffee and chocolate breaks, the parties and the funny moments. Then, I couldn't help mentioning Patrizia, for the morning, daily and nightly conversations.

I would like to deeply thank everybody who provided me with a bed and some food in my last vagrancy months. I will return the favours somehow!

My special thanks to Lucia, Stefano and Francesco for having been the best doctorate mates I could have ever had, warts and all, and to all the others PhD students who have shared with me the office, the nearly never working printer, the broken chairs, the fast lunches, the bad coffee and so on.

Obviously, I would like to warmly thank my parents, for being so close to me despite the distance, and to my brother for listening to every my complaint.

But above all, my loving thanks go to the stylist of this thesis for his patience and good care of me.

Introduction

Given the global challenges related to climate change and resource shortages, both high efficiency energy supply and intensive utilization of renewable energy sources are required, especially in the building sector which worldwide accounts for over 40% of primary energy use and 24% of greenhouse gas emissions[*].

Combined Heating, Cooling and Power (CHCP) systems coupled with Solar Thermal Collectors (STC) set an example of high efficiency and renewable energy facility, suitable for those civil buildings which feature relevant electricity, heating and cooling needs. CHCP systems offer on one hand on site power generation for appliances and cooling, on the other hand, heat (necessary by-product of the power production) usable not only for heating and domestic hot water production but also for cooling by means of heat driven chillers. As for solar thermal collectors (STC), they offer renewable heat which can be similarly used for heating, domestic hot water production and cooling.

To the knowledge of the author, five CHCP systems combined with STC installations have been built in Europe. Beside the above mentioned advantages, such installations feature complicated layouts and control strategies which make the same plants difficult to be managed. Moreover, for one installation, monitoring data have shown that the prime mover and the solar collectors can interfere in their operation and compete from the energy and economical points of view.

As such critical issues are strictly dependent on the design of the plant, a tool based on a spreadsheet and dynamic simulations has been elaborated to assist the planning phase. The present document describes the tool and shows its application to a real case.

[*] Voss, K., Reley M., 2008. IEA Joint Project: Towards Net Zero Energy Solar Buildings (NZEBs). November 2008

Executive Summary

The present work focuses on CHCP systems, made up of gas engine as prime mover and absorption chiller as cooling device, combined with Evacuated Tube solar thermal Collectors (ETC).
Such an energy system has provided the EURAC building with heating and cooling since 2002 and has been monitored since 2005. Thanks to the monitoring data, critical aspects have been highlighted concerning the size selection of some components, the overall layout and control strategy (Chapter 1). On the basis of this outcome, a procedure for optimal designing CHCP plus ETC systems has been defined and includes:

1. the layout and the control strategy selection (Chapter 2): beside the already mentioned basic components, the layout also includes a biomass boiler, as a further renewable heat source, and a compression chiller, as a cooling back up device;
2. the definition of a sizing procedure for each component of the layout (Chapter 3): this procedure is based on a spreadsheet which requires the heating and cooling demand of the building and a first sizes selection concerning the absorption chiller, the cogenerator and the solar collectors in order to output the sizes of all the left plant components;
3. the development of a TRNSYS deck which simulates the designed plant at off design conditions (Chapter 5): to this end, two new models have been developed in MATLAB respectively for a gas engine based cogeneration unit and a biomass boiler (Chapter 4).

Such design procedure has been applied in order to select the sizes suitable to match the EURAC heating and cooling demand. On this subject, by repeating the sizing procedure with different initial sizes of the major plants component and by considering different control strategies, various configurations have been output. Such configurations have been simulated in TRNSYS to calculate the Primary Energy Consumptions (PEC), the Operation Costs (OC) and the CO_2 emissions which can be saved by the examined system with respect to a conventional system.
By comparing the savings turned out of all the simulations, the optimal size of the cogeneration unit, the biomass boiler, the absorption and the compression chiller have been identified. The obtained results have also been discussed from the point of view of the Discounted Pay Back Period (Chapter 6).

1 Trigeneration Systems Assisted by Solar Thermal Energy: Experiences

1.1 Overview on Existing Installations

Within the Task 38 project supported by the International Energy Agency (IEA) under the "Solar Heating and Cooling" program [1], data have been collected about world wide large scale solar assisted heating and cooling installations in order to define the state of the art of solar cooling [2]. According to such review, solar thermal collectors are usually combined with further technologies to match the overall heat demand for both heating and cooling purposes. To this end, gas boilers are usually employed, except in five installations which make use of gas engine based cogeneration systems.
In Bolzano, the capital of the most northern Italian Province, three buildings are equipped with a gas engine based cogeneration system plus solar thermal collectors plus an absorption chiller:

1. the seat of the institute for applied research EURAC [3];
2. the L. Einaudi Professional Training Centre and
3. the main fire-fighters quarter of the city.

The first building dates back to Italian rationalism (1936) but was enlarged and refurbished (1995-2002) to a solar active building in order to house the regional institute for applied research EURAC. Its energy facility (Figure 1.1) has been monitored since 2005, so a huge amount of data has been collected which are in detail presented and discussed in the next subchapters.
The second building is a school which houses training courses in summer time too. Its facility has been planned by the same engineers as in the EURAC case. This explains the numerous resemblances between the two installations (Figure 1.1 and Figure 1.2). Actually, according to [4], the L. Einaudi installation apparently turns out to be an improved version of EURAC installation. The major difference concerns the hydraulics: in the Einaudi case, a high temperature loop and a low temperature loop can be identified, whereas in the EURAC case the hydraulic separation is a lack, as it will be demonstrated in the next subchapters. The low temperature loop in the Einaudi building is connected to the radiant floor heating system and it partially includes the condensing boilers so that the flue gas can condense. On the contrary, the cogeneration unit and the absorption chiller are included in the high temperature loop, whereas the

solar thermal field can be part of both the loops depending on its produced hot water temperature.

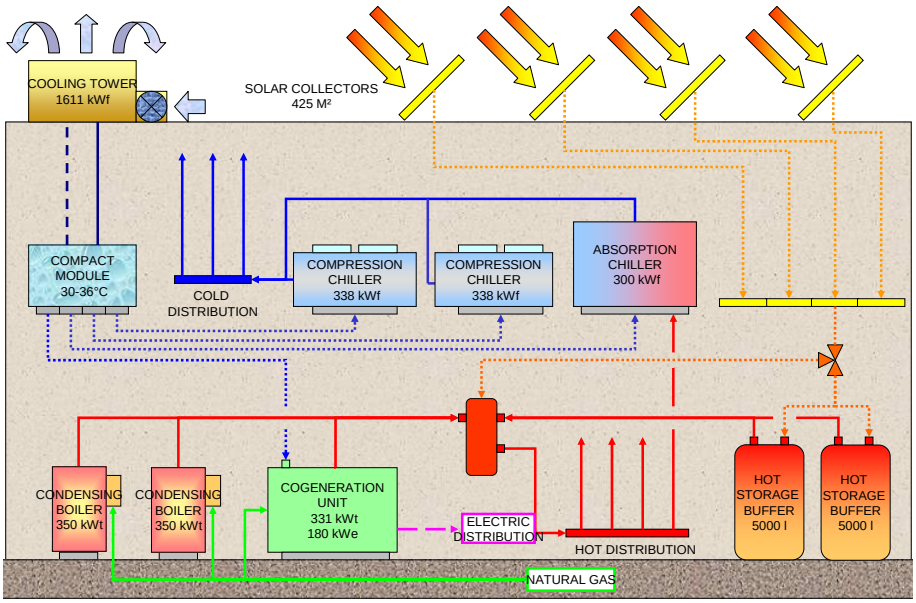

Figure 1.1 EURAC plant layout, Bolzano Italy

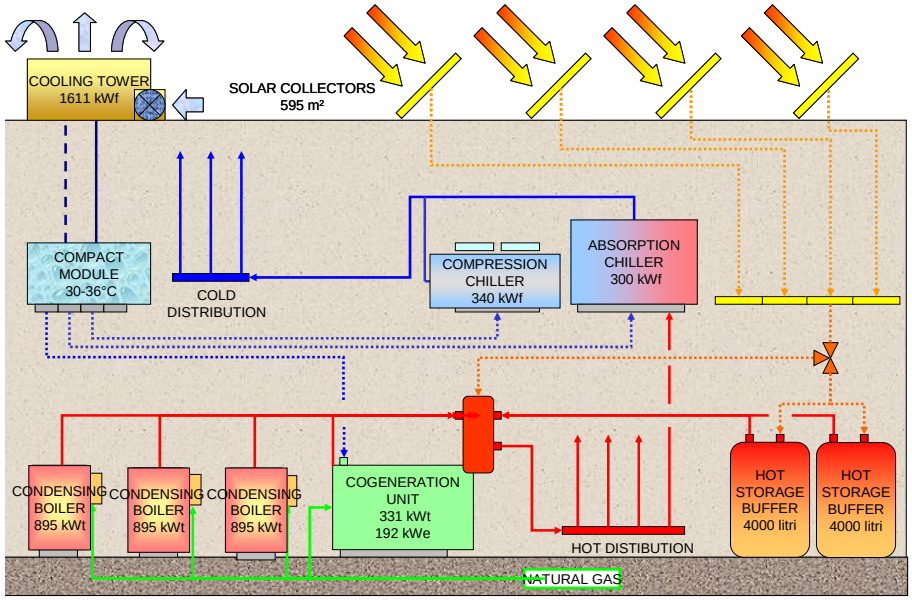

Figure 1.2 L.EINAUDI plant layout, Bolzano - Italy

The plant installed at the main fire-fighters quarter of the city is currently (beginning of 2009) under investigation by the Institute for Renewable Energy of EURAC, as it has never worked properly since its installation. Table 1.1 reports the major components of this installation and their sizes. It has to be added that in this installation the flat plate collectors (FPC) have not been designed to feed the absorption chiller and they have run only to produce hot sanitary water since their installation. On the other hand, the cogeneration unit has rarely run and the heating and cooling demand have been nearly always provided by the heat pump. Such issues are dependent on different factors, mainly the layout, the sizes and the control strategy, but also the management of the plant. Nevertheless, no more can be said about such plant as it is under investigation.

Table 1.1 Sizes of the major components included in the solar heating and cooling instalaltion at the fire-fighters head quarter in Bolzano - Italy

	Components	Model	Sizes	Units
Heat Production	Solar Collectors	FPC	105	m^2
	Cogeneration units	Gas Engine	224/374	kW_e/kW_{th}
	Auxiliary Heater	Heat Pump	133/145	kW_{th}/kW_c
		Gas Boiler	2,160	kW_{th}
Cold Production	Absorption Chiller	H_2O/LiBr	175	kW_c
	Auxiliary Chiller	Heat Pump	133/145	kW_{th}/kW_c
Storage Tanks	Solar Tank	-	11.6	m^3
	Cold Tank	-	-	-

Two further installations which make use of an engine based cogenerator system plus solar thermal collectors plus an absorption chiller are respectively located in Langenau (Germany) and in Skive (Denmark).
The first system was put in operation in 1997 and serves an office area of 415 m^2 of the company Ott & Spiess. The Evacuated Tube solar thermal Collectors (ETC) field (Table 1.2) provides heat both for driving the absorption chiller in the cooling season and for heating in winter. In case of low solar gains, additional heat is obtained from the CHP unit for combined heat/electricity production. If the heat demand still exceeds the capacity of the solar system or of the CHP unit, additionally a gas burner is involved in the operation.
The chilled water from the absorption chiller is provided at a temperature of 13°C due to the employment of chilled ceilings and displacement ventilation.

Table 1.2 Sizes of the major components included in the solar heating and cooling installation at the Ott & Spiess company, Langenau - Germany

	Components	Model	Sizes	Units
Heat Production	Solar Collectors	ETC	45	m^2
	Cogenerator	Gas Engine	8/19.5	kW_e/kW_{th}
	Auxiliary Heater	Gas Boiler	50	kW_{th}
Cold Production	Absorption Chiller	H_2O/LiBr	35	kW_c
	Auxiliary Chiller	-none	-	-
Storage Tanks	Solar Tank	-	2	m^3
	Cold Tank	-	1	m^3

According to [5], in 1999 the annual Coefficient of Performance COP (useful cold / driving heat) of the chiller was 0.56. and approximately 9 % of the total heat input into the building for cooling and heating was provided by the solar system. The same source also states that, “due to the limited power of the CHP unit, the recovered heat does not conflict with the gains from the solar system; hence a high utilisation of both the solar thermal system and the CHP unit is achieved under the realized design”.

Lastly, the Municipality of Skive has built a new town hall comprising conference halls, service and administration facilities and a new library with lending departments, public areas and offices for the library administration [6]. Such installation turns to be really complex (Figure 1.3 and Table 1.3). Briefly, the core element is the hot tank which stores not only the solar energy but also the heat recovered by the three diesel engines. It has to be added that such diesel engines have been reconstructed in order to be driven by oil and rape seeds. The absorption chiller is driven with the hot flow coming from the top of the tank and the chilled water is stored in the cold tank. One compression chiller is used in summer to assist the production of the cold water in summer and in winter to supply cold air to an outdoor ice rink. Such compression chiller is electrically driven by means of the CHP units and in winter exploits the hot water returning from the load.

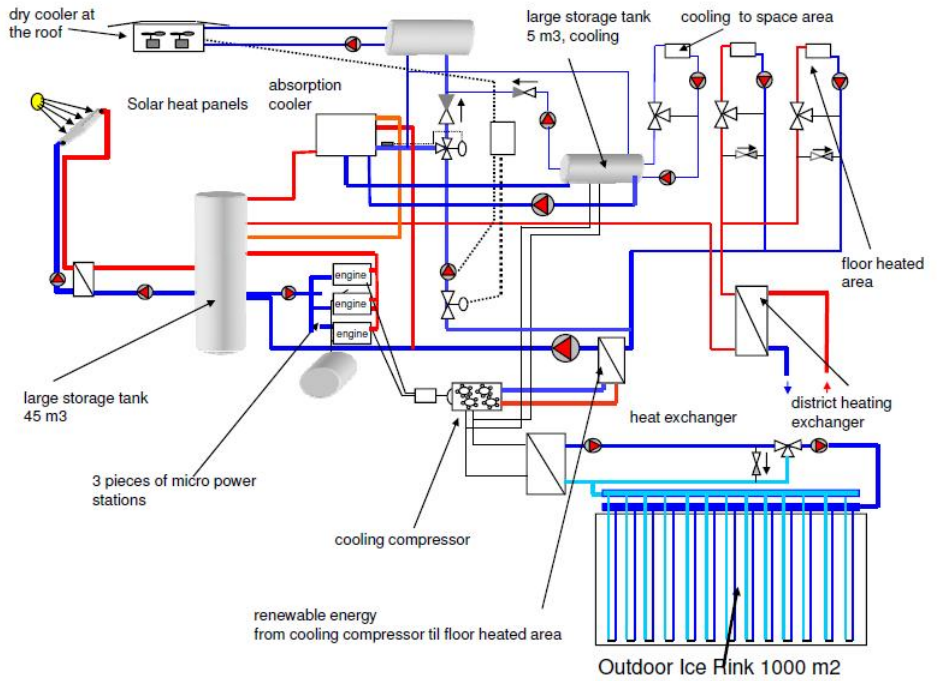

Figure 1.3 Layout of the plant installed at the town hall in Skive (Denmark)

Table 1.3 Sizes of the major components included in the solar heating and cooling installation at the new town hall and library in Skive – Denmark

	Components	Model	Sizes	Units
Heat Production	Solar Collectors	FPC	265	m^2
	Cogenerator	Diesel Engine	75	kW_e
	Auxiliary Heater	Gas Boiler	50	kW_{th}
Cold Production	Absorption Chiller	H_2O/LiBr	70	kW_c
	Auxiliary Chiller	Compression	400	-
Storage Tanks	Solar Tank	Stratified	40	m^3
	Cold Tank	-	5	m^3

The concept implemented in the plant of Skive turns out to be interesting and particularly sustainable, but at the same time largely complex especially from the point of view of hydraulics and the control strategy.

To conclude, the illustrated experiences demonstrate that trigeneration systems combined with solar thermal technologies feature a wide complexity especially of layout and control strategy. This complexity is related to the complexity in

fitting to each other a typically unsteady heat source (the solar radiation) and a system which needs steady working conditions (N.B. the primary function of an engine heat recovery equipment is to cool the engine [7]), to the final end of meeting the heat demand, both in winter and summer [8]. On this subject, the plant in Skive and the Einaudi installation in Bolzano suggest a clear definition of the flows on the basis of their temperature. The next subchapters about the EURAC case are going to demonstrate the relevance of the isolation of different temperature levels and to put the basis for an optimal design of similar energy facilities.

1.2 The EURAC Case Study

1.2.1 General data

Since 2002 the institute for applied research EURAC resides in a building which combines innovative architecture with an innovative energy system (Figure 1.4). The building houses not only offices for ca. 180 collaborators but also lecture halls, a library and a cafeteria within a total cubic space of 55'000 m³, 37'000 m³ of which are heated and cooled.

Figure 1.4 The EURAC building: magenta parts are protected parts of the building (1936, Italian rationalism), the construction in glass, concrete and steel was added by Austrian Architect Klaus Kada (2002).

For climatisation purposes, the building relies on one hand on a double glazed façade (Figure 1.5), on the other hand on an HVAC (Heating, Ventilation and Air Conditioning) system with solar thermal collectors, cogenerator and absorption chiller as its key components [9].

According to the local climate, the architectural features and the final use of the building, the engineers calculated the heating load to amount to 785 kW and the cooling load to amounts to 890 kW, even if in 95% of the cases the actual cooling load would have been lower than 70% of the designed value [9]. Nevertheless, the energy bills paid up to the beginning of 2005 resulted in energy consumptions higher than the predicted ones [9]. Therefore a monitoring system was installed during summer 2005 in order to evaluate the performance of the system and to achieve an in-depth understanding of the technologies applied.

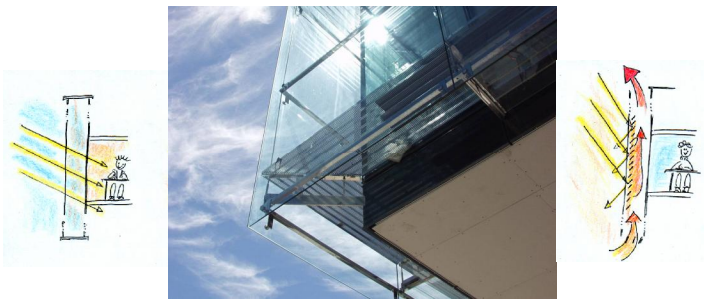

Figure 1.5 The double façade allows for passive use of solar energy in the heating season (heat buffer), while solar gains to the office space can be contained in summer (chimney releases heat captured by blinds).

1.2.2 Energy facility and monitoring equipment

The energy flows chart is reported in Figure 1.6.
The cooling system consists of the absorption chiller (300 kW, 480 kW_{th}), two compression chillers (316 kW each), and a cold storage (5000 l), where chilled water is stored at 7-8°C. The heat for the absorption chiller is provided by the solar thermal collectors (424 m² ETC net area) and a cogenerator (330 kW_{th}). The latter ha been planned to be the building's main heat source during winter, assisted by two condensing boilers (350 kW each). Hot water from the solar thermal collectors can either be directed immediately to heat distribution or accumulated in two hot storages (5000 l each). Besides their contribution to the cold production, the solar thermal collectors supply the sanitary hot water and contribute to heating [9].
The monitoring system includes 13 heat meters and 3 electricity meters. Values are measured every minute and gathered at a central server where mean values on a five minutes, hourly and daily basis are elaborated. Their position is also indicated in Figure 1.6.

1.2.3 Design energy flows

Before the implementation of the system, two terms energy balances (October to April, May to September) had been calculated by the planners [11].
As shown in Figure 1.7 left side, for the summer term a solar contribution of 190'000 kWh (38%) to the heat demand of the absorption chiller was predicted, the latter providing with 270'000 kWh 47% of the total cooling demand. With the supply of the remaining heat demand (307'000 kWh) by the cogenerator, an electricity production of 178'500 kWh is connected. This is more than twice the amount the compression chillers need for the supply of the missing cold demand, so that only two thirds (219'800 kWh) of the total electricity demand for ventilation, pumping and cooling tower (320'700 kWh) have to be drawn from the grid.
In winter term (Figure 1.8), all the heat generator are expected to run, but the contribution of the condensing boilers to the heating demand is predicted to be very low (16%) compared to 55% from the cogenerator and 29% from solar and internal sources .

1.2.4 Monitoring results

After two years of operation of the monitoring system the energy flows turned out to be far from the design ones as it is shown in Figure 1.7 and Figure 1.8 [12].
During summer 2006 (Figure 1.7, right side), 403'000 kWh of cooling energy were supplied to the building, 75% being provided by the absorption chiller and 25% by the compression chiller. The total heat delivered to the absorption chiller amounted to 639'000 kW_{th}, resulting in an overall COP of 0.51. 70.5% of this heat was supplied by the condensation boilers, 23.5% by the cogeneration unit and 6% by the solar collectors.
During winter 2005/2006 (Figure 1.8, right side), the heating demand amounted to 781'000 kWh. This heat was basically provided by the condensing boilers (75%) and the cogeneration unit (nearly 25%), solar fraction being very small (the system was supplied only with 6'230 kWh).

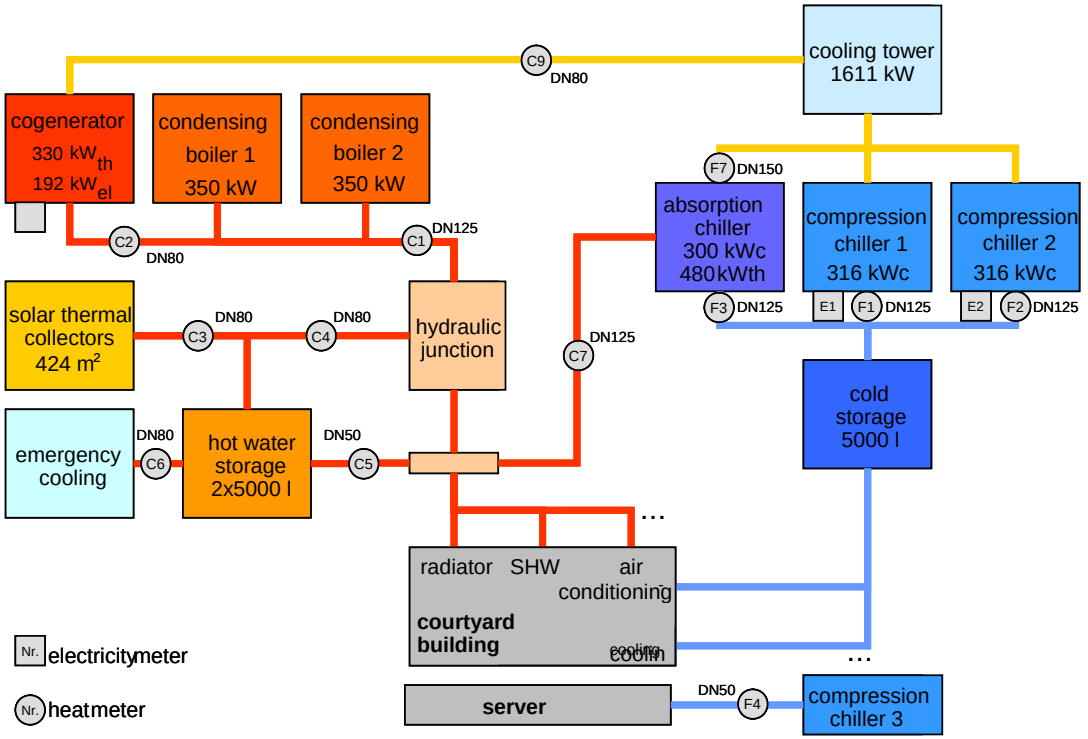

Figure 1.6 Energy flows chart and sensors position

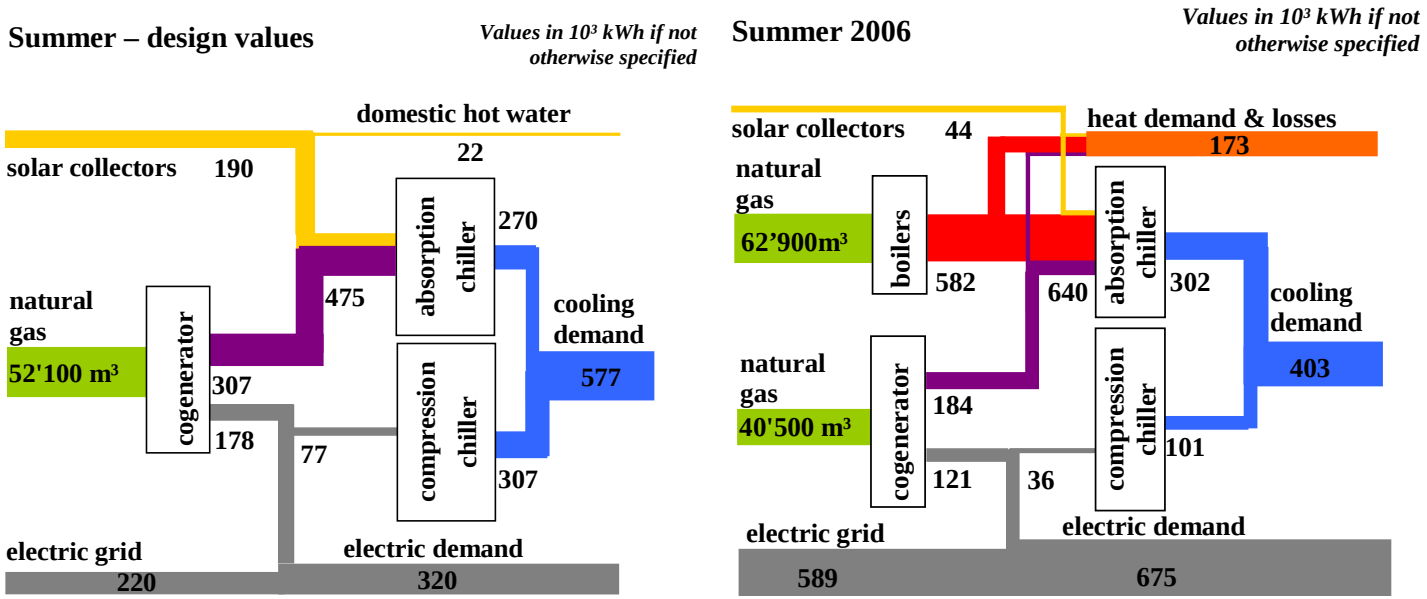

Figure 1.7 Energy flows for summer operation – Comparison between design values (15 April-15 October) and measured values (21 April - 31 October, 2006). The design electric demand counts only the electricity requested by the energy facility and not by the all building.

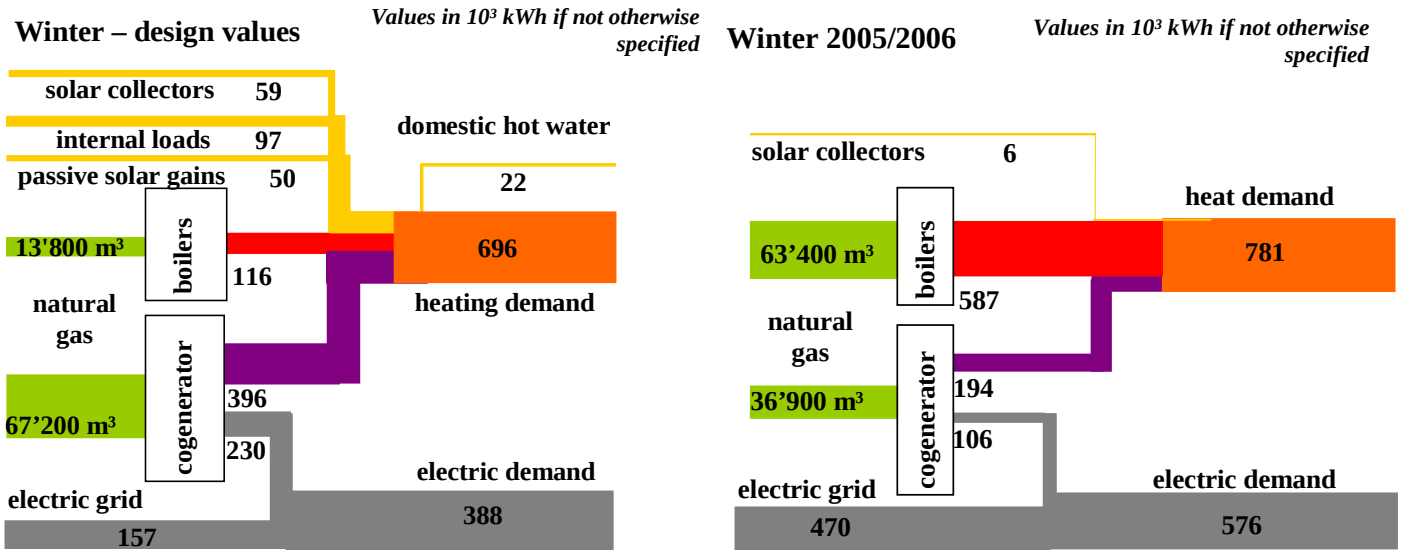

Figure 1.8 Energy flows for winter operation – Comparison between design values (15 October – 15 April) and measured values (1 November 2005 – 20 April 2006). The design electric demand counts only the electricity requested by the energy facility and not by the all building.

To summarize the monitored energy flows, it can be concluded that:

- the solar fraction was smaller then predicted by the planners, both in winter and in summer;
- the condensing boilers were used as the main heat back-up system instead of the cogeneration unit, even in summer when they shouldn't run at all.

Such results can be motivated by an improper control system operation which has been highlighted by the monitoring system too [12]. The major lacks concern:

1. The solar collectors

The measured yearly solar fraction amounted to 50'400 kWh_{th}, which represents 20% of the value predicted by the planners. A detailed analysis about the energy flows between the solar collectors, the hydraulic junction, the storages and the distributing collector (Figure 1.9) showed that a heat flow occurred towards the solar collectors. This backflow was due to the pump for the secondary solar circuit and to the pump for the circuit which connects the storage and the heat distributor manifold. Actually, these pumps are respectively controlled by a time schedule and by a static set temperature instead of a temperature gap between the tank and the hot manifold. Avoiding the backflow towards the solar collectors, more energy could be delivered to the system, maximum around 82'000 kWh_{th}, measured on the secondary solar circuit. However, this input is still low and far below the design value and further investigations are being currently carried out.
A too high set temperature for the pump of the solar secondary circuit could be the main cause for the low solar energy obtained during winter. In fact, in this season, the temperature that allowed the heat to be exchange between the primary and the secondary solar circuit was to high (90) °C. Thereby, the winter solar fraction only amounted to 10% of the corresponding design value and actually it was concentrated in the beginning of April.

2. The cogeneration unit

The cogeneration unit is driven by the electricity, and not by the heat demand of the building. Under this condition, the heat requirements were mostly matched by means of the condensing boilers, since also the solar fraction was insufficient.

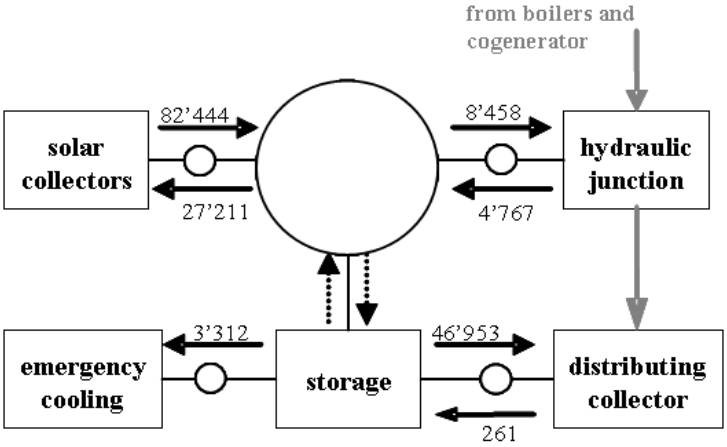

Figure 1.9 Heat flows from the system towards the solar collectors and then to the environment.

3. The absorption chiller

According to the summer monitoring data, the absorption chiller ran both during the day and night in order to provide with chilled water at a temperature lower than 8°C. As the chilled water temperature grew up this value, heat was requested by the generator of the machine. Whenever no thermal energy was available from the cogenerator or the solar circuit, the boilers automatically switched on to produce it. Thus, they had been always working during the summer nights. Further more, as the COP of the absorption chiller during the night amounted to 20% (Figure 1.10), the seasonal performance of the chiller decreased to approximately 50%.

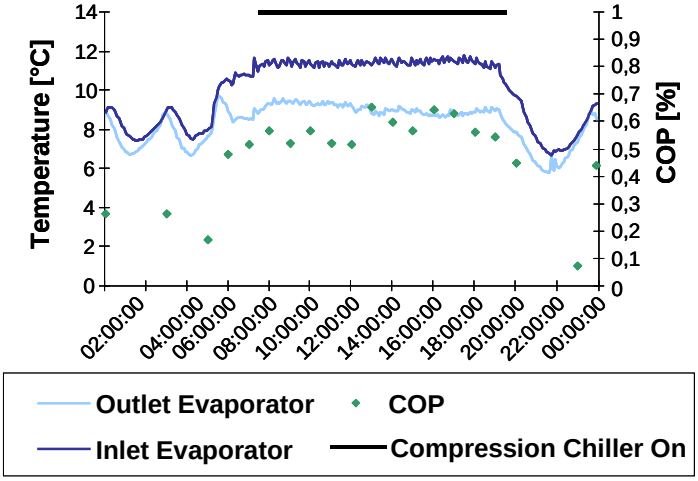

Figure 1.10 One day operation of the absorption chiller, chilled water temperatures and COP.

1.2.5 Optimization procedures

On the basis of the outcome of the monitoring system, since October 2006 different procedures have been implemented to optimize the overall plant performance [12].

As the monitoring data showed that the major critical issues were strictly related to the control strategy, some control settings were changed. However, since the control equipment is not easy accessible, manual modifications were necessary.

The first one concerned the set temperature on the secondary solar circuit during winter 2006-2007 which has been moved to 50°C.

Moreover, a new working priority was applied within the machines at the beginning of summer 2007. In particular, boilers have been switched off for the most part of day, thus the heat demand has been mainly provided by the solar collectors and the cogenerator. Hence, the absorption chiller has worked only when hot energy was available from solar collectors or cogenerator; whereas, the compression chillers ran not only during the day to match the peak demand, but also during the night.

Thanks to this changes, in 2007 the absorption chiller produced less cold water in comparison with summer 2006 (Figure 1.11) and the cogeneration unit was its main heat source (Figure 1.12).

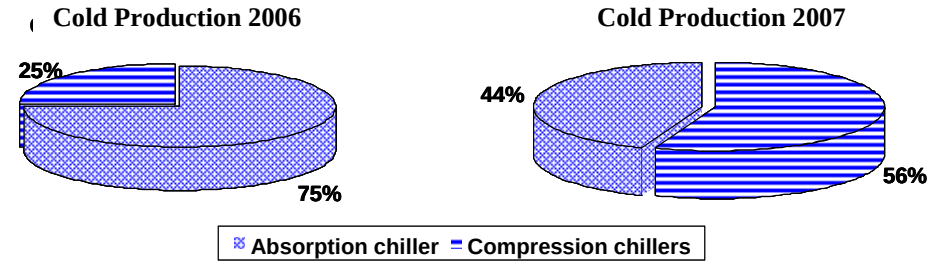

Figure 1.11 Cooling produced by the absorption and compression chiller in summer 2006 and 2007

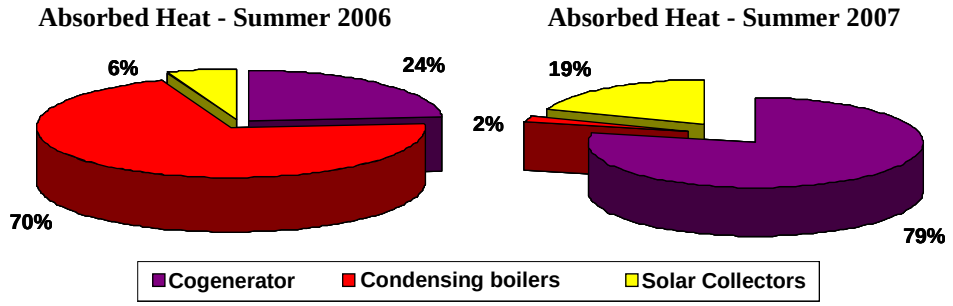

Figure 1.12 Heat produced by the cogeneration unit, the solar collectors and the boilers in summer 2006 and 2007

Table 1.4 reports the comparison between the monitoring data about summer 2007 have been analyzed and compared to the 2006 ones to verify the results.

Table 1.4 Comparisons between 2006 and 2007 summer operation. The 2007 control settings have led to lower costs and CO_2 emissions. The calculation of CO2 emissions does not include those ones coming from the cogenerator. Actually, since the emission rate from the cogenerator is lower than Italians electricity grid's average, the heat cogenerated has been considered "CO_2 neutral".

		summer 2006	summer 2007
Cooling Degree Hours (26°C)		1,994	1,563
cold production	absorption chiller [kWhc]	288,446	112,227
	compession chiller 1[kWhc]	0	65,949
	compession chiller 2 [kWhc]	80,575	22,480
Total		369,021	200,656
heat production	cogenerator [kWhth]	168,720	169,114
	boilers [kWhth]	514,578	5,175
	solar [kWhth]	45,688	59,498
Total		728,987	233,787
energy consumption	absorption chiller [kWhth]	600,312	176,449
	compession chiller 1 [kWhe]	0	22,589
	compession chiller 2 [kWhe]	30,448	9,392

primary energy	total gas [m³]	92,696	37,730
consumption	electricity [kWhe]	30,448	31,982
Costs	Gas	45,172	14,561
	Electricity	4,099	4,305
Total		49,271	18,867
Specific cost	€/kWhc	0.13	0.09
CO2	gas [kg]	107,015	1,076
	electricity [kg]	21,314	22,387
total CO2		128,329	23,463
Specific Emission	CO_2 kg/kWhc	0.35	0.12

1.2.6 Remarks on the design

The EURAC monitoring system has demonstrated that the control strategy plays a crucial role in the overall plant performance and that significant improvements can be achieved by only optimizing it. Nevertheless, the EURAC installation presents some critical issues in the overall design which could have been avoided during the planning phase.

Firstly the heat distribution system includes different technologies (radiant panels, radiators and fan coils) which require different temperature levels. However, the heat facility does not feature any hydraulic separation, so heat is always produced at a high temperature level. On one hand, this does not allow for the solar collectors to be well exploited for heating purposes, on the other hand boilers nearly never run in the condensing mode.

As far the component sizes are concerned, the monitoring system output a cooling peak demand not higher than 350 KW both in 2006 and 2007 summer, whereas the cooling capacity installed amounts to 930 kW. However it has to be underlined that the facility was built in 1999-2002 and the solar cooling technology was not well known.

As already said, the cogenerator tracks the electricity demand and no tanks are available to store the produced heat when the latter exceeds the demand. Such a situation especially occurs in spring and autumn, when the building does not require high amounts of heat but the electricity demand is still relevant. Under this condition, heat can not be removed from the engine and it gets switched off.

Although the mentioned aspects, the most critical one is the presence of a hydraulic junction where all the hot and cold streams are planned to be mixed, in particular the ones of the cogenerator and the solar loop which often have different temperatures, especially in winter[8]. In fact, a three way valve (Figure 1.13) addresses the solar flow to the hydraulic junction only when its temperature is higher than the one in the top of the junction. As heat has to be delivered at high temperature (ca 80°C), solar energy is nearly always stored in winter time.

On the contrary, in summer, high temperatures are delivered by the solar loop, increasing the main temperature in the hydraulic junction. In this case, when the absorption chiller works at partial loads (i.e. the “V Abs” in Figure 1.13 reduces the mass flow entering the generator of the absorption chiller, thus the mass flow between the hydraulic junction and the valve is recirculated), the return stream risks to be too high to cool the engine which gets switched off.

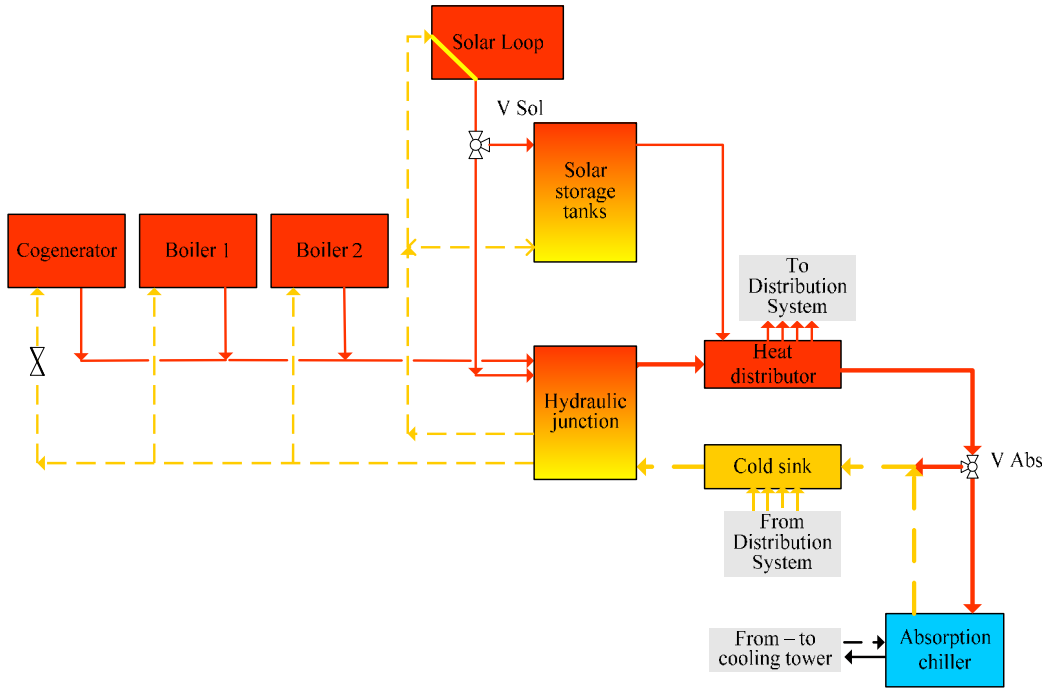

Figure 1.13 Hydraulics connecting the heat facility and the the absorption chiller in the EURAC installation.

Furthermore, the nominal hot mass flow entering the generator of the absorption chiller is higher than the sum of the nominal flows of the cogenerator and the solar loop, thus the boilers have to be used if the absorption chiller has to be run at nominal conditions. Whenever not all the heat generators run and the cooling peak load is reached at the same time, the stream temperature entering the generator decreases and the COP of the chiller gets worse.

1.3 Conclusions

The EURAC energy supply system feature an interesting energy concept based on high efficiency and renewable source exploitation, but turns out to be really complex to manage. Most of its complexity resides in the layout and control strategy, so it is strictly related to the planning process. Some design issues have been discussed in the previous subchapter, other ones can be extracted from [13] and currently some more ones are still under investigations.
Also considering the others existing trigeneration systems combined with solar thermal technologies it can be concluded that planning such systems can be rather complex. For this reason it has been decided to create a tool able to support the design of such energy supply system from three points of view:

- the selection of a layout
- the selection of a control strategy;
- the definition of a sizing procedure.

2 Layouts and Control Strategies for Trigeneration Systems Assisted by Solar Thermal Energy

2.1 Coupling Solar Collectors and Cogeneration Units for Heating and Cooling Purposes

Combined Heat, Cooling and Power (CHCP) systems feature on one hand a large variety of components: turbines or engines as prime movers, absorption chiller or compression chiller as cooling devices, gas heaters or heat pumps as auxiliary heat generators, the heat pumps being also usable for cooling purposes; on the other hand, CHCP also features a large variety of layouts and control strategies. Figure 2.1 shows some configurations for trigeneration systems which have been selected in [15].

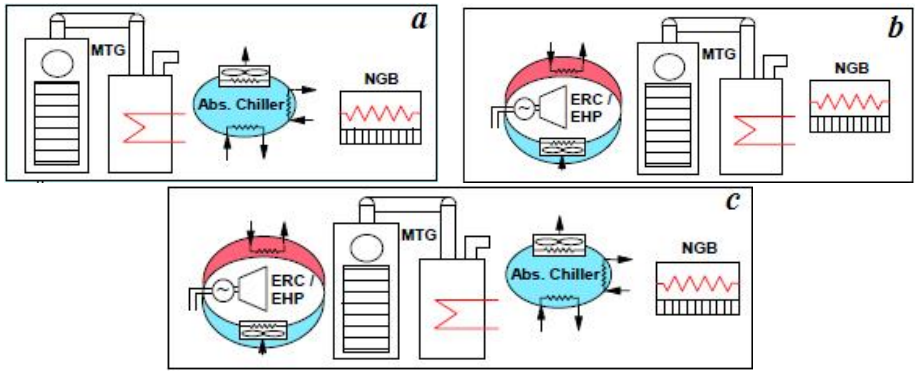

Figure 2.1 Some layouts selected in [15]: a) prime mover with heat recovery assisted by an auxiliary heater, and absorption chiller; b) prime mover with heat recovery assisted by an auxiliary heater and a heat pump, the latter being used also for cooling purposes; c) prime mover with heat recovery assisted by an auxiliary heater, heat pump for both cooling and heating purposes and absorption chiller.

Although the wide literature about co/tri-generation systems, very few documents have been found concerning how to couple a gas engine based cogeneration system with low temperature solar thermal collectors. Thereby, some layouts have been drawn by following different lines of reasoning.
Basically, as the investigated plant configuration includes low temperature solar thermal collectors, the gas engine is planned to produce hot water by recovering heat from both engine jacket and exhaust gases. In a typical configuration heat is recovered from the oil, the engine jacket and the exhaust gases in series like in Figure 2.2 [15] Nevertheless, in the present investigation, parallel heat

recuparators have also been taken into account: such an example is shown in Figure 2.3 [16]

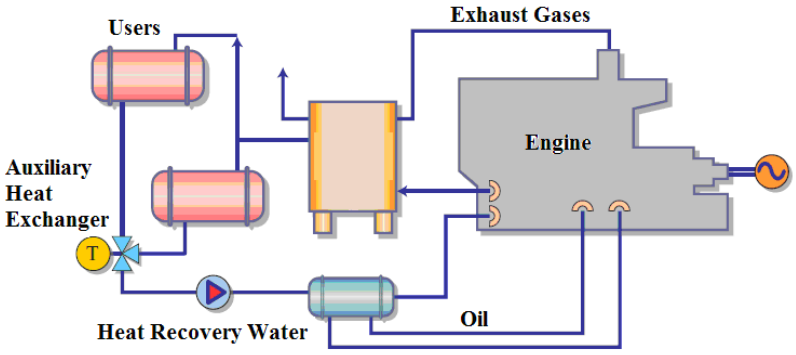

Figure 2.2 Typical configuration with heat recuperators in series according to increasing temeperature levels.

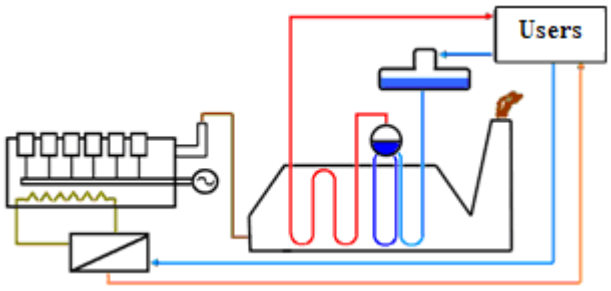

Figure 2.3 Example of a parallel heat recovery from the engine jacket and exahust gases

Parallel and series connections have also been considered for the combination of a cogeneration unit and a solar collectors field, like in the configurations shown in Figure 2.4 and Figure 2.5. In the first case, the collected solar heat is added to the heat recovered from the engine (the heat recovery from the exhaust gas occurs in series with the engine jacket). In the second case, the solar loop flow is additionally heated up by the heat recovery on the flue gases (the heat recovery from the engine jacket occurs in parallel to the one on the exhaust gases). Hybrid connections can also be considered: for instance solar collectors can be planned for working in series during winter, to make them to reach the temperature required by users easier or in parallel during summer, when it's more probable they reach the relative high temperature needed by the absorption chiller.

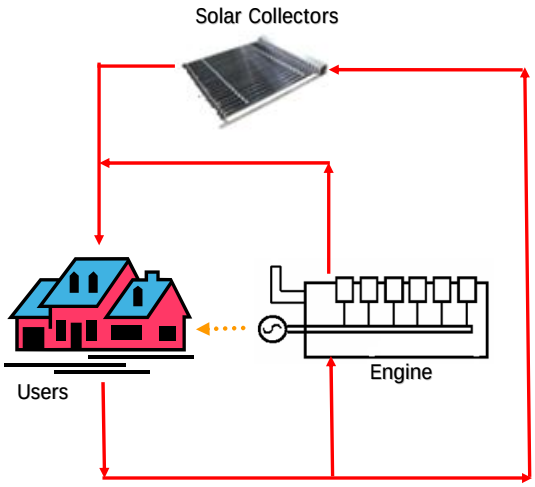

Figure 2.4 Possible scheme for a solar collectors field to be connected in parallel to a cogeneration unit

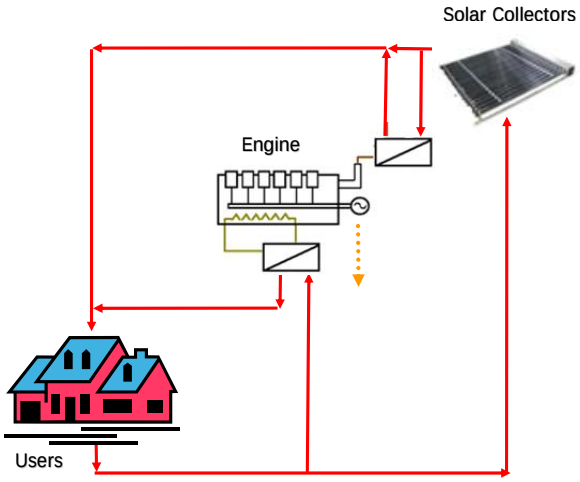

Figure 2.5 Possible scheme for a solar collectors field to be connected in series to a cogeneration unit: exhaust gases are here used to heat up the secondary solar loop mass flow

According to these remarks, different layouts can be designed, but only one has been selected for the present investigation. Such selection features an engine whose heat exchangers are connected in series, whereas solar collectors work in parallel with the engine, just like in Figure 2.4. Such a configuration has been preferred because it has looked like the simplest one to be implemented, not only in the present research work but also in the reality. The selected

configuration represents the major hypothesis of all the present research work as it conditions:

- the whole plant project in terms of sizes and control;
- the modelling of the cogeneration unit and the biomass boiler illustrated in chapter 4;
- the implementation in a TRNSYS model reported in Chapter 5.

2.2 Layout Selection

Firstly, the distribution system (DS) has been selected as it sets the temperatures of the hot and cold water to be delivered to the users. On this subject, radiant panels and fan coils have been respectively selected for heating and cooling purposes in order to have, on one hand, a low temperature heat distribution, on the other hand, comfortable air moisture. The water delivery temperatures which have been set are 40°C and 8° respectively for the radiant panels and the fan coils.
Secondly, a heat exchanger has been planned to separate the medium flowing through the DS from the one flowing through the facility.
Once the interface between the users and the real facility has been selected, two sub facilities have been designed:

1. the “Heat Facility”, i.e. the heat generator facility (Figure 2.6);
2. the “Cooling Facility” i.e. the cold generator facility (Figure 2.7).

The “Heat Facility” includes:

- Evacuated Tube (ETC) solar thermal collectors,
- one gas engine based cogeneration unit (CHP),
- one biomass boiler and
- two heat storage tanks.

As declared beforehand, the ETC collectors and the CHP unit are connected in parallel. The heat collected by the solar thermal field is assumed to be always stored and used whenever the tank reaches the selected temperature levels and heat is required at the same time.
Also the cogeneration unit is served by a tank which buffers the variable load and prevents that the engine frequently switches on/off.
The biomass boiler has been selected to assist the heat production with one more renewable source.

The “Cooling Facility” includes:

- one absorption chiller,
- one compression chiller and
- one cold tank.

The chillers are connected in parallel. The tank only serves the cooling produced by the absorption chiller and it is used to buffer the variable load and to prevent that the absorption chiller frequently switches on/off.
Two things need to be underlined:

- in the present research work it is not discussed the effect of further units for the same components, e.g. two storage tanks or two absorption chillers;
- possible instability of a machine during the simulations can also be due to its mathematical model.

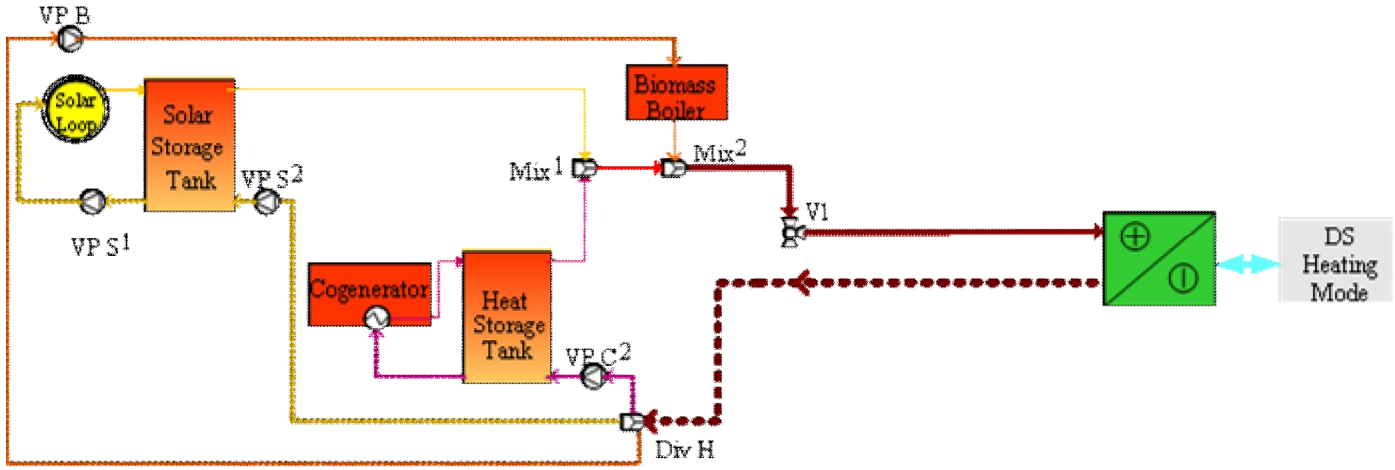

Figure 2.6 Selected layout for a trigeneration system assisted by solar energy in the heating mode

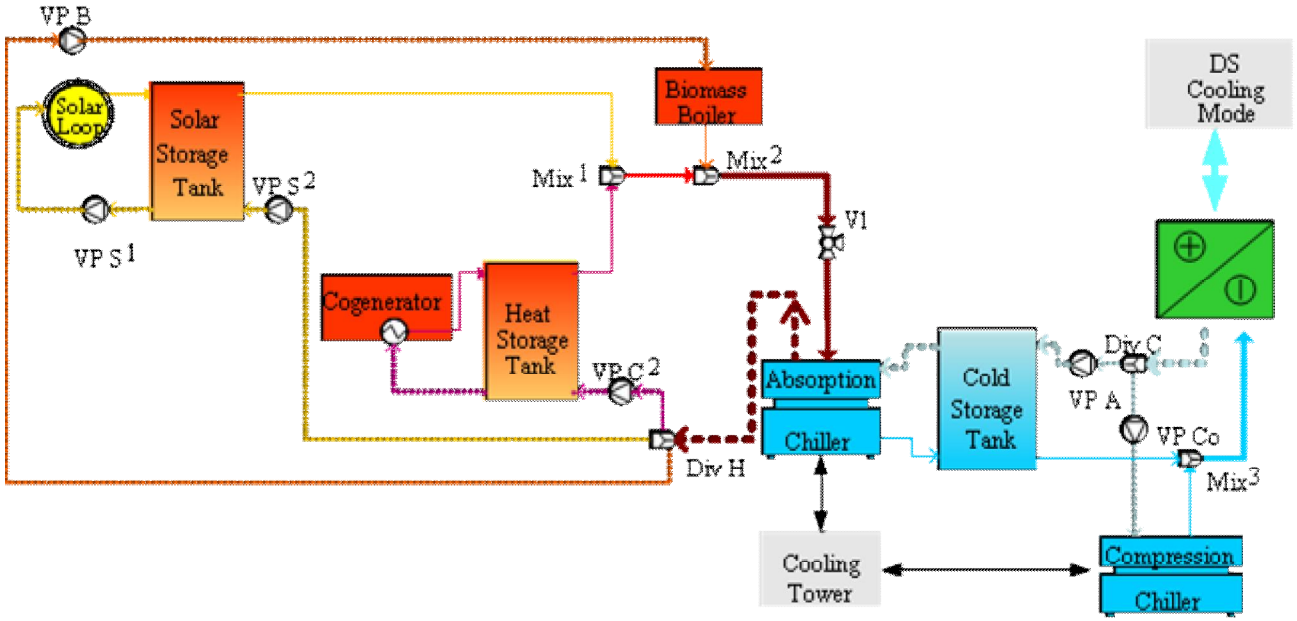

Figure 2.7 Selected layout for a trigeneration system assisted by solar energy in the cooling mode

2.3 Control Strategy Definition

Control strategy is fundamental in managing such a complex plant as it determines how the single machines get involved in the operation.
In figures 2.6 and 2.7 three kinds of devices can be recognized which are responsible for the control:

- Variable speed pumps (VP),
- Diverters (Div) and
- Valves (V).

Actually, the mentioned devices are controlled by specific components such as On/Off or Proportional Integrative and Derivative (PID) controllers.
On one hand, On/Off controllers command the VP to switch on/off: for instance the pumps which draw out the flow from both solar the cogenerator tank (VP S2 and VP C2) are switched on/off depending on the top temperature compared with the temperature returning from the users. On the other hand, On/Off controllers command the machine to be switched on/off depending on the demand: for instance the cogenerator and the absorption chiller are put into operation depending on the top temperature of their tank compared to the set temperature.
Moreover, another On/Off controller commands the opening and the closing of the three way valve (V1 in Figure 2.6 and Figure 2.7) which sets the heating or the cooling mode. It means that, in the cooling mode the valve addresses the hot flow towards the absorption chiller, whereas in the heating mode it addresses the hot flow towards the heat exchanger with the winter DS.
The VP are also regulated by PID controllers which set the mass flow by tracking the set temperature. E.g. a PID controller regulates the mass flow in the primary solar loop in order to reach the winter/summer set temperatures (VP S1 in Figure 2.6); another PID controller regulates the hot mass flow entering the generator of the absorption chiller so that cold water is supplied at the set temperature (Figure 2.7) [7]. To summarize, the goal of using PID controllers for VP is to supply heat and cold energy flows at constant and unique selected values [8].
Lastly, the diverters “DivH” in Figure 2.6 and “Div C” in Figure 2.7 set the hierarchies between the different components. Whenever heat is required, first the top temperature of the solar tank is checked and compared to the desired temperature in order to firstly use the stored solar energy. Then, the top

temperature of the cogenerator tank is checked and compared to the set value in order to secondly use the heat recovered from the engine. However, hot flow is drawn out of the cogenerator tank only for certain ranges of the heat demand. In fact, the cogenerator is not planned to run whenever there are relatively low heat requirements and it is more probable the cogenerator gets automatically switched off. On the contrary, the biomass boiler is designed to supply the left heat demand whenever no enough heat is available from the two hot thanks or whenever the heat requirement is lower than the cogenerator threshold but higher than the capacity of the solar tank.

As far the cooling facility is concerned, the first selected control strategy (named “Abs. Priority”) is based on the exploitation of the absorption chiller for certain ranges of the cooling demand, as in the case of the cogeneration unit. On the contrary, the compression chiller runs to supply the left cooling demand, exactly like in the case of the biomass boiler.

More details about the implemented control strategy are reported in the 5th chapter.

3 Sizing Procedure

3.1 Major Variables Involved in the Sizing Procedure

A sizing procedure has been defined for dimensioning each machine, pump, heat exchanger and tank included in the layout described in Chapter 2.
As many variables are involved in the sizing procedure, the nomenclature is below reported.

Table 3.1 Nomenclature for the variables involved in the sizing procedure

Label	Description
Wtime	Last winter hour
TSetW	Set temperature to be supplied to the users in the heating mode
TsetMachW	Winter set temperature for each heat generator except the solar loop
CollectorArea	Collectors' surface area
SurfaceSlope	Collectors' slope
PrimFlow	Maximum mass flow rate in the primary solar loop
UApsExch	Overall heat exchange coefficient of the heat exchanger between the primary and secondary solar loops
SecondFlow	Maximum mass flow rate in the secondary solar loop and in the loop from the solar tank to the users
SolTankV	Solar tank volume
nSolT1	Height of the 1st node in the solar tank
nSolT2	Height of the 2nd node in the solar tank
nSolT3	Height of the 3rd node in the solar tank
nSolT4	Height of the 4th node in the solar tank
nSolT5	Height of the 5th node in the solar tank
PthCog	Thermal power of the cogeneration unit
Mcog	Mass flow rate entering the cogenerator and maximum mass flow rate in the loop from the cogenerator tank to users
CogTankV	Cogenerator tank volume

n1CogT	Height of the 1st node in the cogenerator tank
n2CogT	Height of the 2nd node in the cogenerator tank
n3CogT	Height of the 3rd node in the cogenerator tank
n4CogT	Height of the 4th node in the cogenerator tank
n5CogT	Height of the 5th node in the cogenerator tank
PthBio	Biomass heater power
MBio	Maximum mass flow rate in the biomass heater
mPmach	Maximum mass flow rate in the overall heat facility
TloadW	Flow temperature returning from the users in winter time
WinterUA	Overall heat exchange coefficient for the heat exchanger between the heat facility and the users in the heating mode
Stime	Last summer hour since the first simulation hour (0 hour)
TSetS	Set temperature to be supplied to the users in summer time
TsetMachS	Summer set temperature for each heat generator except the solar loop
TsetAux	Set temperature for the compression chiller
Qevanom	Nominal cooling power of the absorption chiller
COPnom	Nominal COP of the absorption chiller
QabsNom	Heat power required by the absorption chiller at its maximum cooling rate
mheat	Nominal hot mass flow rate entering the generator of the absorption chiller
mchill	Nominal cold mass flow rate entering the evaporator of the absorption chiller and maximum mass flow rate from the cold tank to the heat exchanger with the distribution system in summer time
mcool	Nominal cold mass flow rate entering the condenser and the absorber of the absorption chiller
QcomprNom	Nominal cooling power of the compression chiller

mchillCompr	Maximum mass flow rate in the loop from the compression chiller to the heat exchanger with the distribution system in summer time
MCold	Maximum mass flow rate in the overall cooling plant
AbsTankV	Cold tank volume for the absorption chiller
n1AbsT	Height of the 1st node in the cold tank
n2AbsT	Height of the 2nd node in the cold tank
n3AbsT	Height of the 3rd node in the cold tank
n4AbsT	Height of the 4th node in the cold tank
n5AbsT	Height of the 5th node in the cold tank
TloadS	Temperature returning from the users in summer time
SummerUA	Overall heat exchange coefficient for the heat exchanger between the cooling facility and the distribution system

3.2 A Spreadsheet as Support to the Sizing Procedure

The sizing procedure is supported by an excel file. This file includes 8 sheets: one sheet for inputs entries, six sheets which calculate the sizes of each component of each core section of the plant and a final sheet for outputs.
Before describing each mentioned sheet, it is necessary to state the major hypothesis which the entire sizing procedure is based on: the temperatures of the stream being delivered to the building and returning from it have been assumed constant, both in winter and in summer, according to the selected distribution system (DS).
Such hypothesis has been mostly necessary to simulate the heating and the cooling demand of the building. In fact, the demanded power has been translated into a “demanded mass flow” at constant temperature gaps. So, during the simulations, the “demanded mass flow” at the assumed return temperature gets elaborated by the designed facility. Under the mentioned hypothesis, checking that what is produced by the facility matches what is required by the building means ensuring that the “demanded mass flow” gets distributed at the assumed delivery temperature[8].

3.2.1 The “Load” sheet

The first sheet, named “LOAD”, includes the hourly heating and cooling demand of a building. Such sheet converts the heating and cooling demand into hot and cold mass flow demand on the basis of constant temperature gaps which depend on the selected distribution system.
In this sheet two factors are set:

- a first size of the absorption chiller,
- a first solar collectors’ surface.

Once the cooling capacity of the absorption chiller is set, the corresponding heat consumption QabsNom is calculate by:

$$\mathrm{QabsNom} = \frac{\mathrm{Qevanom}}{\mathrm{COP}} \qquad 3.1$$

To solve this equation data about Thermax chiller have been used [17]. Actually, the COPnom reported in the manufacturers can not be directly used in this equation as it refers to different mchill inlet and outlet temperatures. In fact, in the current plant design, mheat and mcool inlet and outlet temperatures are supposed to be the same in [17] (90°/80°C and 29/35.65°C respectively). However, the mchill inlet and outlet temperatures have been respectively set at 10°C and 5.3°C, not at 12°C and 7°C as in [17].
Such selection is due to the need for cooling the temperature of the stream circulating the distribution system from 13°C to 8°C (subchapter 2.2).
To determine the appropriate COP, the mathematical model of the absorption chiller developed by Nurzia [18] is simulated in TRNSYS.
In these simulations, the cooling capacity, which is desired the absorption chiller provides with, and the corresponding COP acquired by the manufacturers are entered the model as Qevanom and COPnom respectively. Then the inlet temperatures of mchill, mcool and mheat are set at 10°C, 27°C and 90°C. Given these entries, under steady state conditions, the simulation output the maximum capacity that the chiller can provide with. As the selected temperatures are different from the one specified in the manufacturer’s sheet, the maximum cooling capacity and the COP are different as well. So, further simulations have to be carried out with different selections of Qevanom until the chiller is able to provide the required cooling capacity, i.e. the required flow mass at the selected temperature gaps. Thanks to these simulations the real COP and QabsNom are determined.

By dividing the hourly cooling demand of the building for the real COP, it is possible to draw the summer heat duration curve. By adding the summer heat demand to the winter one, the yearly duration curve is obtained.
At this point, a reasonable selection of the cogeneration unit can be done.
The second feature characterized in the LOAD sheet is the solar thermal collectors' surface. As this choice can depend on external factors, for instance the maximum building surface which is exposed to the sun, no one defined calculation procedure is applied, but an arbitrary decision is taken.
To identify a first volume for the solar tank, the value 60 l/m² [26] has been considered. While the volume of the cogeneration unit and the absorption chiller have been identified via TRNSYS simulations with the aim at avoiding a large number of ignitions/expirations of the cogenerator and the absorption chiller[1]. The respective rates amount to: 40l/kW_{th} and 90 l/kW_c.

3.2.2 The "Heat Exchangers" sheet

In this sheet the heat exchangers between the heating and cooling facilities and the distribution system are sized.
The heating and cooling peak demand, thus the maximum mass flow rates in the distribution system, are here involved. To identify the UA of the heat exchanger the Log Mean Temperature Difference (LMTD) method is used (Figure 3.1 and Equation 3.2). The temperature gaps on the user's side both in winter and summer are set by the selection of the distribution system: 40°C-30°C for radiant panels and 8°C-13°C for fan coils; whereas, on the facility side, the following temperatures have been selected: 48°C-35° C and 10°C-5.3°C. This selection is useful to have no low LMTD, hence no too much high UA for the heat exchanger. Further more, for the cooling mode, the temperature 5.3°C has been selected according to the temperature of the chilled water provided by the absorption chiller with inlet temperatures of the hot and cooling water respectively equal to 90°C 29°C [17].

[1] Note that the mathematical models do not include thermal inertial effects which can also lead to instable simulations of the cogenerator and the absorption chiller

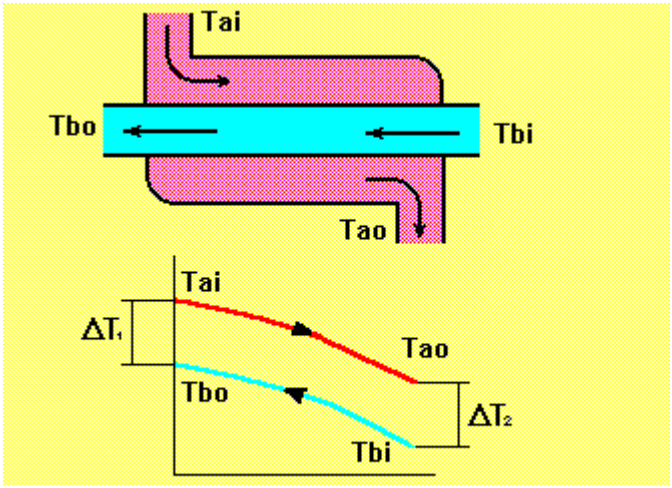

Figure 3.1 Temperature distribution along tube axis in a heat exchanger

$$LMTD = \frac{\left[(T_{ai} - T_{bo}) - (Tao - Tbi)\right]}{\log \frac{(T_{ai} - T_{bo})}{(Tao - Tbi)}} \tag{3.2}$$

Once the heat to be transferred to/from the distribution system ($Q_{transferW}$ and $Q_{transferS}$) is known and the LMTD are fixed, the mass flow rates through the heat and cooling facilities are calculated as follows:

$$mPmach = \frac{Q_{transferW}}{cp*(48-35)} \tag{3.3}$$

$$MCold = \frac{Q_{transferS}}{cp*(10-5.3)} \tag{3.4}$$

So, the UA for the winter and summer heat exchanger are determined according to:

$$WinterUA = \frac{Q_{transferW}}{LMTD_W} \tag{3.5}$$

$$SummerUA = \frac{Q_{transferS}}{LMTD_S} \tag{3.6}$$

3.2.3 The "Solar Loop" sheet

In this sheet the heat exchanger between the primary and solar loop is sized.
A reasonable collector's flow mass per m² of collectors has been identified via TRNSYS simulations and amounts to 25 l/m²*hr. Simulations have been carried out by altering the flow mass in the solar collectors in order to reach the set temperatures in winter and summer under the solar irradiation of Bolzano. The flow mass in the primary loop is determined by:

$$\mathrm{PrimFlow} = 25\frac{\mathrm{l}}{\mathrm{m}^2 \cdot \mathrm{hr}} \cdot \mathrm{CollectorsArea\ m}^2 \qquad 3.7$$

The heat exchanger between the primary and the secondary solar loop is sized using the LMTD method, just like in the previous subchapter.
Table 3.2 reports the temperature differences selected on the hot and cold side of the heat exchanger between the primary and secondary solar loops. Please note that this selection takes into account the temperature differences to be supplied to the users both in summer and in winter. The labels here used refer to Figure 3.1.

Table 3.2

		Winter	Summer	
Hot Stream	Tai	55	95	[°C]
	Tao	40	83	[°C]
Cold Stream	Tbi	35	80	[°C]
	Tbo	48	90	[°C]
LMTD		5.94	3.92	

The cp of the primary solar loop stream, which consists of glycol-water solutions, is calculated with a 33.3% ratio of glycol to water and it amounts to:

$$4.19\frac{\mathrm{kJ}}{\mathrm{kg}*^{0}\ \mathrm{K}} * 0.667\frac{\mathrm{kg}_{\mathrm{H_2O}}}{\mathrm{kg}_{\mathrm{sol}}} + 2.5\frac{\mathrm{kJ}}{\mathrm{kg}*^{0}\ \mathrm{K}} * 0.333\frac{\mathrm{kg}_{\mathrm{glyc}}}{\mathrm{kg}_{\mathrm{sol}}} = 3.62\frac{\mathrm{kJ}}{\mathrm{kg}*^{0}\ \mathrm{K}} \qquad 3.8$$

By respecting the energy balances on the hot stream, the cold stream and on the overall heat exchanger, the UA and the flow mass in the secondary loop are calculated, just like with the equations 3.3, 3.4, 3.5 and 3.6. So, as the heat to be transferred and the LMTD are different for winter and summer, two UApsExch and SecondFlow can be calculated. However, for the heat transfer between the primary and secondary loops it has been decided to have a unique heat exchanger: so the UApsExch maximum is selected, thus the minimum SecondFLow.
The "solar loop" sheet also includes the volume of the tank and it is here used to determine the nodes height for TRNSYS inputs [19] It is supposed that the diameter is 1/3 of the height, thus the following equations system is solved:

$$\mathrm{TankVolume} = \frac{\pi}{4} \cdot \mathrm{TankDiameter}^2 \cdot \mathrm{TankHeight} \qquad 3.9$$

$$\mathrm{TankDiameter} = \frac{1}{3} \cdot \mathrm{TankHeight} \qquad 3.10$$

The height of each node in the tank is determined by supposing that the distance between two nodes in succession is constant.

$$\mathrm{TankHeight}_i - \mathrm{TankHeight}_{i-1} = \frac{\mathrm{TankHeight}}{N} \qquad 3.11$$

N being the total number of the nodes in the tank. Thereby, the height of the first node is exactly:

$$\mathrm{TankHeight}_{i=1} = \mathrm{TankHeight} \qquad 3.12$$

The last variable output by the solar loop sheet is the maximum mass flow rate from the solar tank to the users and is has been set equal to the SecondFLow.

3.2.4 The "Cogeneration Unit" sheet

The nominal heat power of the cogeneration unit, which has been selected in the LOAD sheets, is here used to determine the flow mass entering the cogenerator according to:

$$Mcog = \frac{PthCog}{cp * \Delta T} \quad 3.13$$

The temperature differences to be supplied in winter and summer by the cogenerator are reported in Table 3.3:

Table 3.3 Temperature differences to be supplied with by the cogeneration unit both in winter and summer

	Winter	Summer	
Inlet Temperature	35	80	°C
Outlet Temperature	48	90	°C
ΔT	13	10	°C

To ensure that the cogenerator is able to warm up the flow to the set temperature, the maximum temperature difference, thus the minimum flow is selected. Please note, this flow mass is not the engine jacket chilling flow mass (sub-sub chapter 4.2.1).
The other nominal features of the cogenerator, such as the nominal power, the efficiencies and so on, are calculated according to the equations used in the mathematical model presented in the chapter 4.
The volume of the tank for the cogenerator, which is selected in the LOAD sheet, is here used to determine the height of the entire tank and height of the nodes just like in the solar tank case.
The flow from the cogenerator to the users is set equal to the flow entering the cogeneration unit.

3.2.5 The "Biomass Heater" sheet

The maximum flow mass entering the biomass boiler is derived from:

$$MBio = mPmach - Mcog \quad 3.14$$

Then, the nominal power is calculated, according to the maximum temperature gap the boiler has to provide with:

$$PthBio = MBio * cp * \max \Delta T \quad 3.15$$

The winter and summer ΔTs to be provided are the ones in Table 3.3.
The nominal efficiency is calculated by the mathematical model presented in chapter 4.

3.2.6 The "Absorption Chiller" sheet

In this sheet, the size of the absorption machine, selected in the "LOAD" sheets, and the COPnom deriving from manufacturers are used to determine mchill, mcool and mheat according to the listed temperature gaps (Figure 3.2).

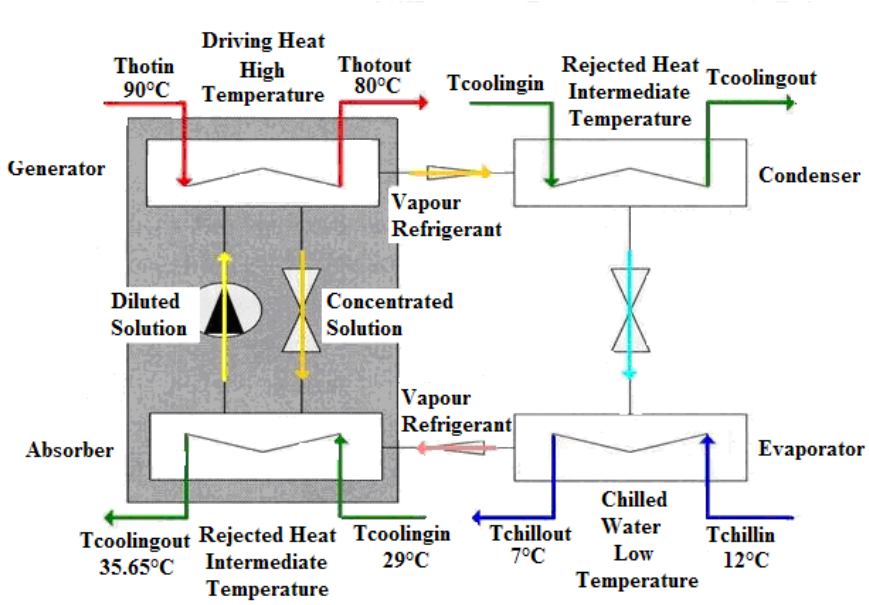

Figure 3.2 Scheme of the cooling cycle in an absorption chiller according to the manufacturers nominal temeperature gaps

So

$$\text{mchill} = \frac{\text{Qevanom}}{\text{cp} * (\text{Tchillin} - \text{Tchillout})} \qquad 3.16$$

The heat requirement and the hot flow mass entering the desorber are given by:

$$\text{DrivingHeat} = \frac{\text{Qevanom}}{\text{COPnom}} \qquad 3.17$$

$$\text{mheatin} = \frac{\text{DrivingHeat}}{\text{cp} * (\text{Thotin} - \text{Thotout})} \quad 3.18$$

The heat to be rejected is given by:

$$\text{Re jectedHeat} = \text{Qevanom} + \text{DrivingHeat} \quad 3.19$$

and:

$$\text{mcool} = \frac{\text{Re jectedHeat}}{\text{cp} * (\text{Tcoolingout} - \text{Tcoolingin})} \quad 3.20$$

The volume of the tank for the absorption chiller, set in the LOAD sheet, is here used to determine the height of the entire tank and of the nodes according to the equations 3.11 and 3.12
The maximum mass flow rate from the absorption to the users is set equal to mchill.

3.2.7 The "Compression Chiller" sheet

Here the compression chiller nominal cooling capacity is determined. The flow mass required on the cold side of the heat exchanger with the summer distribution system is here used to determine the maximum flow which has to be cooled down from the auxiliary cooling machine.

$$\text{mchillCompr} = \text{mCold} - \text{mchill} \quad 3.21$$

Then, according to the temperature gap that the compression chiller has to provide with:

$$\text{QcomprNom} = \text{mchillCompr} * \text{cp} * (\text{Tcompr}_{\text{in}} - \text{Tcompr}_{\text{out}}) \quad 3.22$$

$\text{Tcompr}_{\text{in}}$ and $\text{Tcompr}_{\text{out}}$ being the inlet and outlet temperature of the compression chiller, thus 10°C and 5.3°C.
The corresponding electrical consumption is calculated by supposing a COP equal to 3.

3.2.8 The "Outouts" sheet:

This sheet is used to summarize the outputs of the sizing procedure and it is a clear visualization of the variables which have to be given as inputs to the TRNSYS model described in 5.

3.3 Application of the Sizing Procedure to a Real Case

The sizing procedure has been applied to the EURAC building case study. Thanks to the monitoring system here installed, data about the energy demand of the building have been collected, thus the LOAD sheet has been filled in. The following subchapters present the results of the first application of the sizing procedure to the EURAC case study.

3.3.1 The EURAC heating and cooling demand

To start with implementing the sizing procedure, EURAC monitored data from November 2005 to October 2006 have been used.
Because of missing sensors on the distribution system, it has been assumed that all the heating and cooling produced by the energy supply system respectively coincides with the heating and cooling demand of the building. Actually, the produced energy is expected to be higher than the real demand as it also includes heat losses.
The EURAC monitoring system allows deriving the operation hours of each machine. Thus, considering the time the absorption and the compression chiller have been turned on along the monitored year, it has been possible to define the heating and the cooling season.
As the heat consumption for hot water sanitary is not monitored, it is not possible to distinguish it from the heat for heating use. Nevertheless, as the building is an offices block, the heat production for hot water sanitary use can be assumed negligible with respect to the heating need. So, the winter heat production is supposed to be only used for heating purposes, whereas the summer heat production is supposed to be only used for feeding the absorption chiller.
According to this assumption and to the time the cooling facility was involved into operation along the monitored year, the cooling season started in April, 24^{th} and ended in October 11^{th} thus:

- Wtime = 2737^{th} hr
- Stime = 6817^{th} hr

3.3.2 The "Load" sheet

In this sheet, the heating and cooling demand is translated in a winter and summer mass flow rate demand under constant temperature gaps in the distribution system. Figure 3.3 shows the EURAC heating and cooling demand whereas the Table 3.4 resumes the most interesting data concerning the demand.

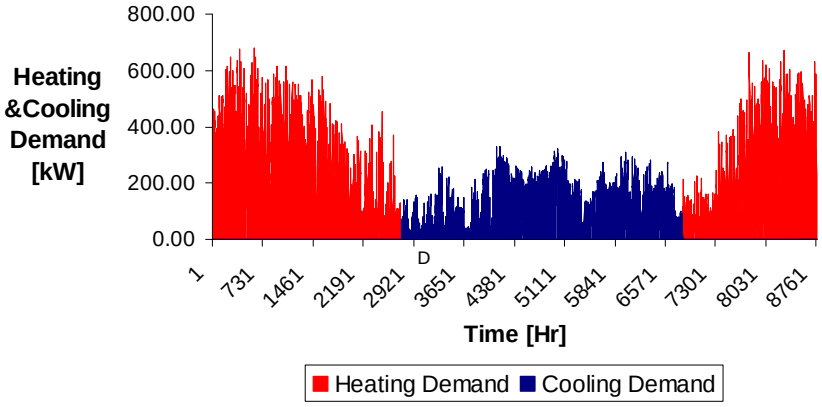

Figure 3.3 EURAC heating and cooling demand

Table 3.4 Major data about the heating and cooling demand of EURAC

Heating Mode	Peak Demand	678	kW
	TsetW	40	°C
	TloadW	30	°C
	DS Max Flow	16.2	kg/s
Cooling Mode	Peak Demand	330	kW
	TsetS	8	°C
	TloadS	13	°C
	DS Max Flow	15.7	kg/s

In the first application of the sizing procedure, the absorption chiller is desired to cover the entire cooling demand[2] and its cooling capacity results to be 355 kW.

[2] Actually, Qevanom is higher than the cooling peak reported in Table 3.4. In fact, according to the model presented in [18] and the manufacturers specifications [15], a 330 kW absorption chiller with 10°C inlet chilled flow temperature can only supply 308 kW. So, by simulating the type 201 created by Nurzia, the appropriate size has been identified in order to supply 330 kW: this size has resulted to be 355 kW.

The volume capacity of the cold tank derives from:

$$90\frac{\mathrm{l}}{\mathrm{kW_c}}\cdot 355\mathrm{kW_c} = 29.7\mathrm{m}^3 \qquad 3.23$$

With a COP of the absorption chiller set at 65%[3] , the summer heat demand has been derived, thus the yearly duration curve shown in Figure 3.4 has been drawn.

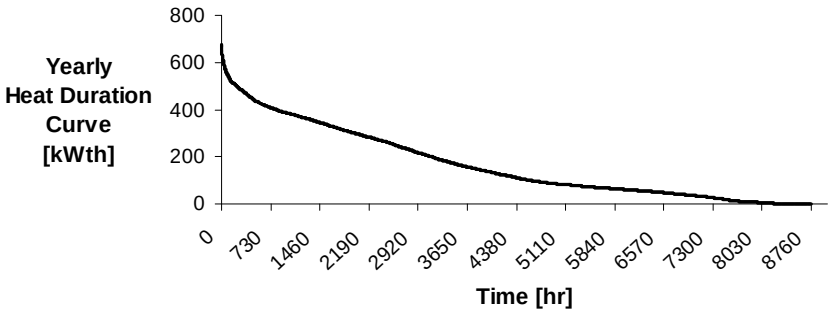

Figure 3.4 Yearly heat duration curve at EURAC

The yearly heat duration curve is useful for a first selection of the cogeneration unit size. To make the cogeneration unit involved in the operation for 3000 hours at least, a 200 kW_{th} capacity has been selected.
According to the ratio reported in the subchapter 3.2.1, t he tank volume for the cogeneration unit amounts to:

$$40\frac{\mathrm{l}}{\mathrm{kW_{th}}}\cdot 200\mathrm{kW_{th}} = 8\mathrm{m}^3 \qquad 3.24$$

In the LOAD sheet an arbitrary solar collectors' surface is selected. It has been set at 200 m². Thus volume tank results in:

[3] According to the manufacturers [15], the COP of a 355 kW chillers is meanly 70%, so the heat demand corresponding to 355 kW amounts to 507 kW. However, according to 1, when the chiller works at its maximum capacity, it supplies with 330 kW, thus the COP amounts to 330/507=65%.

$$60\frac{l}{m^2}\cdot 200m^2 = 12m^3 \qquad 3.25$$

The optimal inclination of the solar collectors has been identified via simulations under the solar irradiation of Bolzano and it amounts to 34°.

3.3.3 The "Heat Exchangers" sizing sheet

Thanks to the data included Table 3.4 and by using the LMTD method, the two heat exchangers between the facility and the distribution systems are sized, one for the heating and the one for cooling mode. Results are respectively reported in Table 3.5 and Table 3.6.

Table 3.5 LMTD method applied to calculate the heat exchanger UA between the heat facility and the winter distribution system for the EURAC case

Hot Stream	Max Flow Mass	12.47[4]	Kg/s
	Cp	4.19	kJ/kg°K
	Tai	48.00	°C
	Tao	35.00	°C
	Heat Transfer	678.63	kW
Cold Stream	Max Flow Mass	16.20	Kg/s
	Cp	4.19	kJ/kg°K
	Tai	30.00	°C
	Tao	40.00	°C
	Heat Transfer	678.63	kW
Exchanger	Mean Log Dt	6.38	°C
	UA	106.32	kW/°k
	Heat Transfer	678.63	kW

[4] The maximum hot flow entering the hot side of the heat exchanger between the facility and the distribution system in the heating mode is also the maximum flow circulating in the heat facility. In fact, the hot flow required by the absorption chiller (see subchapter 3.3.7) is lower than 12.47 kg/s, so mPmach coincides with this value.

Table 3.6 LMTD method applied to calculate the heat exchanger UA between the heat facility and the summer distribution system for the EURAC case

Hot Stream	Max Flow Mass	15.75	Kg/s
	Cp	4.19	kJ/kg°K
	Tai	13.00	°C
	Tao	8.00	°C
	Heat Transfer	329.68	kW
Cold Stream	Max Flow Mass	16.74	Kg/s
	Cp	4.19	kJ/kg°K
	Tai	5.30	°C
	Tao	10.00	°C
	Heat Transfer	329.68	kW
Exchanger	Mean Log Dt	2.85	°C
	UA	115.79	kW/°k
	Heat Transfer	329.68	kW

3.3.4 The "Solar Loop" sheet

A reasonable collector's flow mass per m² of collectors has been identified via TRNSYS simulations and amounts to 25 l/m²*hr. Simulations have been carried out by altering the flow mass in the solar collectors in order to reach the set temperatures in winter and summer under the solar irradiation of Bolzano. So, the flow mass in the primary loop is determined by:

$$25\frac{\mathrm{l}}{\mathrm{hr\,m^2}} * 200\,\mathrm{m^2} = 1.39\frac{\mathrm{kg}}{\mathrm{s}} \qquad 3.26$$

According to Table 3.2, two LMTD exist so two UA can be obtained, as shown in Table 3.7 and Table 3.8.

Table 3.7 LMTD method applied to calculate the heat exchanger UA between the primary and secondary solar loops in the heating mode for the EURAC case

Hot Stream	Max Flow Mass	1.39	Kg/s
	Cp	3.62	kJ/kg°K
	Tai	55.00	°C
	Tao	40.00	°C
	Heat Transfer	75.42	kW
Cold Stream	Max Flow Mass	1.38	Kg/s
	Cp	4.19	kJ/kg°K
	Tai	35.00	°C
	Tao	48.00	°C
	Heat Transfer	75.42	kW
Exchanger	Mean Log Dt	5.94	°C
	UA	12.69	kW/°k
	Heat Transfer	75.42	kW

Table 3.8 LMTD method applied to calculate the heat exchanger UA between the primary and secondary solar loops in the cooling mode for the EURAC case

Hot Stream	Max Flow Mass	1.39	Kg/s
	Cp	3.62	kJ/kg°K
	Tai	95.00	°C
	Tao	83.00	°C
	Heat Transfer	60.33	kW
Cold Stream	Max Flow Mass	1.44	Kg/s
	Cp	4.19	kJ/kg°K
	Tai	80	°C
	Tao	90	°C
	Heat Transfer	60.33	kW
Exchanger	Mean Log Dt	3.92	°C
	UA	15.41	kW/°k
	Heat Transfer	60.33	kW

As one heat exchanger is desired to guarantee the both heat transfers, the maximum UA value is selected. Thus the SecondFlow amounts to 1.44 kg/s as well as the flow from the solar tank to the heat exchanger with the users.
The volume of the solar tank and the height of each node are reported in Table 3.9.

Table 3.9 Height of each node in the solar tank

Solar Tank	Size	Unit
SolTankV	12.00	m³
nSolT1	5.16	m
nSolT2	4.13	m
nSolT3	3.10	m
nSolT4	2.06	m
nSolT5	1.03	m

3.3.5 The "Cogeneration Unit" sheet

A 200 kW_{th} cogenerator has been selected. So, according to subchapter 3.2.4, the mass flow rate entering the cogenerator is:

$$MCog = \frac{200}{4.19 * (48 - 35)} = 3.67 \frac{kg}{s} \qquad 3.27$$

The volume of the cogeneration tank and the height of each node are reported in table 3.10.

Table 3.10 Height of each node in the cogenerator tank

Cogenerator Tank	Size	Unit
CogTankV	8.00	m³
n1CogT	4.51	m
n2CogT	3.61	m
n3CogT	2.71	m
n4CogT	1.80	m
n5CogT	0.90	m

3.3.6 The "Biomass Heater" sheet

The flow mass entering the biomass heater is:

$$12.47 - 3.67 = 8.80 \frac{\text{kg}}{\text{s}} \qquad 3.28$$

So the nominal power of the boiler amounts to:

$$8.80 \cdot 4.19 \cdot (48 - 35) = 479.28\text{kW} \qquad 3.29$$

3.3.7 The "Absorption Chiller" sheet

According to the equations 3.16 through 3.20, the nominal features of the absorption chiller are shown below:

Table 3.11 Nominal mheat, mcool and mchill of the absorption chiller with Qevanom set at 355 kW

Absorption Chiller		Size	Unit
mheat	Flow mass	12.10	kg/s
	Cp	4.19	kJ/kg°K
	Inlet Temperature	90.00	°C
	Outlet Temperature	80.00	°C
	Driving Heat	507.14	kW
mchill	Flow Mass	16.95	kg/s
	Cp	4.19	kJ/kg°K
	Inlet Temperature	12.00	°C
	Outlet Temperature	7.00	°C
	Evaporated Heat	355	kW
mcool	Flow mass	30.94	kg/s
	Cp	4.19	kJ/kg°K
	Inlet Temperature	35.65	°C
	Outlet Temperature	29	°C
	Rejected Heat	862.14	kW

Data on the cold tank are reported in the Table 3.12.

Table 3.12 Height of each node in the cold tank

Cold Tank	Size	Unit
AbsTankV	29.7	m³
n1AbsT	6.98	m
n2AbsT	5.59	m
n3AbsT	4.19	m
n4AbsT	2.79	m
n5AbsT	1.40	m

3.3.8 The "Compression Chiller" sheet

By selecting the maximum size for the absorption chiller, mchill coincides with the total flow to be circulated in the cooing facility, so it represents the so called MCold. Under this selection the flow to be circulated in the compression chiller is zero and its nominal cooling capacity as well.

3.3.9 The "Outputs" sheets:

The following tables summarize the outputs of the sizing procedure which represents the entry to the simulations.

Table 3.13 All the outputs of the sizing procedure applied to the EURAC concerning the heat facility and the heating mode

TSetW	40.00	°C
TsetMachW	48.00	°C
CollectorArea	200.00	m²
SurfaceSlope	34.00	°
PrimFlow	5,000.00	kg/hr
UApsExch	55476	kJ/hrK
SecondFlow	5,184	kg/hr
SolTankV	12.00	m³
nSolT1	5.16	m
nSolT2	4.13	m
nSolT3	3.10	m
nSolT4	2.06	m

nSolT5	1.03	m
PSolTank	100.00	kJ/hr
PthCog	200.00	kW
Mcog	13,218	kg/hr
CogTankV	8.00	m³
n1CogT	4.51	m
n2CogT	3.61	m
n3CogT	2.71	m
n4CogT	1.80	m
n5CogT	0.90	m
PthBio	479	kW
MBio	31,676	kg/hr
mPmach	44,895	kg/hr
TloadW	30.00	°C
WinterUA	382752	kJ/hr

Table 3.14 All the outputs of the sizing procedure applied to the EURAC concerning the cooling facility and the cooling mode

Stime	6,817.00	hr
TSetS	8.00	°C
TsetMachS	90.00	°C
TsetAux	5.30	°C
Qevanom	355.00	kW
COPnom	0.70	
mheat	12.10	kg/s
mchill	16.95	kg/s
mcool	30.94	kg/s
mheat_hr	43,573	kg/hr
mchill_hr	61,002	kg/hr
mcool_hr	111,390	kg/hr
QcomprNom	0.00	kW
mchillCompr	0.00	kg/hr

MCold	60,268	kg/hr
AbsTankV	29.70	m^3
n1AbsT	6.98	m
n2AbsT	5.59	m
n3AbsT	4.19	m
n4AbsT	2.79	m
n5AbsT	1.40	m
TloadS	13.00	°C
SummerUA	416829	kJ/hr

4 Modelling of a Cogeneration Unit and a Biomass Boiler for TRNSYS Simulations

4.1 Introduction

To simulate the plant designed in Chapter 2, the mathematical models included in the TRNSYS standard library [19] can be used for most of the components included in the selected layout. However, as any standard type exists for a cogeneration unit and not even for a biomass boiler, two new mathematical models have been developed which are described in details in this chapter.
In the development of the two models, both the components have been considered as black boxes which transfer heat to an entering stream according to internal control logics.
The development of the models has been carried out with the aim at reproducing both the design and off design behaviour of the components. In particular, each model:

- calculates the main nominal features once the size of each component has been selected;
- simulates the operation of the component according to its internal control logics and operating characteristic curves;
- calculates the primary energy consumption;
- calculates the outlet state of the fluid.

The models have been written in MATLAB which appeared suitable to implement the instructions and the equations for modelling the operation of both the components. Furthermore, the TRNSYS includes a specific type, “TYPE 155- Calling MATLAB”, which easily makes the TRNSYS and MATLAB communicating between each other.

4.2 Modelling a Gas Engine Based Cogeneration System

4.2.1 Hypotheses

1. The model for the cogeneration system groups the gas engine, the electric generator, the internal heat recuperators and the heat exchanger with the external side in one unit. This unit represents a black box which provides with power and heat in compliance with internal control logics and operating curves.

2. Two separated models have been developed depending on the control strategy: one for a heat load tracking cogenerator and one for a power load tracking cogenerator. In each model two types of modulation are available: continue and discrete modulation. In continue modulation the cogenerator can provide every rate of the nominal power included in a certain range (usually 60%-100%); in discrete modulation the cogenerator can provide with specific rates of the nominal power (e.g. only 60% and 100% of the nominal power).
3. The operating curves have been derived from the elaboration of technical specifications acquired by various manufacturers. They refer to the following range of sizes: [70; 500] kWe[5]. Data have been interpolated in order to allow the selection of all the sizes included in the above defined range.
4. The model does not include inertia effects but simulates the component under steady state conditions.

4.2.2 Data collection and elaboration

To model a co-generation system employing a gas engine, specific data of several engine types have been collected and elaborated. Those data have been extrapolated by Thermoflex, a software tool for the design and simulation of thermal power plants [20]. This software includes a database of 377 diesel and gas reciprocating engines. For each engine a technical card, directly derived from manufacturers, reports data about the power and the heat recoverable from exhaust gases and the cooling water jackets. In particular the cards include:

- the nominal power, P_{nom};
- the nominal electrical efficiency,$\eta_{e,nom}$;
- the fuel consumption in Nm^3/hr for three load rates (100%, 70% and 50%), $m_{f,nom}$;
- the exhaust flue gas flow mass in kg/s at nominal working conditions, m_{eg};
- the exhaust flue gas temperature at nominal working conditions, and T_{eg};
- the heat available from the jacket chilling water excluding the heat losses, Q_j.

For the present research, 54 engines have been selected in the database in compliance with the following features:

[5] Such range seemed reasonable for engines to be used in medium-large civil buildings.

- gas as primary energy source;
- frequency of 50 Hz;
- NOx emissions not higher then 250 mg/Nm³ (when specified);
- maximum nominal power of 0.5 MWe.

The above mentioned features for the selected engines have been elaborated to obtain the operating curves of based gas engine cogeneration systems.
First, to estimate the efficiency at partial load rates, the gas Low Heating Value (LHV) assumed for each engine has been calculated according to:

$$LHV = \frac{\dot{P}_{nom}}{\eta_{e,nom} \cdot \frac{\dot{m}_{f,nom}}{3600}} \quad \frac{kJ}{Nm^3} \tag{4.1}$$

Once LHV has been obtained, the primary consumption E_p at nominal and partial load rates has been calculated according to:

$$\dot{E}p_i = LHV \cdot \frac{\dot{m}_{f,i}}{3600} \quad kW \quad for\, i = 1, 0.75, 0.5 \tag{4.2}$$

Then the electrical efficiencies at 75% and 50% load rates have been calculated according to:

$$\eta_{e,part} = \frac{\dot{P}_{part}}{\dot{E}p_i} \quad nd \quad for\, part\, and\, i = 0.75, 0.5 \tag{4.3}$$

The heat available from the engine has been obtained as explained below.
On one hand, the exhaust gas mass flow and its temperature at nominal working condition have been used to calculate the maximum heat flow obtainable from the flue gas at full load. Gases have been supposed to be chilled to a 120°C with a Specific Heat (cp_{eg}) of 1.2 kJ/kg*K.

$$\dot{Q}_{eg} = \dot{m}_{eg} \cdot cp_{eg} \cdot (T_{eg} - 120) \quad kW \tag{4.4}$$

On the other hand, the heat recoverable from the jacket chilling water is directly available from Thermoflex and it already excludes the heat losses declared by the manufacturers.
The entire recoverable heat at nominal working condition is obtained by summing the two above amounts.

$$\dot{Q}_{rec,nom} = \dot{Q}_{eg} + \dot{Q}_{j} \quad kW \tag{4.5}$$

Hence, the first law efficiency η_I is calculated by:

$$\eta_I = \frac{\dot{P}_{nom} + \dot{Q}_{nom}}{\dot{m}_{f,nom} * LHV} \quad \% \tag{4.6}$$

and the nominal thermal efficiency $\eta_{th,nom}$ results in

$$\eta_{th,nom} = \eta_I - \eta_{e,nom} \quad \% \tag{4.7}$$

To calculate the thermal efficiency at partial loads, the first law efficiency has been assumed constant. Thus, given the electrical efficiencies at partial load rates, the corresponding thermal efficiency can be calculated by the difference:

$$\eta_{th,part} = \eta_I - \eta_{e,part} \quad \% \quad for\ part = 0.75, 0.50 \tag{4.8}$$

Given E_p and $\eta_{th,part}$, the global heat available at partial loads is equal at:

$$\dot{Q}_{rec,part} = \eta_{th,part} * \dot{E}p_{part} \quad kW \quad for\ part = 0.75, 0.50 \tag{4.9}$$

The just described data elaboration is summarized in Table 4.1.

Table 4.1- Summmary of the inputs and outputs for the data elaboration about the cogeneration units.

Inputs	Equation number	Outputs
Pnom , ηe,nom, $\dot{m}_{f,nom}$	$LHV = \frac{\dot{P}_{nom}}{h_{e,nom} * \frac{\dot{m}_{f,nom}}{3600}}$	LHV [kJ/Nm³]
LHV, $\dot{m}_{f,i}$	$\dot{E}p_i = LHV * \frac{\dot{m}_{f,i}}{3600}$	Epi [kW]
Ppart, Epi	$h_{e,part} = \frac{\dot{P}_{part}}{\dot{E}p_i}$	ηe,part [%]
$\dot{m}_{eg}$, T_{eg}	$\dot{Q}_{eg} = \dot{m}_{eg} * cp_{eg} * (T_{eg} - 120)$	Qeg [kW]
Q_{eg}, Q_j	$\dot{Q}_{rec,nom} = \dot{Q}_{eg} + \dot{Q}_j$	Qrec,nom [kW]
P_{nom} , $Q_{rec,nom}$, $\dot{m}_{f,nom}$, LHV	$h_I = \frac{\dot{P}_{nom} + \dot{Q}_{nom}}{\dot{m}_{f,nom} * LHV}$	ηI [%]
η_I,$\eta_{e,nom}$,	$h_{th,nom} = h_I - h_{e,nom}$	ηth,nom [%]
η_I,$\eta_{e,part}$	$h_{th,part} = h_I - h_{e,part}$	ηth,part [%]
$\eta_{th,par}$, Ep_{part}	$\dot{Q}_{rec,part} = h_{th,part} * \dot{E}p_{part}$	Qrec,part [kW]

4.2.3 Design and off-design operating curves

The above described data elaboration has been used to obtain the operating curves for a gas engine based cogeneration unit.
First of all, the relationship between the nominal power P_{nom} and heat $Q_{rec,nom}$, i.e. the Electrical Index (EI), has been observed (Equation 3.1 and Figure 3.1):

$$P_{nom} = 0.6148 \cdot Q_{rec,nom} + 0.9282 \quad kW \qquad 4.10$$

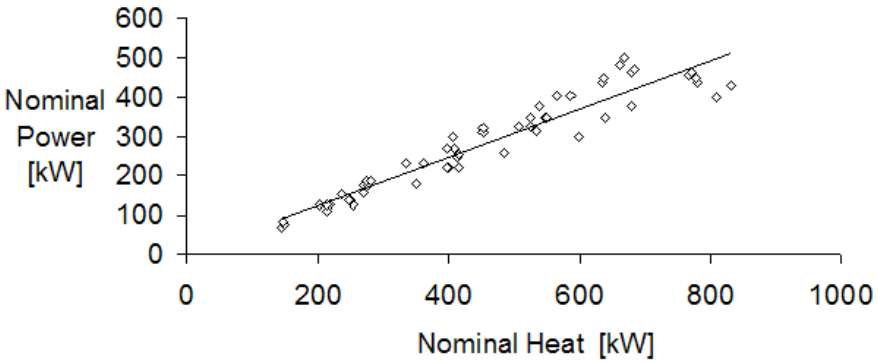

Figure 4.1 Relationship between the nominal power and the nominal heat

Electrical, thermal and first law efficiencies have been turned out to depend on different nominal electrical power according to the following equations as shown in Figure 4.2.:

$$\eta_{e,nom} = 0.0061P_{nom} + 31.284 \quad \% \qquad 4.11$$

$$\eta_{th,nom} = -0{,}0133P_{nom} + 58{,}266 \quad \% \qquad 4.12$$

$$\eta_{I,nom} = -0{,}0071P_{nom} + 89{,}51 \quad \% \qquad 4.13$$

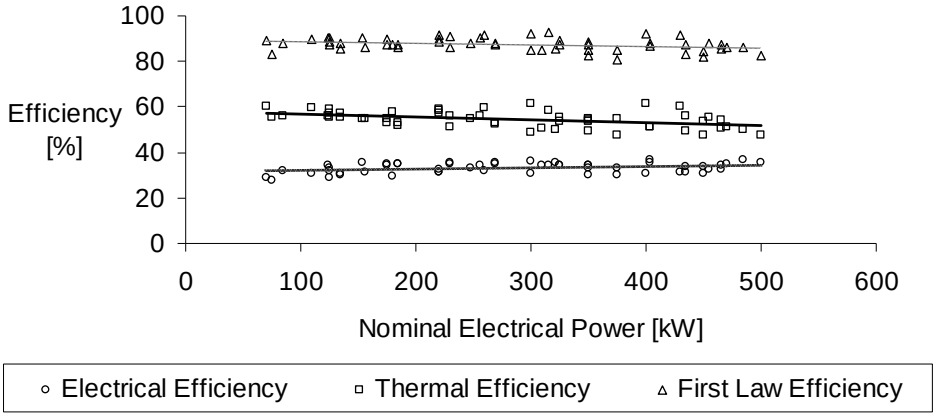

Figure 4.2 Electrical, thermal and First Law efficiencies dependence on Nominal Electrical Power.

A linera trendline has been assumed for the dependency between the electrical and thermal load rates, as in Figure 4.3, according to the following equation:

$$\frac{\dot{Q}_{rec,part}}{\dot{Q}_{rec,nom}} = 0.6685 \cdot \frac{\dot{P}_{part}}{\dot{P}_{nom}} + 0.3315 \quad \% \qquad 4.14$$

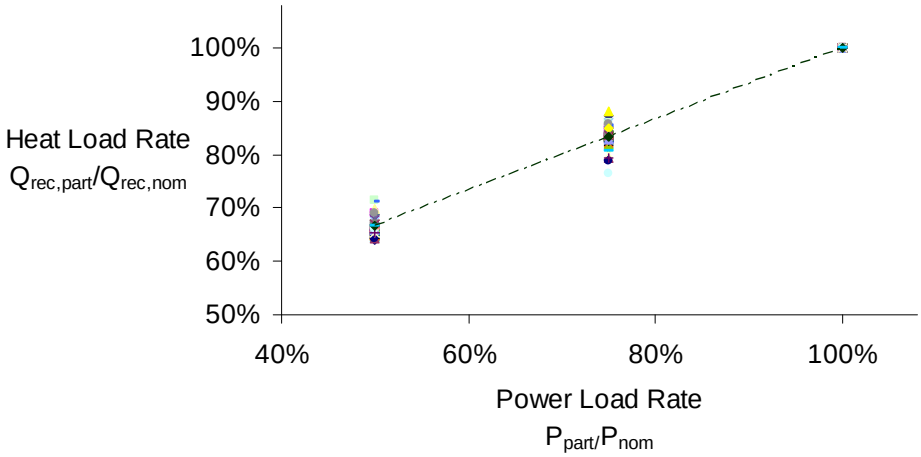

Figure 4.3 Selection of one trendline as average curve for the relationship between the Heat Load Rate and the Eectrical Load Rate

Then, the dependency of the electrical efficiency on the power load rates has been highlighted Figure 4.4.

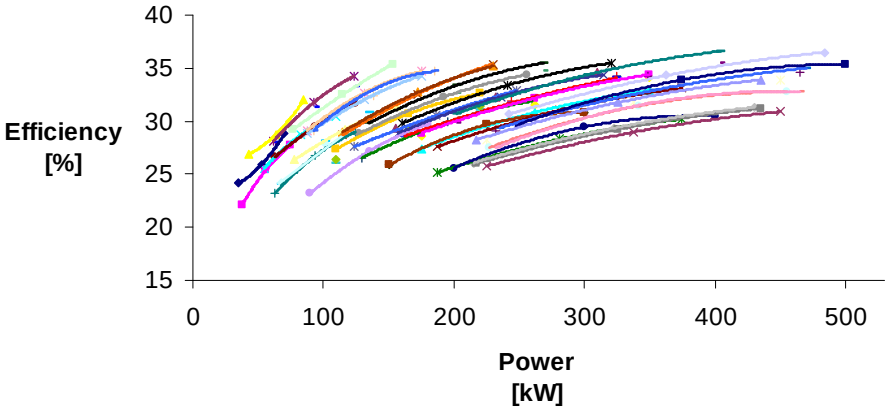

Figure 4.4 Dependency of the Electrical Efficiency on power load rates for each engine included in teh database

As that dependency appears stronger for engines with a power lower then 185 kW (curves are more tilted), two ranges have been identified (Figure 1.5). Therefore, two relationships have been derived expressing an average for the efficiency rates at partial loads.
For nominal powers below 185 kW:

$$\frac{\eta_{e,part}}{\eta_{e,nom}} = -0,32\left(\frac{P_{part}}{P_{nom}}\right)^2 + 0,86\left(\frac{P_{part}}{P_{nom}}\right) + 0,46 \quad \% \qquad 4.15$$

Whereas for nominal powers above 185 kW:

$$\frac{\eta_{e,part}}{\eta_{e,nom}} = -0,40\left(\frac{P_{part}}{P_{nom}}\right)^2 + 0,96\left(\frac{P_{part}}{P_{nom}}\right) + 0,44 \quad \% \qquad 4.16$$

4.2.4 MATLAB modelling of a gas engine based cogeneration unit

The data elaboration and the curves above drawn have been used to model a gas based co-generation system in MATLAB.
The model has been built according to the main aim of this investigation, i.e. deriving nominal and off design features for a gas engine to be simulated under two control strategies: head tracking and power tracking.
In this subchapter, the model of a heat tracking co-generator is described.
In this case, the first input to be given to the model is the nominal heat of the cogenerator.
The nominal heat is used to calculate the corresponding nominal power through the equation 4.10
Then, the nominal electrical, thermal and the first law efficiencies are calculated through the equations 4.11, 4.12 and 4.13.
With the regard to the off-design features, the model includes some instructions for the engine to be modulated in dependence on the heat load of a building. First of all, the model calculates the heat required for the entering stream to be heated up to a previous selected temperature. Then, two options are available: discrete modulation (modulation=0) and continue modulation (modulation=1). Discrete modulation means that the engine can only work at fixed load rates within the range [Qmin, Qnom], whereas continue modulation means that the engine can work at all load rates included in the range [Qmin, Qnom]. In the

first case, the code requires an array Lrp including the possible power load rates, e.g. [0.60; 0.80; 1]; in the second case, the code only requires the minimum load rate, e.g. 0.60.
Once the modulation is defined and the required heat is calculated, the code identifies the recoverable heat as:

- the minimum load rate between Qmin and Qnom, which does not exceed the required heat Qreq, in discrete modulation, or
- as an amount equal to the required heat for Qreq included in [Qmin, Qnom], in continue modulation.

Once the recoverable heat is identified, the heat load rate is determined as the rate between such heat and the nominal heat. Afterwards, the corresponding electrical load rate is calculated according to the equation 4.14
Therefore, the equation 4.15 and 4.16 give the electrical efficiencies at partial loads.
Subsequently, supposing the first law efficiency to be constant, the thermal efficiency at partial load is obtained by means of the difference between the first law efficiency and the electrical efficiency at partial loads as in the equation 4.8 .
At the end, the primary energy consumption is calculated as the rate between the power and the electrical efficiency.

4.2.5 Adapting the m-file for TRNSYS simulations

The model of the cogeneration unit has been written in MATLAB but it has to be simulated in TRNSYS. To this end, TRNSYS type 155 has been used. Such type connects the two programs so that:

- firstly, TRNSYS gives the inputs needed by the model to MATLAB,
- secondly, MATLAB executes the model and gives the outputs to TRNSYS

To make the two programs interact, it is mainly needed to declare:

- the parameters, variables constant with time;
- the inputs, variables in input not constant with time; and
- the outputs, the variables calculated by the code.

For the co-generation model the variables can be classifies as follows:

Parameters

- modulation: discrete variable which can be 0 (modulation discrete) or 1 (continue modulation);
- LRp, Load Rate power: an array or single value including the available power load rates which are usually expressed in terms of the nominal power;
- cp: heat capacity of the entering stream which is supposed to be constant under the present working temperatures;

Inputs

- Qnom: the nominal heat;
- Tset: the set temperature the stream entering the cogenerator is wanted to reach;
- m: the mass flow of the entering stream;
- Tin: the inlet temperature of the entering stream;
- onoff: signal for the cogenerator to be switched on/off by an external control.

Outputs:

- Pnom: the nominal power corresponding to the selected nominal heat;
- etaenom: the nominal electrical efficiency;
- etaInom: the first law efficiency;
- etathnom: the nominal heat efficiency;
- Qcog: the recoverable heat in a certain time step according to the required heat and to the selected modulation;
- P: the power generated in a certain time step corresponding to Qcog;
- etae: the electrical efficiency corresponding to the power load rate in a certain time step;
- etath: the thermal efficiency corresponding to the heat load rate in a certain time step;
- Ep: the primary energy consumption in a certain time step;
- mout: the outlet mass flow;

– Tout: the outlet temperature of the stream.

The communication between the TRNSYS and MATLAB is represented in Figure 4.5. Note that the m-file is called by the TRNSYS at each time step of the simulation.

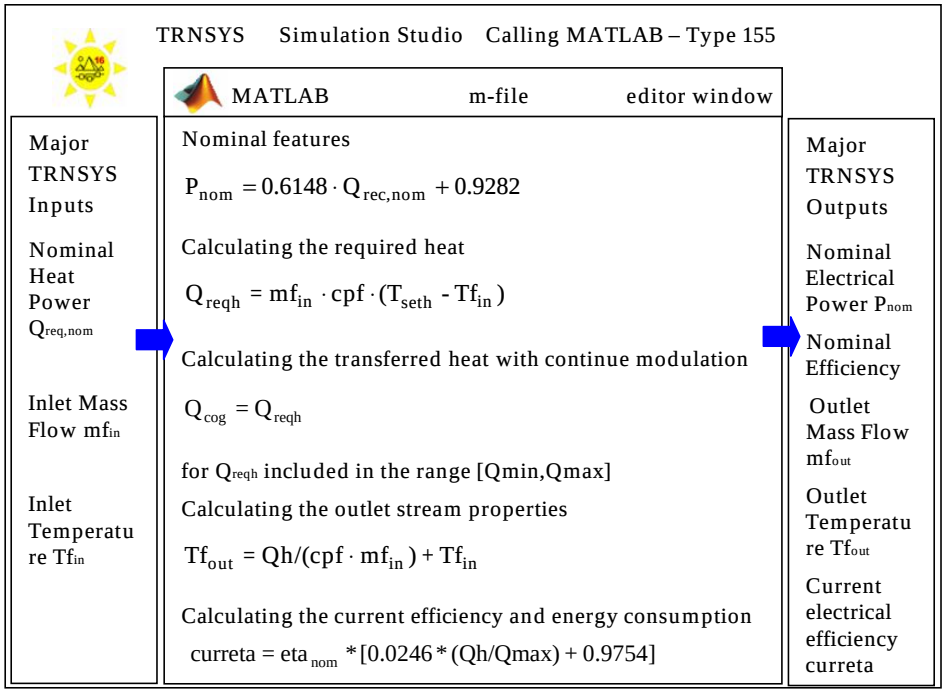

Figure 4.5 Logic representation of the TRNSYS type 155

4.3 Modelling of a Biomass Heater

4.3.1 Hypotheses

1. In this model, the biomass boiler is represented as a black box which provides heat in compliance with internal control logics and operating curves.
2. Two modulations are available, just like for the cogenerator: continue and discrete modulation. In continue modulation the boiler can provide every rate of the nominal heat included in a certain range (25%-100%); in discrete modulation the boiler can provide with specific rates of the nominal power (e.g. 50% and 100%).

3. The operating curves have been derived by the elaboration of technical specifications acquired by various manufacturers as described in the subchapter 1.3.2. They refer to the following range of sizes: [15; 1000] kWth[6]. Data have been interpolated in order to allow the selection of all the sizes included in the above defined range.
4. The model does not include inertia effects but simulates the component under steady state conditions.

4.3.2 Data collection and elaboration

To model a biomass heater, specific data have been collected from manufacturing sheets. A database including 50 heaters, to be fed up with wood biomass (pellets or chips), has been created. Heaters manufactured by Fröling, UNiconfort, KWB and Kalorina, with a nominal heat power up to 1 MW have been included in such database.
The following data have been collected:

- nominal heat;
- minimum load rate;
- primary energy consumption or/and total heat efficiency at nominal and at minimum load rate.

Unfortunately, not all these data have been available for each heater type; nevertheless significant results could be drawn.

4.3.3 Design and off-design operating curves

The collected data have been used to draw operating curves for biomass heaters. The available data show that wood heaters with nominal heat lower than 100 kW have the highest efficiencies at nominal condition (Figure 4.6 Overall heat efficiency of various biomass boilers depending on their nominal heat Figure 4.6) according to:

$$\eta_{nom} = -2.6733 \ln \dot{Q}_{max} + 101.61 \quad \% \qquad 4.17$$

[6] Such range seemed reasonable for boilers to be used in medium-large civil buildings.

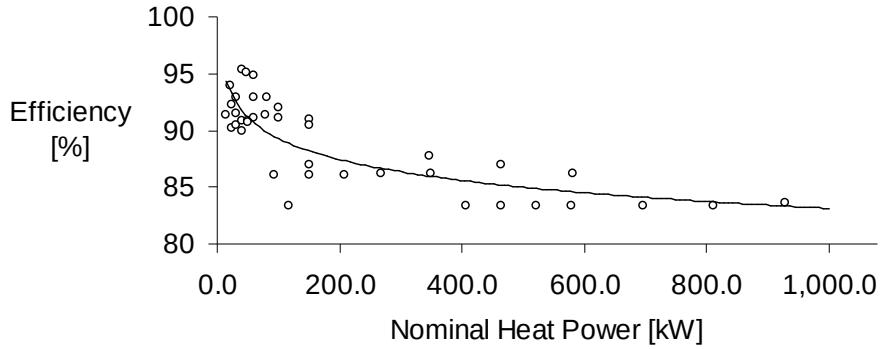

Figure 4.6 Overall heat efficiency of various biomass boilers depending on their nominal heat

Most of the wood heaters can run at partial loads too. Modern heaters can be continuously modulated between the nominal and the minimum heat rate, which usually amounts to 25%. Observing the efficiency at partial loads it has turned out that no uniform trend exists. In fact, biomass heaters efficiencies at partial rates can be higher or lower than the nominal ones depending on the model (Figure 4.7).

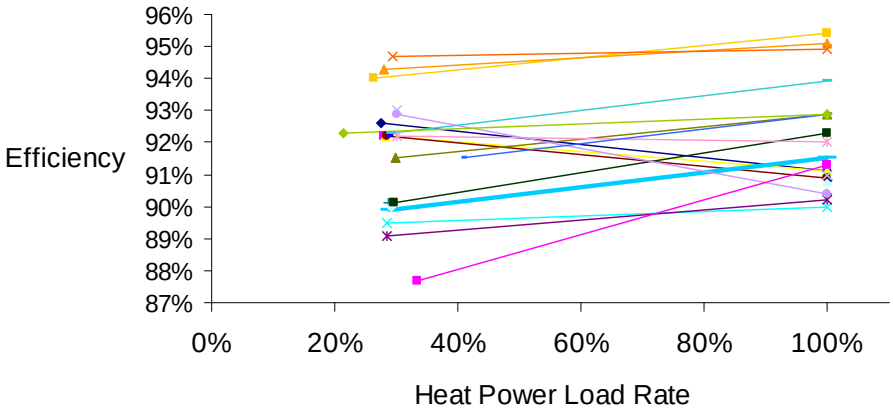

Figure 4.7 Heat efficiency values at minimum and maximum heat rate and their trends for different boilers

Because of this variance, to model a biomass heater only one curve has been selected and it corresponds to the following equation (Figure 4.8):

$$\frac{\text{curreta}}{\text{eta}_{\text{nom}}} = 0.0246 \cdot \frac{\dot{Q}h}{\dot{Q}m_{ax}} + 0.9754 \quad \% \qquad 4.18$$

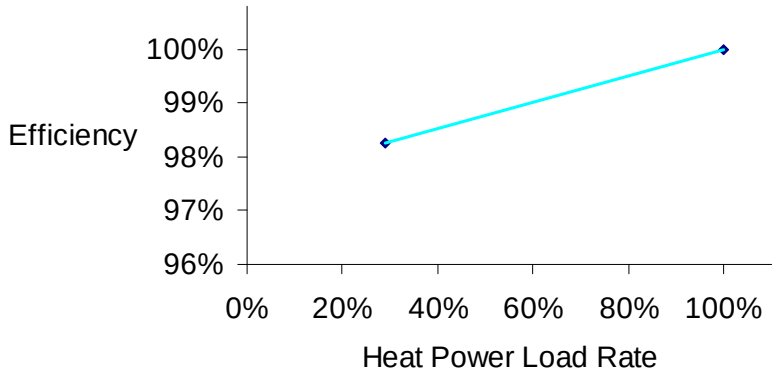

Figure 4.8 Selection of a trend to model the relationship between the overall thermal efficiency and various heat rates in a biomass boiler

4.3.4 MATLAB modelling of a biomass boiler

The data elaboration and the curves above drawn have been used to model a biomass boiler in MATLAB.
The model has been built according to the main aim of this investigation, i.e. deriving nominal and off design features for a biomass boiler to be simulated.
The first input to be given to the model is the nominal thermal power which identifies the properties of the boiler, e.g. the efficiency at full heating rate according to the equation 4.17.
With the regard to the off-design features, the model includes some instructions for the boiler to run in order to supply an entering stream with heat and to make it reach the desired temperature.
In fact, firstly, the model calculates the heat required to increase the entering stream up to the desired value. Secondly, the boiler will transfer certain heat amounts in dependence on its modulation mode. If the modulation is discrete, the heat transferred to the fluid is:

- higher than the required heat, whenever the latter is lower than the minimum heating rate;
- equal to the required heat, whenever the latter coincides with the minimum or the maximum heating rate;

- lower than the required heat, whenever the latter is higher thsn the maximum heating rate.

In continue modulation, the heat transferred to the fluid will be exactly the heat required except in two cases:

- whenever the heat required is higher than the maximum heating rate, thus the heat transferred will be the nominal one;
- whenever the heat required is lower than the minimum heating rate, thus the heat transferred coincides with the minimum heating rate.

In both the modulation modes, the heater is supposed to work even when the required heat is lower than the minimum heating rate. This choice depends on the fact that the heater is the last back up machine to supply the heat demand.
Once the heat to be transferred is calculated, the outlet stream temperature is calculated through an energy balance. This temperature is not supposed to be affected by losses through the envelopment of the heater, as UA values are difficult to be known by the manufacturers.
Once the current transferred heat is determined, the current efficiency is calculated according to the equation 4.18.
Finally, the primary energy consumption is determined.

4.3.5 Adapting the m-file for TRNSYS simulations

As for the interaction between the MATLAB cogeneration unit model and the TRNSYS, also for m-file for the biomass boiler needed to be adapted and inputs, parameters and outputs have been declared.
In this case, some variables which are actually parameters, have been declared as inputs. In this way, it is possible to define a default value in the TRNSYS proforma of type 155.
According to such remark, the following variables have been declared:

Inputs

- cpf= heat capacity of the entering stream supposed to be constant considering the present working temperatures;
- Modul= discrete variable which can be 0 (discrete modulation) or 1 (continue modulation);
- Qmax= the nominal heat;
- Tseth= the desired temperature for the stream to be heated up;

- Tfin= the inlet temperature of the entering stream;
- mf= the flow mass of the entering stream;
- OnOff= signal for the cogenerator to be switched on/off by an external control.

Outputs:

- Qreqh: the heat required by the stream to be heated up to the desired temperature;
- Qh: the heat provided by the boiler according to the selected modulation;
- Tfout: the outlet temperature of the stream in a certain time step;
- mfout: the outlet flow mass in a certain time step;
- etanom: the nominal overall efficiency;
- curreta: the overall efficiency at partial load rate in a certain timestep;
- Qcomb: the primary energy consumption in a certain timestep.

Similarly to the cogeneration unit case, the biomass boiler model is called by the TRNSYS at each time step of the simulation.

5 Building the TRNSYS Deck

5.1 Introduction

In the present chapter the TRNSYS deck is described[7]. It represents the translation in TRNSYS of the layout and control strategy presented in Chapter 2. The inputs to most TRNSYS types derive from the sizing procedure presented in Chapter 3. In fact, the outputs of the sizing procedure (e.g. Table 3.13 and Table 3.14) are set as parameters in two EQUATIONS, "Inp/param_Winter" and "Inp/param_Summer" (Figure 5.1). All the types which need such variables as inputs refer to the two EQUATIONS. In this way, it is enough to change the value of one input in these two EQUATIONS that the new value is considered by all the types which use it.

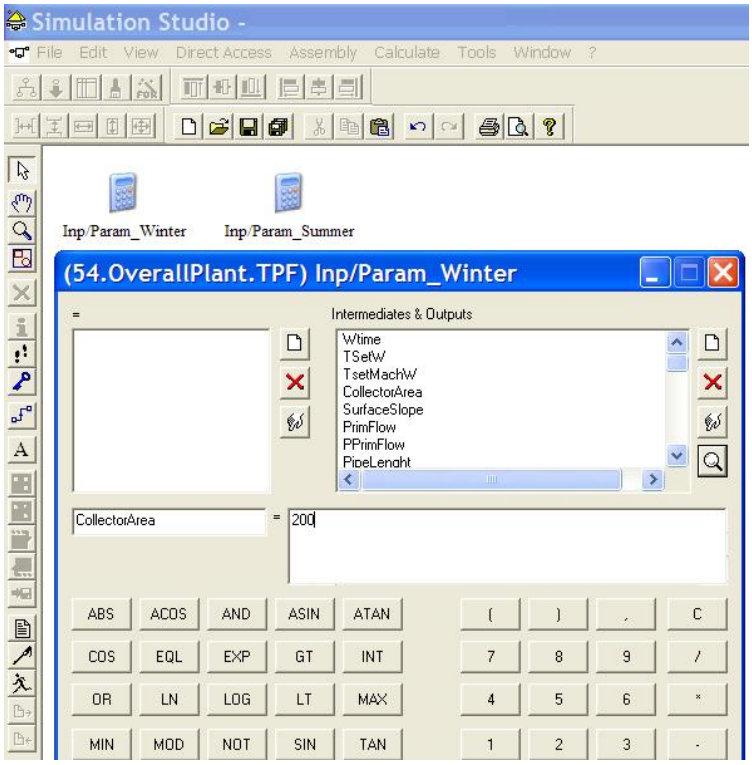

Figure 5.1: The solar collectors surface selected in the sizing procedure (200 m²) is entered as parameter into the "Inp/param_Winter" EQUATION

[7] Please, refer to [19] for a better understanding of this chapter.

In particular, the “Inp/param_Winter” includes all the variables concerning the heating mode and, in general, the heat facility; on the contrary, the “Inp/param_Summer” includes all the variables concerning the cooling mode and, in general, the cooling facility.
The following chapters describe each sub-facility and the way they get involved in the yearly simulation. Please, remember that the simulations refer to the EURAC case as its heating and cooling demand is used.

5.2 Heat Facility Simulations

As already stated in Chapter 2 the term “Heat Facility” refers to the part of the energy facility which provides with heat for both heating and cooling purposes. This part includes the following 3 macros:

1. the solar loop;
2. the cogeneration;
3. the biomass boiler.

Each one of them will be differently simulated depending on the heating and the cooling mode already shown in Figure 2.6 and Figure 2.7.

5.2.1 The heating mode

The section representing the heat facility in the heating mode is reported in Figure 5.2.
The DATA READER, named “Heating Load”, includes as text file the heating demand deriving from the “LOAD” sheet of the sizing procedure. An On-Off controller (Type 2b-4) discriminates the range of the flow mass demand which make the heat facility to run in the heating mode. The minimum heat amount to be supplied has been selected by observing the heating demand of EURAC and by identifying the minimum step.
The “PID Wint” controller outputs a signal which regulates the flow mass in the hot side of the “Winter Heat Exchanger”. It sets the flow mass which is needed at 48°C (set point temperature for the heat generators in the heating mode) to heat up 40° the stream in the distribution system, its return temperature being 30°C. The signal output by the “PID Wint” controller is entered into the “Pump_HotMach” through the “Sig_PumpHotMach” EQUATION which has been included in the deck only to discriminate between the heating and cooling mode (Subchapter 5.3.1).

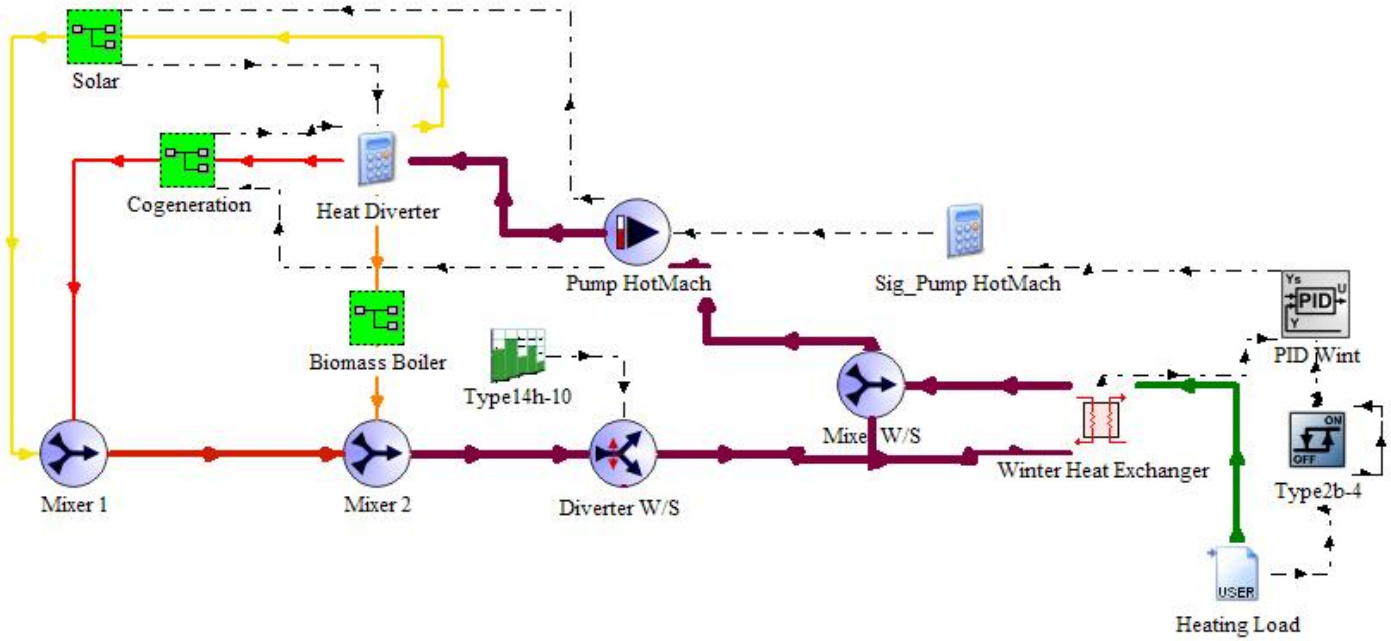

Figure 5.2 TRNSYS deck: focus on the heat facility

Please note, the “Pump_HotMach” is a virtual pump: it is only used for an easy identification of the total flow in the overall heat faciliy and for the next EQUATION named “Hot Diverter”. This EQUATION sets the flow mass to:

1. the solar tank, after that the temperature at the top of the tank has been checked to be at least 10°C degrees higher than the one returning from the load;
2. the cogenerator tank, after that the temperature at the top of its tank has been checked to be at least 10°C higher than the one returning from the load;
3. the biomass boiler.

The selected hierarchy gives the priority to the solar energy, whenever it is available at the selected temperature. In fact, once the temperature in the top of the tank is higher than the outlet hot temperature of the winter heat exchanger, solar energy is exploited depending on the required flow (reqflow), determined by the “PID wint”, according to:

$$\begin{aligned} \text{solflow} = \text{le}(\text{solav}, \text{reqflow}) * \text{solav} + \\ \text{gt}(\text{solav}, \text{reqflow}) * \text{reqflow} \end{aligned} \qquad 5.1$$

where “solav” is the nominal flow rate which can be drawn out of the solar tank. The second heat source to be involved in the operation is the cogenerator tank. However in this case, beside the temperature in the top of the tank is checked by an on/off controller (output signal cogav1), the required flow is compared to a certain minimum flow. This minimum amounts to 30% of the nominal flow rate which can be drawn out of the cogenerator tank, according to the typical minimum flow rate of variable speed pumps. The “Heat Diverter” compare the flow needed, named flowtocog, which derives from:

$$\text{flowtocog} = \text{reqflow} - \text{solflow} \qquad 5.2$$

to the minimum flow for the cogenerator tank, according to the following instruction:

$$\begin{aligned} cogflow = cogav1 * (lt(flowtocog,0.30MCog) * 0 + \\ ge(flowtocog,0.30MCog) * le(flowtocog,MCog) * \\ flowtocog + gt(flowtocog,MCog) * MCog) \end{aligned} \quad 5.3$$

being cogflow the actual flow from the cogenerator tank and MCog is the nominal flow rate (see Table 3.13).
The reqflow amount which can not be heated up by the solar tank, not even by the cogenerator tank, is addressed to the boiler according to:

$$heatflow = reqflow - solflow - cogflow \quad 5.4$$

According to this hierarchy, for certain ranges of the "reqflow" it can be possible that solar fraction gets only assisted by the biomass boiler.
After the flows have been elaborated in each macros, they are mixed in ttwo TEE PIECE types here named "Mixer 1" and "Mixer 2".

5.2.2 The "Solar" macro

The Solar macro in Figure 5.2 TRNSYS deck: focus on the heat facility, includes the secondary solar loop and another macro for the primary solar loop macro which is shown in Figure 5.3.
The WEATHER DATA type simulates the weather conditions of Bolzano according to an internal database. This type outputs different variables which are mostly given as inputs to the VTC (Vacuum Tube Collector) type, such as the ambient temperature, the solar radiation for tilted surface, the angle of incidence etc. On the other hand, the ambient temperature is also given as inputs to the "OutPipe" which represents the external pipes and it can be used to calculate the heat losses in the primary loop.
As far the VTC standard type is concerned, performance coefficients are required. Thus, a specific model of VTC has been selected among the listed models in Its technical specifications are reported in the table 1.

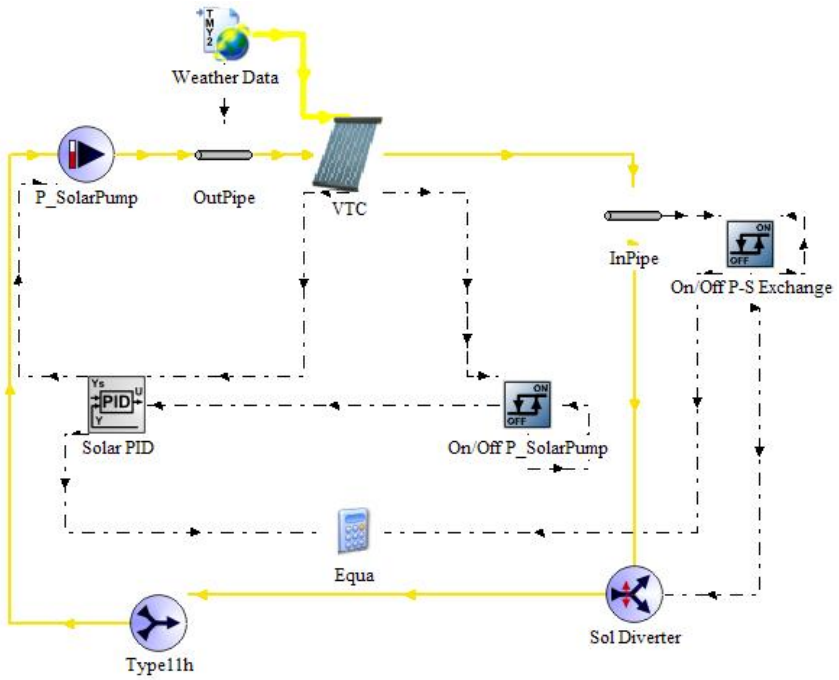

Figure 5.3 Primary solar loop

Table 5.1 Major data of the model for VTC which has been selected in [20]

Solar collector factsheet	SPF-Nr.C601
Model	Mazdon 20 - TMA 600S
Manufacturer	Thermomax Ltd
Glycol rate	33,3%
Glycol density (15°C)	1127 kg/m³
Density acqua	1000 kg/m³
Coefficient 1	-2.772 kJ/hr m² K
Coefficient 2	0.01548 kJ/hr m² K²

The control strategy on the primary solar loop includes the "On/Off P_SolarPump" connected to the "Solar PID" to regulate the mass flow in the circuit and the "On/Off P-S Exchange" to control the heat transfer from the primary to the secondary solar loop.
The "Solar PID" outputs a signal which regulates the mass flow in "P_ SolarPump" so that the outlet fluid temperature of the solar collectors achieves

the set value. This value depends on the temperature levels required by the distribution systems, thus on the operation mode. A set point of 55°C has been chosen to provide heat at 40°C for radiant panels during winter, whereas a set point of 95°C has been selected to supply the heat driven cooling with heat at 90°C. The signal output is included in the range [0.3; 1], thus the flow mass will be in the range of 30%-100% of the nominal flow rate (the minimum value has been selected according to the literature on the variable speed pump; it will be kept into account also for other pumps PID controllers). The PID is switched on by the"On/Off P_SolarPump". This controller generates a control function that can have a value of 0 or 1 depending on the temperature sensed in the collectors and on the set band gaps. The on-off controller compares the collectors temperature with an absolute temperature (20°C in winter and 60°C in summer) to switch on or off the pump on the primary solar loop. Comparing the collectors temperature with selected absolute (and not relative values) avoids transient during early morning or late afternoon. The controller works sensing the temperature, thus avoiding fast radiation changes, even if it will make the pump run also when the temperature is lower than the requested one (but the selected values and bands make that to rarely happen).

The OnOff P-S Exchanger in Figure 5.3, allows the stream to bypass or not the heat exchanger between the primary and the secondary loop which is shown in Figure 5.4. The controller outputs 1 when the temperature at the outlet of the solar collectors is higher of the temperature in the top of the solar tank at least of 5 °C and it is switched off when the two temperatures are equal.

The "Equa" in Figure 5.3 multiplies the signal outcome from the OnOff P-S Exchanger and the one from the "Solar PID" to output a signal for the variable speed pump to be regulated on the secondary loop (S-Pump in Figure 5.4). In this way the "S-Pump" follows the "P-Solar_Pump". So, the higher the heat collected is, the more the tank is charged.

The "On/Off SolTank" for the tank to be discharged is also shown in Figure 5.4. As said before, its signal is used to switch on the "Sol-Pump" depending on the temperature gap with the top of the tank and the return temperature. As already said, the flow mass in the "Sol-Pump" depends on the "Heat Diverter" (subchapter 5.2.1).

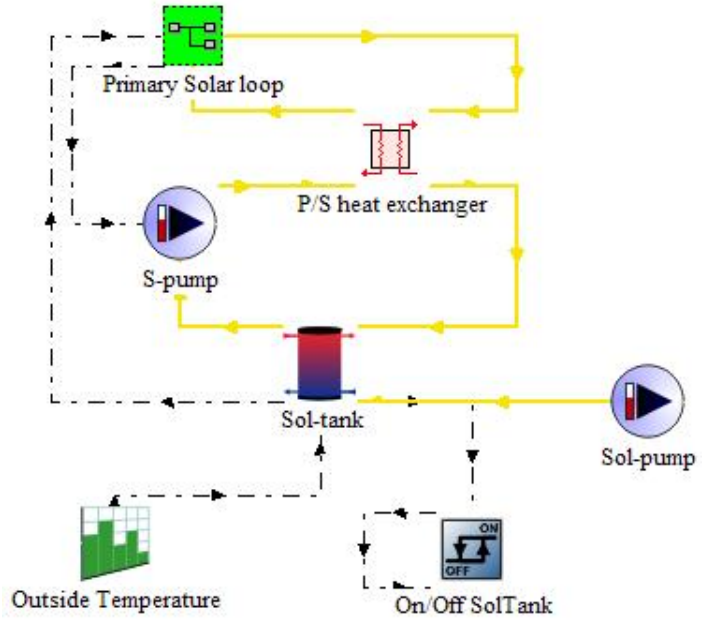

Figure 5.4 Secondary solar loop

5.2.3 The "Cogeneration" macro

The cogeneration macro is shown in Figure 5.5.
The "OnOff CogTank" senses the temperature in the top of the cogenerator tank and compares it with the one coming from the load. It discharges the tank if the temperature gap is at least higher then 10 degrees in winter and 6 degrees in summer. The flow elaborated by the "Cog Pump" is set in the "Heat Diverter" as said in subchapter 5.2.1).
The On/Off controller 2b-10, senses the temperature in the top of the tank and compare it to the set temperature in summer and in winter, 90 and 48 respectively. As the temperature in the top of the cogenerator tank is 4 degrees lower than the set points at least, the constant speed "C-pump" is switched on and the engine as well.

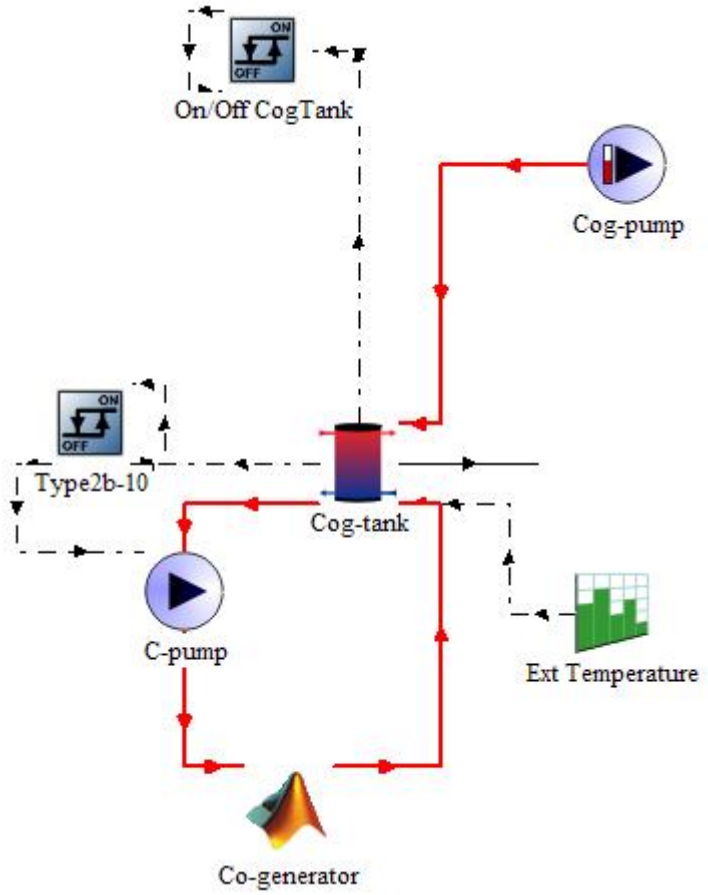

Figure 5.5 Cogeneration unit macro

5.2.4 The "Biomass Boiler" macro

The biomass boiler macro is shown Figure 5.6. It includes the "BH-pump" which receives the mass flow set by the "Heat Diverter" according to the sub chapter 5.2.1 and directs it towards the "Biomass Heater". The heater will supply with as heat as the stream needs to reach the winter and summer set temperatures (48°C and 90°C respectively).

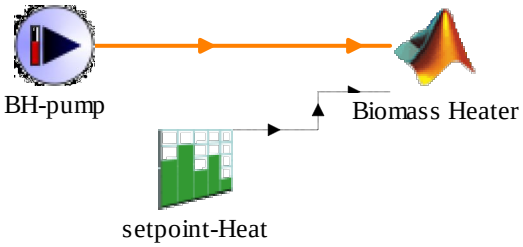

Figure 5.6 The Biomass Heater macro

5.3 Cooling Facility Simulations

The term “Cooling Facility” refers to the part of the energy system which supplies the users with cold. It mainly includes two macros:

1. the absorption cooling;
2. the auxiliary cooling.

The connection between the single parts and their control strategy are described below.

5.3.1 The cooling mode

The “EURAC Cooling Load” (Figure 5.7) includes the cooling flow mass demand of the building which derives from the “LOAD” sheet of the excel file about the sizing procedure.
An On-Off controller discriminates the range of flow mass demand which requires the cooling facility to be put into operation. The minimum cold energy to be supplied has been selected by observing the trend of the EURAC cooling demand and by identifying the minimum step.
A PID controller outputs a signal which regulates the flow mass in the cold side of the summer heat exchanger: it sets the flow mass (ReqMchill) to be cooled by the chillers up to 5.3°C in order to supply users with 8°C cold water, the inlet temperature being 13°C.

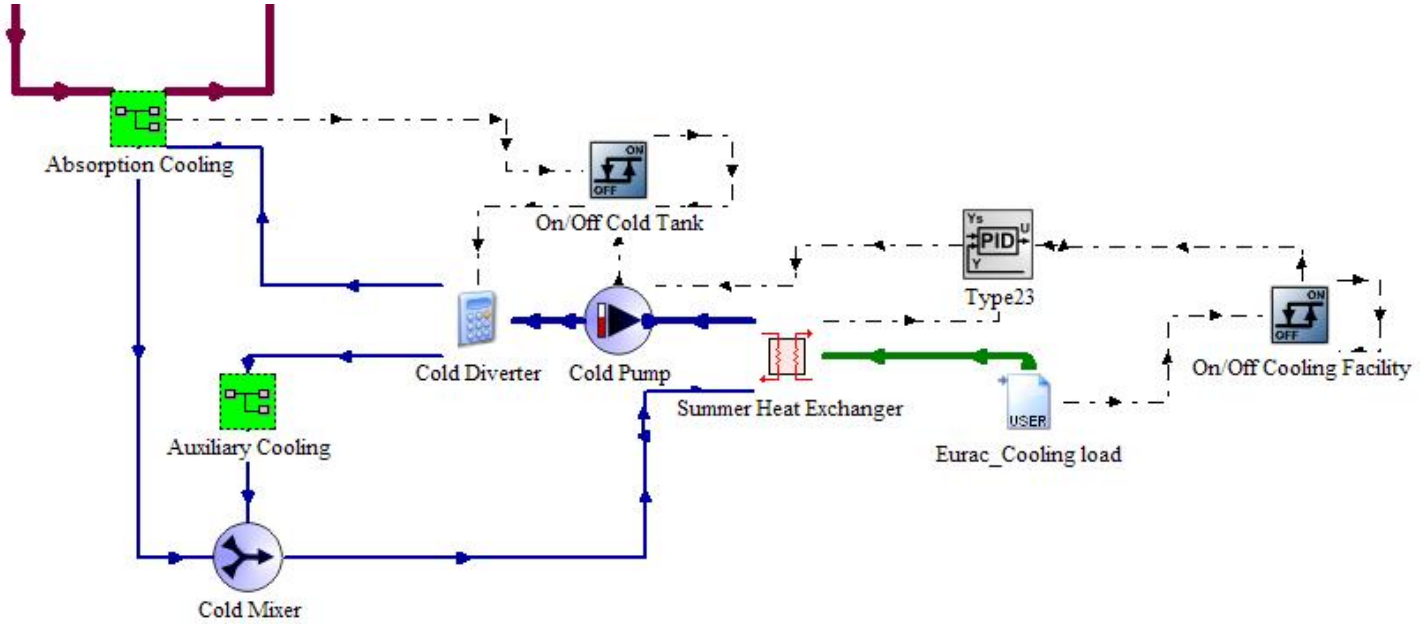

Figure 5.7 Cooling Facility

The “Cold Diverter” EQUATION acts as the “Heat Diverter” of the heat facility. It diverter set the flow rate to be cooled by the absorption machine and the one to be cooled by the compression chiller. For the absorption chiller a minimum flow to be elaborated (minMchill) has been set. This minimum amount has been set at 30% of the nominal rate.
The auxiliary cooling device is supposed to cover the left demand. On one hand, the “Cold Diverter” compares the minimum possible flow for the absorption chiller (minMchill) with the one required (ReqMchill). The latter is calculated by the type 23. On the other hand, it receives an input from an on/off controller which senses the temperature in the bottom of the tank. If this temperature is below the temperature coming back from the distribution system, 2 degrees at least, then cold flow can be pumped from the tank to the users (CtankOn=1), according the equation:

$$\begin{aligned} FlowToAbs = {} & CtankOn * (lt(ReQMchill, minMchill) * 0 + \\ & ge(ReqMchill, minMchill) * le(ReqMchill, mchill\_hr) * \\ & ReqMchill + gt(ReqMchill, mchill\_hr) * mchill\_hr) \end{aligned} \qquad 5.5$$

Afterward, the flow to the auxiliary cooling is calculated:

$$FlowAux = ReqMchill - FlowToAbs \qquad 5.6$$

Both the flows are mixed into the “Cold Mixer” TEE-PIECE type.
The cooling facility includes two macros: “Absorption Chiller” and “Auxiliary Cooling”.

5.3.2 The “Absorption Cooling” macro

When the “On/Off cold tank” (Figure 5.7) outputs 1 and the cooling demand is higher then the minimum flow for the absorption chiller, the “CTank Pump” (Figure 5.8) is switched on and its flow rate is set at “FlowToAbs”, $FlowAux = ReqMchill - FlowToAbs$ 5.6. Hence, the “CTank Pump” regulates the discharging of the tank under its external temperature varying with the season (type “Environmental Temperature).
The equation “On/Off ABS” controls the absorption chiller and outputs a signal depending on the temperature at the top of the tank (controlled by the Type 2b-6)

and on the operation mode (Type 14b-3 outputs 1 when the cooling mode is required).

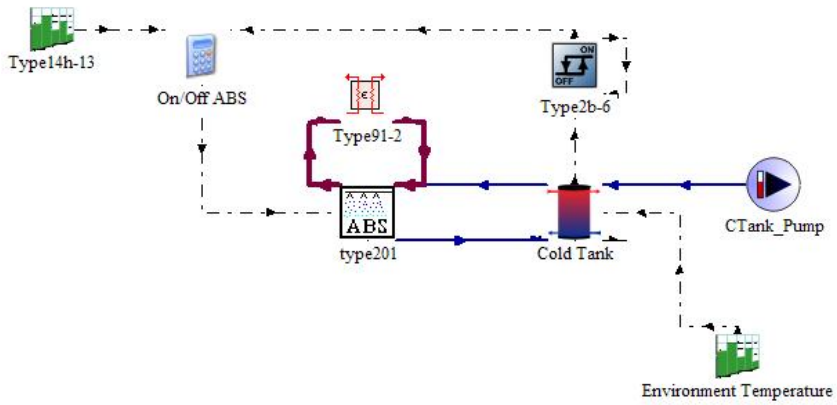

Figure 5.8 ”Absorption Chiller” macro

When the model for the absorption chiller which is used in the simulations was developed, it was not foreseen to run under variable flow masses [7]. In fact, this model only simulates the off-design conditions due to inlet temperature changes. Under inlet mass flows different from the nominal ones but constant inlet temperatures, the absorption chiller reacts with too large temperature gaps. For instance, under the minimum mass flow set for the absorption tank, the temperature outlet the generator can also be near 0°C.
An expedient was needed to use the same model also under mass flows changes. First of all, constant flows have been set between the absorption chiller and the cold tank. Secondly the virtual heat exchanger “Type91-2” (constant effectiveness=1) has been included in the simulations to separate the mass flow entering the generator of the absorption chiller and the mass flow coming from the heat generators. In this way, the hot flow entering the absorption chiller is kept constant, whereas the one in the heat generators can be varied. To this end, it has been necessary to find out an equation for the regulation of the flow in the heat facility. Such equation had to comply with the following need: finding out the mass flow to be heated up to the summer set temperature (90°) by the heat facility so that chilled water is produce at the set temperature (5.3 °C).
To this end, the model created by Nurzia [18] has been used to generate en equation which correlates the hot flow temperature Thin entering the generator to the flow temperature entering the condenser Tcon The goal was to identify the needed Thin to produce 5.3°C cold water, under different Tcin.

$$Thin = 7.0942 \cdot Tcin + 19.034 \qquad 5.7$$

Once Thin is identified at each time step of the simulation, the mass flow to be circulated in the heat facility, i.e. in the hot side of the virtual heat exchanger in Figure 5.8, is regulated in order to heat the mass flow entering the generator of the absorption chiller up to Thin. In this way, the model still receives constant flows but the hot mass flow regulation is achieved. Further more, as the effectiveness of the virtual exchanger has been set at 1, the temperature of the flow to be heated up in the heat facility is the same as the temperature outgoing the generator the absorption chiller. So, the results obtained by using such expedient should not be so far from the case of an absorption chiller with regulation of the hot mass flow.
The regulation of the hot flow in summer time is controlled by the by the EQUATION “ABS Tset” which, according to the equation 5.7 sets:

$$\begin{aligned} Thin = {} & le(tcin,8) * 75 + gt(tcin,8) * lt(tcin,10) * \\ & (7.0942 * tcin + 19.034) + ge(tcin,10) * 90 \end{aligned} \qquad 5.8$$

This temperature represents a set temperature for the “PID summ” which identifies the flow to be circulated in the “PumpHot Mach”. The “Sig_Pump HotMach” simply receives the signal output by the “PID sum” in summer, and by the “PID wint” in winter, and passes it to the “Pump HotMach”. The entire flow is then distributed to the single heat generators according to the subchapter 5.2.
In the cooling mode, the Diverter W/S receives the signal 1 from the Type 14h-10 and the hot flow enters the absorption chiller and not the winter heat exchanger. Then the outlet hot flow goes to the “Mixer W/S”.

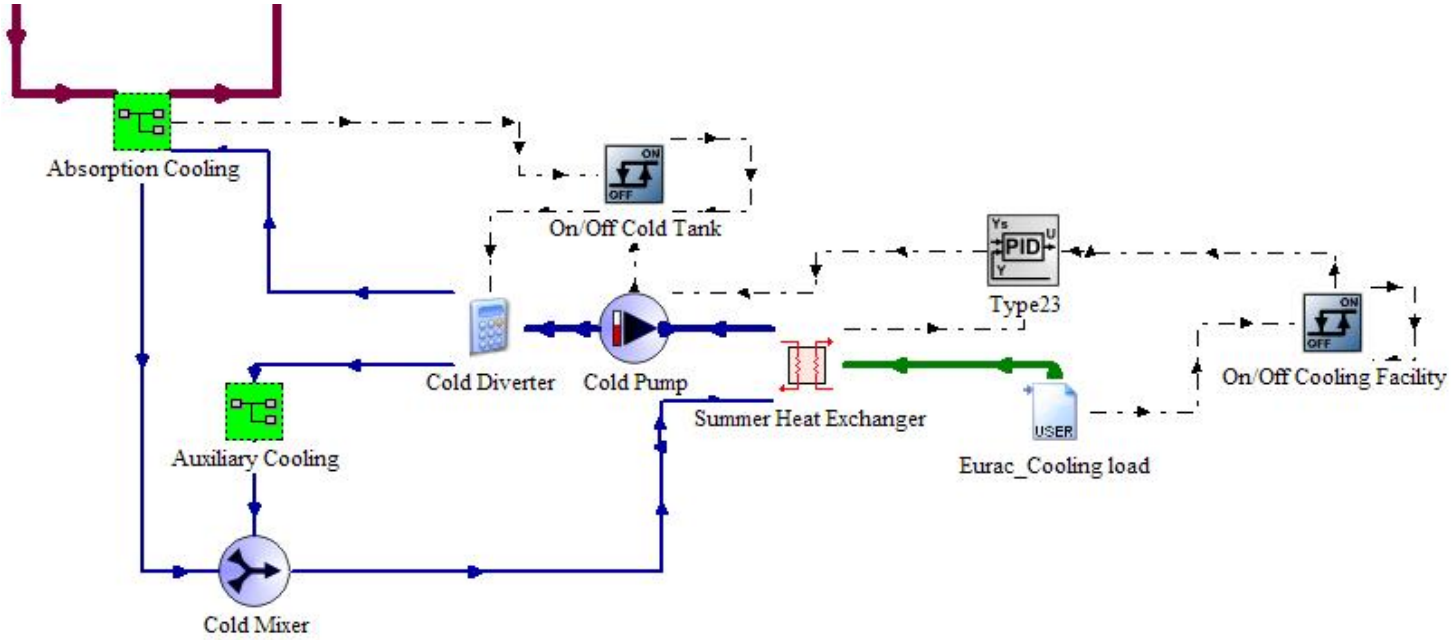

Figure 5.9 Connection between the heat facility and the cooling facilit

5.3.3 The "Auxiliary Cooling" macro

Type 92 has been used to simulate an auxiliary cooling. It does not specifically simulate a compression chiller but simply models a device which cools down the entering stream, in this case the "AuxFlow" (Equation 5.5), to a desired temperature (5.3°C). For subsequent calculations, it is supposed that this type consumes electricity with a COP equal to 3. As such value is typical of compression chillers, the AUXILIARY COOLING type is referred to as compression chiller.

Figure 5.10 The "Auxiliary" Cooling macro

5.4 Simulations Plots

Some plots of the simulations are shown in Figure 5.11 through Figure 5.14. The first two figures report the typical simulations plots for the heating mode, whereas the last two figures report the typical simulations plots for the cooling mode.

Figure 5.11 shows the mass flows and the temperature in the heat exchanger between the heat facility and the winter distribution system. MUseWint is the mass flow in the distribution system which needs to be heated up from 30 °C to 40°C. Mheating is the hot mass flow circulating in the heat facility. It enters the heat exchangers at c.a. 48°C (Theatingin) in order to supply the users with around 40°C (TUseWInt).

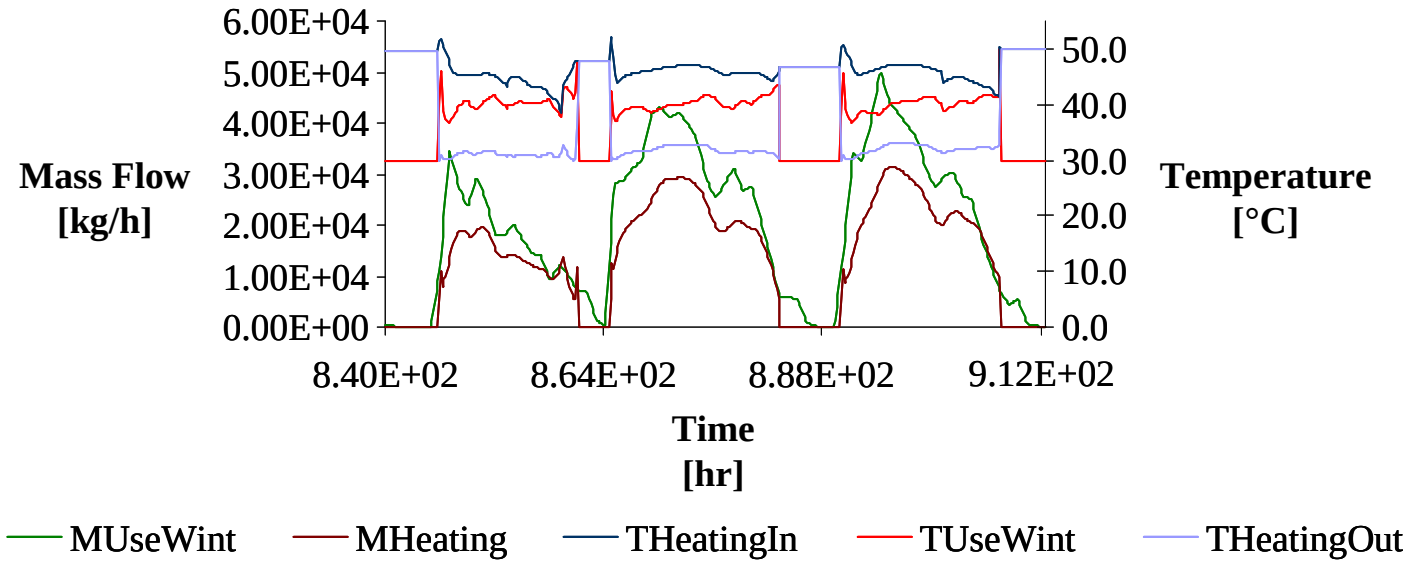

Figure 5.11 Simulations of some day of operation in the heating mode: focus on the winter heat exchanger between the heat facility and the winter distribution syystem.

Figure 5.12 shows the contribution to Mheating and Theating from each heat generator, i.e. the mass flow from the solar tank “Solar”, the cogenerator tank “Cogen” and the biomass boiler “Biomass” and their temperatures (TSolar, TCogen and Tbiomass respectively). The TTbeIncreased represents the temperature entering the two tanks and the biomass boiler, ie. the temperature returning from the heat exchanger with the winter distribution system named Theatingout in Figure 5.11. Please note that the biomass boiler produces exactly 48°C according to the set temperature for winter heat production whereas the flow from the cogenerator is a little bit colder. The control on the top temperature of the cogenerator tank has a band which allows the flow to be already drawn out at 45° C, in order not to be to restrictive around the set point which could lead to repetitive switching on/off of the controller.
Figure 5.12 also shows that the solar contribution that is null for some hours of the first and third day and for all the second day. In fact, flow is drawn out of the solar tank only when the latter top temperature is 10 °C higher than the one returning from the load (TToBeIncreased).
Figure 5.13 shows a typical summer operation day. It focuses on the heat exchanger between the cooling facility and the summer distribution system. MuseSum is the mass flow which circulates in the summer distribution system and needs to be cooled down up to 8°C.Mcooling is the mass flow in the cooling facility which enters the summer heat exchanger at around 5.3 °C (TcoolinIn) to supply users with 8°C (TuseSum). It is reminded that this simulated configuration includes 355 kW absorption chiller and no compression chiller (refer to the subchapter 3.3 about the application of the sizing procedure to the EURAC case): Hence Mcooling represents the flow drawn out of the cold tank.

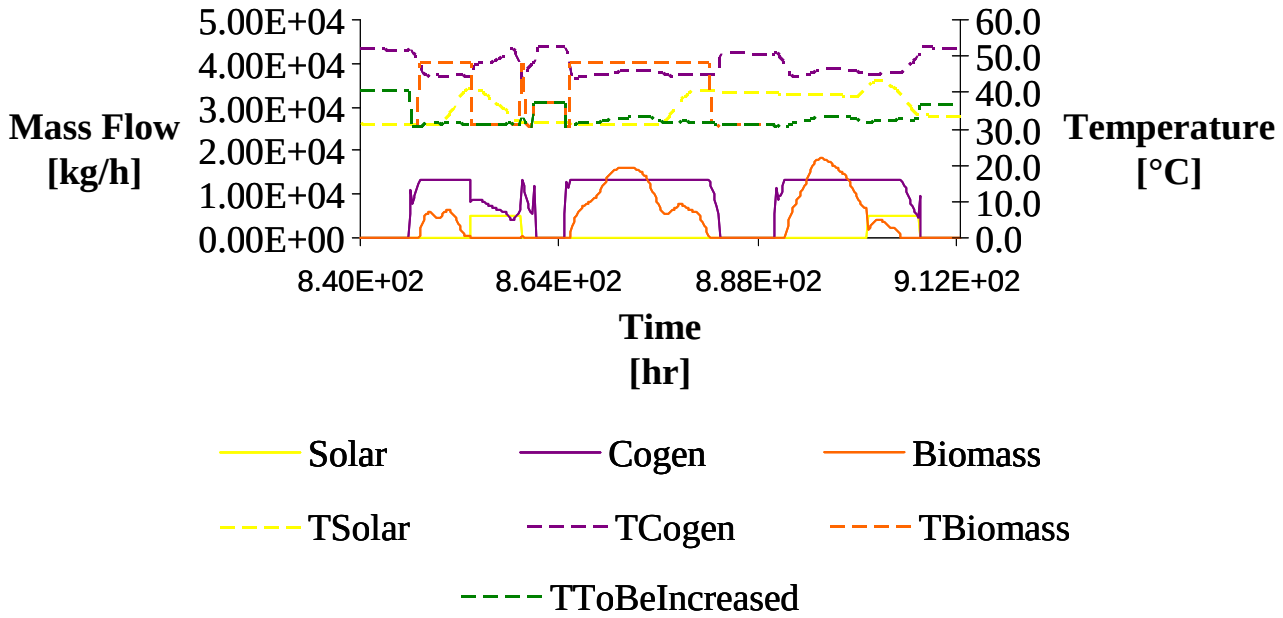

Figure 5.12 Mass flows and outlet temperatures of each heat generator in the heating mode

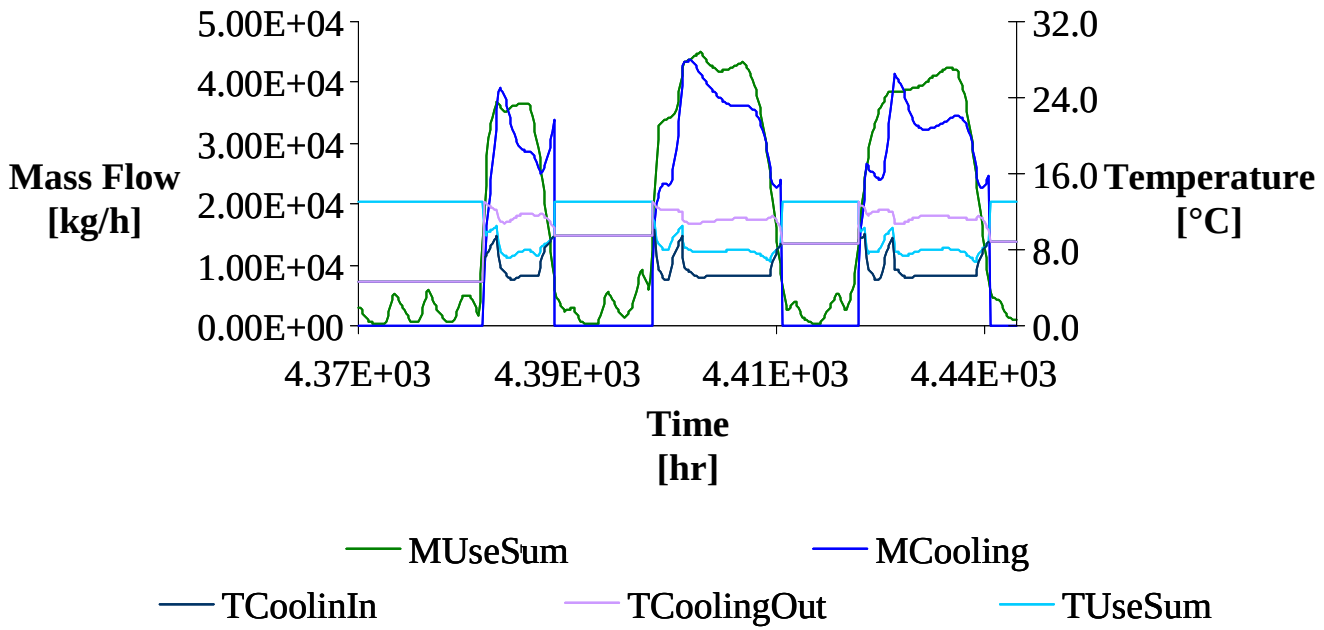

Figure 5.13 Simulations of some day of operation in the cooling mode: focus on the summer heat exchanger between the cooling facility and the summer distribution system.

Figure 5.14 shows the cold water temperature at the outlet of the condenser of the absorption chiller (TChillingOut). As this temperature goes below 5°C, the absorption chiller does not need hot flow mass anymore, i.e. it is switched off. Thereby, Solar, Cogen and Biomass flows disappear, whereas Mcooling is still drawn out of the cold tank because its temperature is still in a range suitable to the users. When the cold tank temperature reaches 10°C, it is cooled down again and hot flows are required by the absorption chiller one more time. Such instalbility is mainly due to the large size of the absorption chiller and could be avoided with to large volume of the solar tank

Figure 5.15 shows the Solar, Cogen and Biomass mass flows and their temperatures Tsolar Tcogen and Tbiomass. Also in this figure it can be seen that solar contribution is null for the first two days and some hours of the 3rd day. In fact flow is drawn out of the solar tank only when the latter top temperture is at least 5°C higher than the temperature returning from the desorber of the basorption chiller (ToutDesorber). It can also be seen that the hot water temperature produced by the biomaas boiler is excatly the winter set temperature whereas the temeprature of the flow coming from the cogenerator can also be some degrees colder.

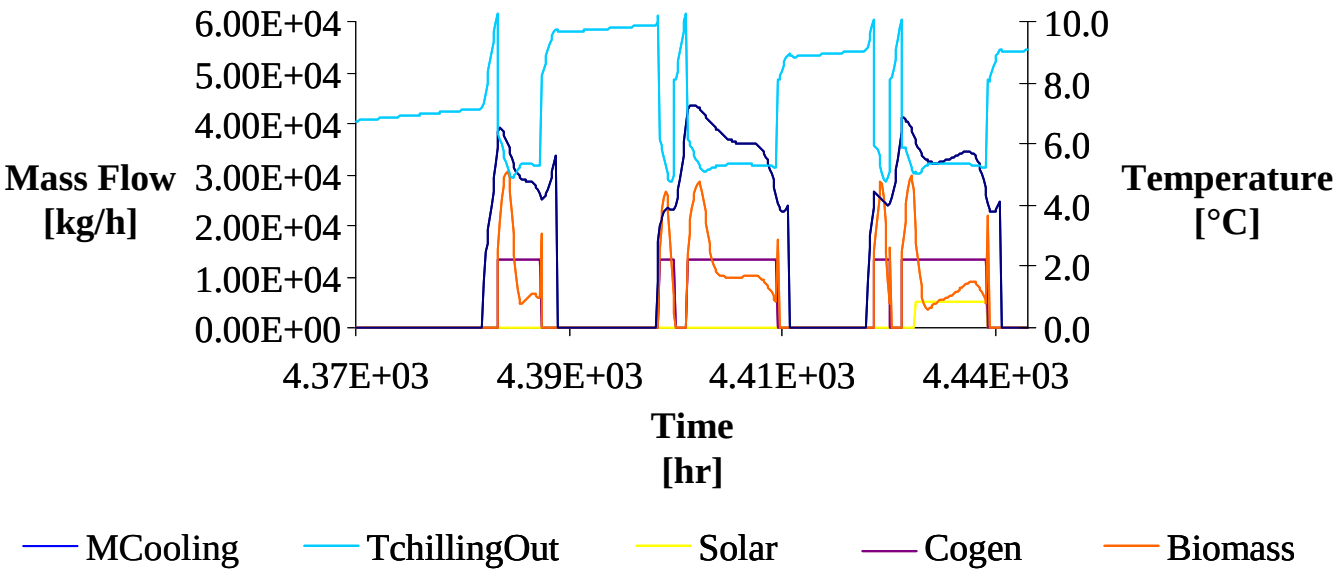

Figure 5.14 Beahviour of the heat generators in the cooling mode

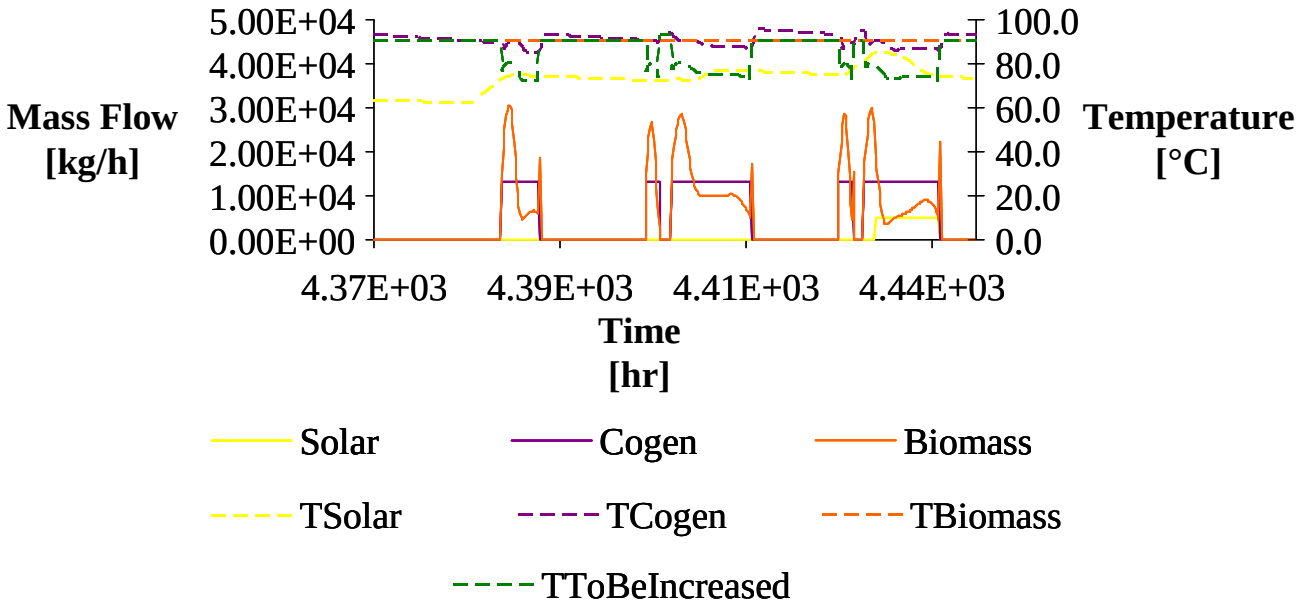

Figure 5.15 Mass flows and temperatures produced by the heat generator in the cooling mode

6 Optimization Procedures by Means of TRNSYS Simulations

6.1 Introduction

In chapters 2 and 3, a trigeneration system combined with solar thermal technology has been designed from three points of view: layout, control strategy and sizes. In chapter 5, the project has been translated into a TRNSYS deck which simulates the operation of the entire plant along one year at off-design conditions. The simulations can be used to assist the design process itself, in particular the control strategy definition and the sizes selection. In fact, by simulating different components' sizes under different control strategies, it is possible to find out the configuration which can lead to the minimum fuel consumption or to the lowest operation costs or rather to the smallest amount of CO_2 emissions.
Such an approach has been applied to identify the optimal size for the major components of the designed plant under the energy demand of the EURAC building. This optimization process needs the sizing procedure (Chapter 3) to be continuously repeated. For instance, whenever a new size is selected for the absorption chiller or the cogenerator, the sizes of all components related to them, such as the compression chiller, the biomass boiler, the pumps and so on, have to be modified too. As the sizing procedure is able to automatically recalculate the size of each component, it is continuously used to generate new configurations to be simulated. In practice, it is enough to change one factor in the "Load" sheet (Sub chapter 3.2.1) of the sizing excel file to generate a new "Outputs" sheet (Sub chapter 3.3.9) which gives the values to be entered into the TRNSYS deck and simulated. Thereafter, at the end of each simulation, three analyses are carried out:

- Primary Energy Consumption analysis;
- Operation Costs analysis;
- CO_2 emissions analysis.

The goal of each analysis is to identify the configuration which respectively leads to low PEC/OC/CO_2 compared with a conventional system. A detailed description of the methodology used to assess the quality of each simulated configuration is presented in the following subchapter.

The optimization process presented in this chapter mainly concerns the absorption chiller and the cogenerator, as such components have resulted to play a crucial role in the overall performance of the plant since the first simulations.

6.2 PEC, OC & CO_2 Analysis: Hypotheses and Approach

The PEC, OC and CO_2 analysis take into account on one hand the energy resource consumption of the cogeneration unit, biomass boiler and compression chiller (please note, the energy consumption of the absorption chiller is included in the one of the cogeneration unit and the biomass boiler), on the other hand the free heat supply due to the solar collectors.
As EURAC hourly electricity demand is missing, it is not possible to identify how much of it is purchased from the grid or provided by the cogeneration unit. However, the bills show a very large electricity consumption in the building (1 million kWh_{el}), so that two hypotheses can be assumed:

1. the electricity consumption of the compression chiller is acquired by the local grid;
2. the electricity produced by the engine is totally used in house and not sold to the grid (as it is in the reality).

The PEC of each machine is accounted in kWh_{th}. The PEC of the cogeneration unit and the biomass boiler are directly calculated by the models presented in chapter 5, while the electricity consumption of the compression chiller is converted into heat consumption on the basis of the electrical efficiency declared by the Italian grid (40% [25]).
Under these hypotheses the PEC of the examined system is given by:

$$PEC_{ExamS} = PEC_{Cog} + PEC_{BioHeat} + PEC_{ComprChill} \qquad 6.1$$

The conversion of the PEC into gas volumes and biomass kilos is based on the following LHV:

$$LHV_{Gas} = 9.45 \quad \frac{kWh}{m^3_{Gas}} \qquad 6.2$$

$$LHV_{Chips} = 3.40 \quad \frac{kWh}{kg_{Chips}} \qquad 6.3$$

Regarding the CO_2 emissions two approaches have been used:

1. On one hand the examined system has been considered CO_2 neutral. This approach is effective for cases, as far as EURAC, which biomass supply chain can be considered short[8].
2. On the other hand a CO_2 emissions rate EmR_{Bio} of 1.8 kg/kg_{Bio} has been calculated according to [23].

So, under the 1st approach the examined system emits:

$$CO_{2_{ExamS}} = CO_{2_{Gas,Cog}} + CO_{2_{kWh_{el},ComprChill}} \quad 6.4$$

whereas under the 2nd approach it emits:

$$CO_{2_{ExamS}} = CO_{2_{Gas,Cog}} + CO_{2_{Bio}} + CO_{2_{kWh_{el},ComprChill}}$$

being

$$CO_{2_{Gas,Cog}} = V_{Gas,Cog} \cdot EmR_{Gas} \quad 6.5$$

$$CO_{2_{kWh_{el},ComprChill}} = kWh_{el,ComprChill} \cdot EmR_{Grid} \quad 6.6$$

$$CO_{2,Bio} = M_{Bio} \cdot EmR_{Bio}$$

and

$$EmR_{Gas} = 1.69 \frac{kg_{CO_2}}{m^3_{Gas}} \quad 6.7$$

$$EmR_{Grid} = 0.47 \frac{kg_{CO_2}}{kWh_{el}} \quad 6.8$$

As to OC of the examined system, they can be calculated as follows:

[8] DECRETO 18 dicembre 2008:Incentivazione della produzione di energia elettrica da fonti rinnovabili, ai sensi dell'articolo 2, comma 150, della legge 24 dicembre 2007, n. 244.

$$OC_{ExamS} = C_{Gas} * V_{GasCog} + C_{Biomass} * M_{Biomass} + C_{Grid} * kWh_{el,ComprChill} \quad 6.9$$

being:

$$C_{Gas} = 0.34 \ \frac{€}{m^3}^{9} \quad 6.10$$

$$C_{Biomass} = 0.07 \ \frac{€}{kg} \ [22] \quad 6.11$$

$$C_{Grid} = 0.149 \ \frac{€}{kWh_{el}} \ [25] \quad 6.12$$

The examined system is compared to a reference system RS which is based on:

- a gas boiler for heating purposes;
- a compression chiller for cooling purposes;
- and the local electrical grid.

The examined and the reference system are compared assuming that the reference system provides with as much energy as the examined system does. Under this hypothesis, the PEC of the reference system results to be:

$$PEC_{RefS} = PEC_{GasHeat} + PEC_{Compr,Chill} + PEC_{kWhel,ExamS}^{10} \quad 6.13$$

The CO_2 emissions are:

$$CO_{2RefS} = CO_{2Gas,Boil} + CO_{2kWh_{el},ComprChill} + CO_{2kWh_{el},ExamS} \quad 6.14$$

The OC amounts to:

[9] EURAC bills 2006-2007

[10] kWhel,ExamS refer to the electricity production due to the cogeneration unit in the examined system which in a reference system should be acquired by the grid.

$$OC_{RefS} = C_{Gas} * V_{GasHeat} + C_{Grid} * (kWh_{el,ComprChill} + kWh_{el,ExamS}) \quad 6.15$$

The LHV, the specific costs and the specific emission rates used for the reference system have been supposed to be equal to the ones used for the examined system (equations 6.2, 6.3, 6.7, 6.8, 6.10, 6.11 and 6.12). For the PEC due to the electricity consumption, 40% electrical efficiency is considered, whereas for the PEC due to the gas consumption, 90% thermal efficiency of the boiler is supposed.
To compare the examined and the reference systems the following variables are calculated:

$$PEC_{Saved} = PEC_{RefS} - PEC_{ExamS} \quad 6.16$$

$$CO_{2\,Saved} = CO_{2\,RefS} - CO_{2\,ExamS} \quad 6.17$$

$$OC_{Saved} = OC_{RefS} - OC_{ExamS} \quad 6.18$$

These factors are calculated for each i-th simulation in order to find out the maximum PEC, OC and CO_2 savings according to:

$$\max_{i=1:N} PEC_{saved_i} \quad 6.19$$

$$\max_{i=1:N} CO_{2\,saved_i} \quad 6.20$$

$$\max_{i=1:N} OC_{saved_i} \quad 6.21$$

being N the total number of carried out simulations.

6.3 Optimization of the Absorption Chiller Size

The first parametric study which has been developed has concerned the absorption chiller. Various simulations have been carried out with different size of the absorption and compression chillers.

The parametric study has been firstly carried out under the control strategies already set in the TRNSYS deck, named “Abs. Priority” (see also Chapter 2). Under this control strategy, the absorption chiller is involved in the operation to meet the cooling demand up to its maximum cooling capacity, so that the compression chiller matches the peak demand. The equations included in the “ColdDiverter” are:

$$\begin{aligned}\mathrm{FlowToAbs} = \mathrm{CtankOn} \cdot (\mathrm{le}(\mathrm{ReqMchill}, \mathrm{mchill\_hr}) \cdot \\ \mathrm{ReqMchill} + \mathrm{gt}(\mathrm{ReqMchill}, \mathrm{mchill\_hr}) \cdot \mathrm{mchill\_hr})\end{aligned} \quad 6.22$$

$$\mathrm{FlowToAux} = \mathrm{Re\,qMchill} - \mathrm{FlowToAbs} \quad 6.23$$

Thereafter, two further control strategies have been implemented and tested:

1. “Compr. Priority”: the compression chiller is involved in the operation to meet the overall cooling demand up to its maximum cooling capacity, so the absorption chiller only matches the peak demand. In this case the control executed by the “Cold Diverter” is expressed by the following equations:

$$\begin{aligned}\mathrm{FlowToAux} = \mathrm{le}(\mathrm{Re\,qMchill}, \mathrm{mchillCompr}) * \mathrm{Re\,qMchill} + \\ \mathrm{gt}(\mathrm{Re\,qMchill}, \mathrm{mchillCompr}) * \mathrm{mchillCompr}\end{aligned} \quad 6.24$$

$$\mathrm{FlowToAbs} = \mathrm{CTankOn} * (\mathrm{Re\,qMchill} - \mathrm{FlowToAux}) \quad 6.25$$

2. “Compr/Abs Threshold”: the absorption chiller is involved in the operation only when the cooling demand is included in the range [30%, 100%] of its maximum cooling capacity. In this case, the compression chiller can match the base and the peak cooling demand. The equations included in the “ColdDiverter” are:

$$\begin{aligned}\mathrm{FlowToAbs} = \mathrm{C\,tan\,kOn} * (\mathrm{lt}(\mathrm{Re\,qMchill}, \mathrm{min\,Mchill}) * 0 + \\ \mathrm{ge}(\mathrm{reqMchill}, \mathrm{min\,Mchill}) * \mathrm{le}(\mathrm{Re\,qMchill}, \mathrm{mchill\_hr}) * \\ \mathrm{Re\,qMchill} + \mathrm{gt}(\mathrm{Re\,qMchill}, \mathrm{mchill\_hr}) * \mathrm{mchill\_hr})\end{aligned} \quad 6.26$$

$$FloAux = ReqMchill, FlowToAbs \quad 6.27$$

Table 6.1 lists the values of the major parameters 11 per each simulated configuration[12]. The results of the parametric studies related to the only summer operation[13] are reported in the next subchapters.

Table 6.1 Selected sizes of the absorption and compression chiller per simulation.

Simulations	Qevanom [kW]	QcomprNom [kW]
1st Run	330	0
2nd Run	300	27
3rd Run	250	78
4th Run	200	128
5th Run	150	178
6th Run	100	228
7th Run	50	279

6.3.1 "Abs. Priority" control strategy

As the size of the absorption chiller is decreased, its contribution to the overall cooling demand decreases too, as shown in Figure 6.1, except in the range [330, 250] kW where the cooling demand is practically only matched by the absorption chiller. This is due to the fact that high cooling requirements occur very few times during the simulated year, so the cooling produced by the compression chiller is nearly zero.

Obviously, as the size of the absorption chiller is decreased, its heat demand decreases too with almost the same trend of its falling cooling production, as shown in Figure 6.2. Actually, as the size approximates 250 kW, the absorption chiller better tracks the cooling demand, the on/off behaviour is smoothed and

[11] Other parameters include the cold tank volume, the pump flow rates and so on according to the sizing procedure.

[12] Not all of the listed configurations are carried out for each control strategy, e.g. it would no make sense to use 330 kW absorption chiller under the "Compr. Priority" control strategy.

[13] As in this first optimization process, no variables related to the heat generators are changed, the winter operation give the same results in all the simulations.

the performance increases. Consequently, its heat demand is better fitted to the range guaranteed by the cogeneration unit (30% of the nominal flow from the tank) which gives its maximum contribution at 250 kW absorption chiller size.
As the size of the absorption chillers is further reduced to 50 kW, the heat demand of the absorption chiller becomes so small that it goes below the range guaranteed by the cogeneration tank. Thus, the boiler is forced to supply most of the heat demand (Figure 6.2).

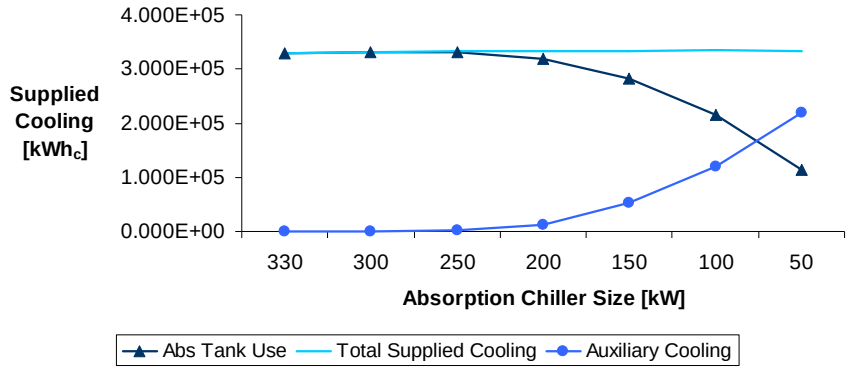

Figure 6.1 Total cooling supply and cooling supplyed by each chiller under the ”Abs. Priority” control strategy

Solar fraction amounts to 6% of the total heat supply in all the simulations except in the last two ones where it is around 8% and 14%. On the other hand, the cogeneration unit contribution grows from 50% of the heat demand in the first case to 60% of the heat demand in the second-last case.

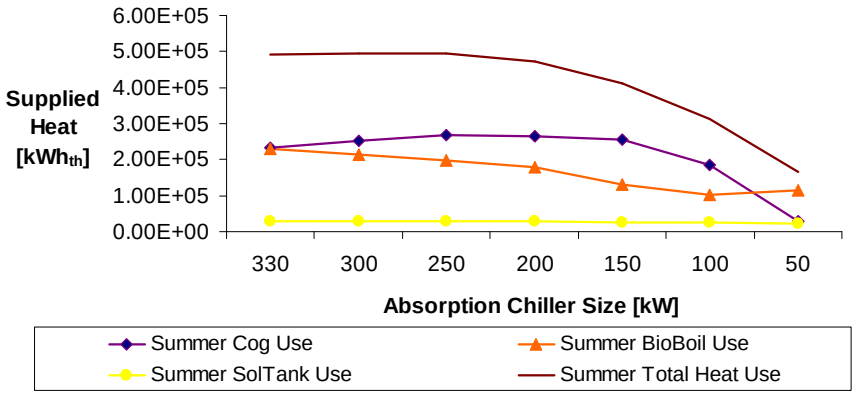

Figure 6.2 Total heat demand of the absorption chiller and contribution from each heat generator under the ”Abs. Priority”

Table 6.2 PEC comparisons between the examined and the reference system under the "Abs. Priority" strategy

Simulations	PEC [kWhth]		
	Examined System	Reference System	PECsaved
1st Run	7.05E+05	6.26E+05	-8.00E+04
2nd Run	7.22E+05	6.56E+05	-6.57E+04
3rd Run	7.30E+05	6.75E+05	-5.47E+04
4th Run	7.07E+05	6.53E+05	-5.31E+04
5th Run	6.55E+05	6.24E+05	-3.11E+04
6th Run	5.67E+05	5.38E+05	-2.98E+04
7th Run	3.85E+05	3.26E+05	-5.93E+04

According to Table 6.2, the PEC of the examined system turns out to be higher than the PEC of the reference system mainly because the COP of the absorption chiller is significantly lower than the COP of the compression chiller.
Secondly, it has to be considered that the biomass boiler plays a crucial role in each simulation, as its contribution varies from 30% to 40% of the heat demand.
Finally, it has to be highlighted that the electrical efficiency declared by the Italian grid has been significantly increased in the last ten years.
Here is an example which shows the effect of each above mentioned factor on the PEC_{saved}.
It supposed to calculate the PEC spent to produce 1 kWh_c by using on one hand the reference system, on the other hand the examined system.
The PEC of the reference system amounts to:

$$\frac{1}{COP_{Compr} * \eta_{el,Grid}} = \frac{1}{3 * 0.40} = 0.83\ kWh_{th} \qquad 6.28$$

The heat requested by the absorption chiller according to the COP turned out of the simulations (67%) amounts to:

$$\frac{1}{COP_{Abs}} = \frac{1}{0.67} = 1.49\ kWh_{th} \qquad 6.29$$

Then, assuming to supply 60% of the heat required with the cogeneration unit (best case turned out of the simulations), 32% with the biomass boiler and 8%

with solar collectors, the PEC spent to produce 1 kWh_c in the examined system amounts to:

$$\frac{0.60 \cdot 1.49}{0.53} + \frac{0.32 \cdot 1.49}{0.84} = 1.69 + 0.57 = 2.26\ \mathrm{kWh_{th}} \qquad 6.30$$

0.53 and 0.84 being respectively the thermal efficiency of the cogeneration unit and the efficiency of the biomass boiler, both turned out of the simulations. From this calculation, the PEC obtained for the examined system results to be around 2.7 times higher than the PEC of the reference system. However, another factor has to be accounted for: the PEC of the cogeneration unit is also related to an electricity production. In fact, with 1.69 kWh_{th} PEC of the cogeneration unit, not only 0.89 kWh_{th} have been produced, but also:

$$0.30 \cdot 1.69 = 0.51\ \mathrm{kWh_{el}} \qquad 6.31$$

30% being the mean electrical efficiency of the cogenerator turned out of the simulations. To produce the same amount of electricity in the reference system, it would be necessary to consume:

$$\frac{0.51}{\eta_{el,Grid}} = \frac{0.51}{0.40} = 1.27\ \mathrm{kWh_{th}} \qquad 6.32$$

Thereby, the total PEC that would be spent by the reference system to produce 1 kWh_c and 0.51 kWh_{el} amounts to:

$$0.83 + 1.27 = 2.10\ \mathrm{kWh_{th}} \qquad 6.33$$

From this calculation, the PEC of the examined system is still lower than the PEC of the reference system but not so far from it.
To go more in detail, it is supposed to consider the only cooling produced by the cogeneration unit, 0.60 kWh_c and the corresponding electricity, 0.51 kWh_{el} (Equation 6.31). To produce the same amount of energy, a reference system would consume:

$$\frac{0.60}{COP_{Compr} \cdot \eta_{el,Grid}} + \frac{0.51}{\eta_{el,Grid}} = \\ = \frac{0.60}{3 \cdot 0.40} + \frac{0.51}{0.40} = 0.50 + 1.27 = 1.77 \text{ kWh}_{th} \quad 6.34$$

which is higher than the PEC of the only cogeneration unit, i.e. 1.69 kWh_{th} (Equation 6.30).

If only the cooling produced by the biomass boiler is considered, i.e. 0.32 kWh_c, and its PEC, i.e. 0.57 kWh_{th} (Equation 6.30) it can be shown that the reference system would consume less primary energy to produce the same cooling effect. In fact, the PEC of the reference system would amount to:

$$\frac{0.32}{COP_{Compr} \cdot \eta_{el,Grid}} = \frac{0.32}{3 * 0.40} = 0.27 \text{ kWh}_{th} \quad 6.35$$

which is considerably lower than 0.57 kWh_{th}.

The example demonstrates that on one hand the PEC of the examined system can be higher than the one of the reference system, on the other hand that the biomass boiler can negatively affect the PEC_{saved}. Consequently, the example explains the reason why the maximum PEC_{saved} corresponds to the 6^{th} run, (100 kW absorption chiller), i.e. when the absorption chiller size supply with 64% of the entire cooling demand, 60% of its heat demand is met by the cogeneration unit and the biomass boiler is less involved in the operation.

Whereas the PEC_{saved} is always negative, the CO_{2saved} is always positive under the assumption of null emissions from the biomass, even if it decreases together with the size of the absorption chiller, as shown in Table 6.3. This result is mainly due to:

- the positive effect of the biomass boiler whose emissions are considered zero;
- the positive effect of the cogeneration unit due to both cooling and electricity yields.

The latter can be explained considering the results of the previous example. The fuel consumption of the cogeneration unit related to the production of 0.60 kWh_c and 0.51 kWh_{el} amounts to:

$$\frac{PEC_{Cog}}{LHV_{Gas}} = \frac{1.69}{9.45} = 0.18\ m^3{}_{gas} \quad 6.36$$

which emit an the following CO_2 amount:

$$0.18 * 1.69 = 0.30\ kg\ CO_2 \quad 6.37$$

The electricity consumed/produced in a reference system would be:

$$\frac{0.60}{3} + 0.51 = 0.71\ kWh_{el} \quad 6.38$$

which emit an amount of CO_2 equal to:

$$0.71 * 0.47 = 0.33\ kg\ CO_2 \quad 6.39$$

which is a little bit higher than the CO_2 emissions of tthe cogeneration unit in he examined system. This result explains the reason why the maximum CO_2saved, resulting from the simulated fuel consumption and calculated under the CO_2 neutral approach, corresponds to the largest use of the absorption chiller, thus for 330 kW absorption chiller (Table 6.3).

Table 6.3 CO2 emissions comparisons between the examined and the reference system. under null emissions from the biomass

Simulations	CO2 [kg]		
	Examined System	Reference System	CO2saved
1st Run	7.62E+04	1.18E+05	4.14E+04
2nd Run	8.26E+04	1.23E+05	4.09E+04
3rd Run	8.75E+04	1.27E+05	3.94E+04
4th Run	8.73E+04	1.23E+05	3.55E+04
5th Run	8.89E+04	1.17E+05	2.83E+04
6th Run	7.99E+04	1.01E+05	2.12E+04
7th Run	4.58E+04	6.13E+04	1.55E+04

Nevertheless, considering the 2nd approach for the CO_2 emissions evaluation, the results are completely different, as shown in Table 6.4. The emissions of the

examined system considerably increase and result in negative CO_2 savings by the comparison with the reference system. Obviously, such result depends on the emissions of the biomass. It can be shown how the biomass boiler affects the overall results as far as the example above.
Considering the cooling effect driven by the biomass boiler in the examined system, i.e. 0.32 kWhc, and the corresponding PEC, i.e. 0.57 (Equation 6.30), the consumed fuel amounts to:

$$\frac{\mathrm{PEC}_{\mathrm{Bio}}}{\mathrm{LHV}_{\mathrm{Bio}}} = \frac{0.57}{3.40} = 0.17\ \mathrm{kg}_{\mathrm{Bio}} \tag{6.40}$$

which emit, according to the considered emissions rate of the biomass:

$$0.17 \cdot 1.8 = 0.31\ \mathrm{kg}_{\mathrm{CO_2}} \tag{6.41}$$

In the reference system the same amount of cooling would require:

$$\frac{0.32}{3} = 0.17\ \mathrm{kWh}_{\mathrm{el}} \tag{6.42}$$

which emit, according to the emission rate of the electricity production declared by the Italian gri:

$$0.17 \cdot 0.47 = 0.08\ \mathrm{kg}_{\mathrm{CO_2}} \tag{6.43}$$

According to these calculations, the biomass boiler emits 3.87 times the CO_2 emissions and this explains the results shown in Table 6.4. The maximum CO_2 saved occurs for the second last simulation (100 kW absorption chiller) in correspondence with a smallest use of the biomass boiler (see also Figure 6.2)

Table 6.4 CO_2 emissions comparisons between the examined and the reference system. under not null emissions from the biomass

Simulations	CO2 [kg]		
	Examined System	Reference System	CO2saved
1st Run	2.22E+05	1.18E+05	-1.04E+05
2nd Run	2.18E+05	1.23E+05	-9.48E+04
3rd Run	2.12E+05	1.27E+05	-8.54E+04
4th Run	2.01E+05	1.23E+05	-7.79E+04
5th Run	1.71E+05	1.17E+05	-5.40E+04
6th Run	1.45E+05	1.01E+05	-4.38E+04
7th Run	1.19E+05	6.13E+04	-5.75E+04

Generally, the OC_{saved} is positive in all the cases (Table 6.5). By calculating the OC for the cooling effect due to each heat generator in the examined system and by comparing it with the reference system, it can be shown that the positive OC_{saved} are mainly due to the financial savings related to the electricity production of the cogenerator. In fact, the maximum OC_{saved} corresponds to the largest amount of electricity cogenerated, i.e. the large use of cogeneration unit, i.e. the 3rd parametric run shown in Table 6.5. (see also Figure 6.2 at 250 kW absorption chiller). It has to be added that also the biomass boiler produces a positive effect on the OC_{saved} due to the very low specific cost of the biomass (Equation 6.11).

Table 6.5 OC comparisons between the examined and the reference system.

Simulations	OC [€]		
	Examined System	Reference System	OCsaved
1st Run	2.12E+04	3.73E+04	1.61E+04
2nd Run	2.21E+04	3.91E+04	1.70E+04
3rd Run	2.27E+04	4.02E+04	1.75E+04
4th Run	2.24E+04	3.89E+04	1.65E+04
5th Run	2.22E+04	3.72E+04	1.49E+04
6th Run	2.09E+04	3.20E+04	1.11E+04
7th Run	1.61E+04	1.94E+04	3.37E+03

To show that the cogeneration unit is the major factor which positively influences the PECsaved, the OCsaved and the CO_2 saved in the simulations, the energy, financial and emissions savings due to each heat generator have been isolated, as shown in Figure 6.3, Figure 6.4 and Figure 6.5, which refer to the results of the 3rd parametric run. These curves have been derived by applying the same approach as in the example above reported to the kWh_c produced in the simulations. These figures also show that the solar fraction obviously causes a positive PEC, OC and CO_2 savings as its contribution is free from all the considered points of view. However, its contribution is really low and not significant compared with the other sources, especially with the cogeneration unit.

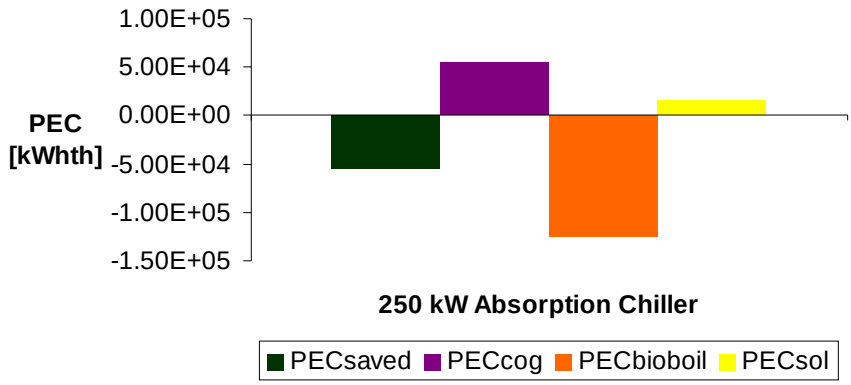

Figure 6.3 Total PECsaved with 250 kW absorption chiller and PECsaved rate due to each heat generator

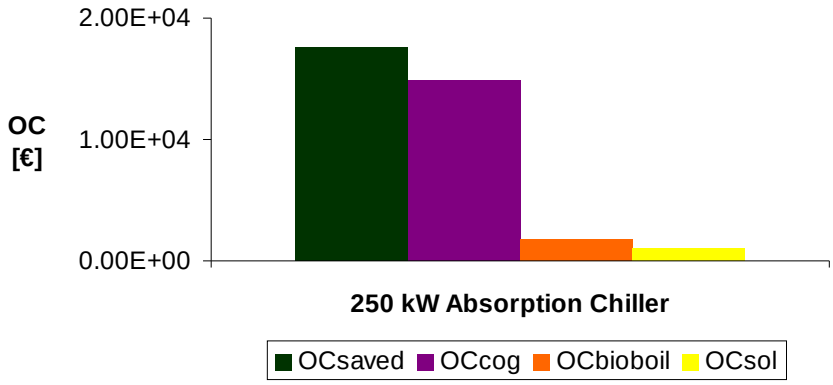

Figure 6.4 Total OCsaved with 250 kW absorption chiller and rate of the OCsaved due to each heat generator

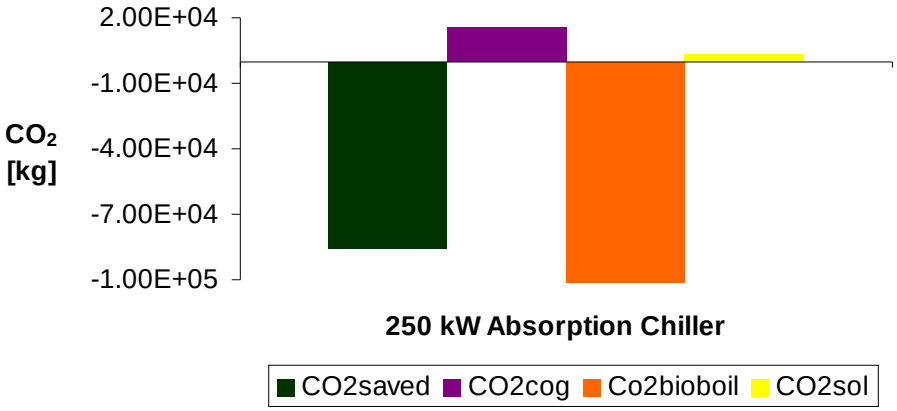

Figure 6.5 Total CO_{2saved} with 250 kW absorption chiller and rate of the OCsaved due to each heat generator

6.3.2 "Compr. Priority" control strategy

With this control strategy, the absorption chiller is involved in operation to meet the cooling peak demand. In this case, the simulation with 330 kW absorption chiller outputs the same results as in the "Abs. Priority" case (that's why the parametric run with 330 kW absorption chiller is missing in the Table 6.6).
Under this control strategy it is not recommendable to select small cooling capacities of the absorption chiller and to use it just to cover the peak, especially when the peak occurs very few times, as in EURAC case (see Figure 6.6).

Table 6.6 Sizes of the absorption and compression chiller per simulation under the ”Compr. Priority” strategy

Simulations	Qevanom [kW]	QcomprNom [kW]
1st Run	300	27
2nd Run	250	77
3rd Run	200	128
4th Run	150	178
5th Run	100	228
6th Run	50	279

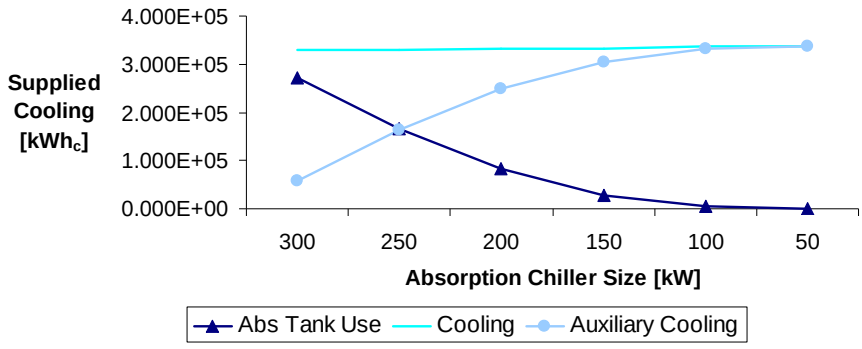

Figure 6.6 Total cooling supply and cooling supplyed by each chiller under the ”Compr. Priority” control strategy

Actually, the cold tank is involved in the operation less time than the absorption chiller, as the control strategy requires having the cold tank always at set temperature (read subchapter 5.3.2). Consequently, under the “Compr. Priority” control strategy there are many losses from the cold tank (see the difference between the cooling produced by the absorption chiller and the cooling leaked out of the tank in Figure 6.7). Similarly, the cogenerator and solar collectors produce more heat than the amounts which get leaked out of the respective tanks as shown in Figure 6.8.

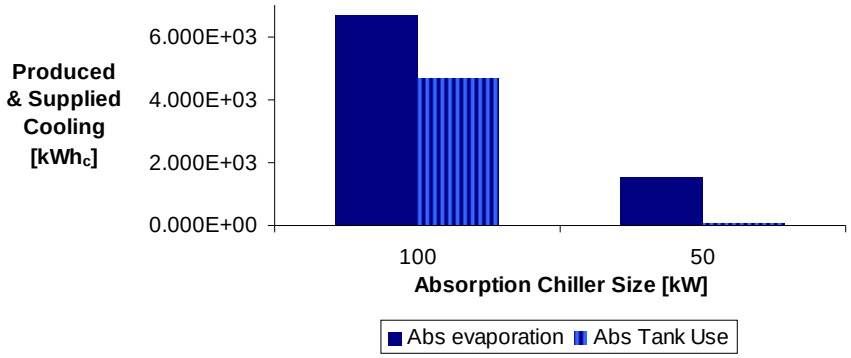

Figure 6.7 Comparison between the cooling produced by the absorption chiller (Abs Evaporation) and the one leaked out of the cold tank (Abs Tank Use) for 100 kW and 50 kW absorption chiller.

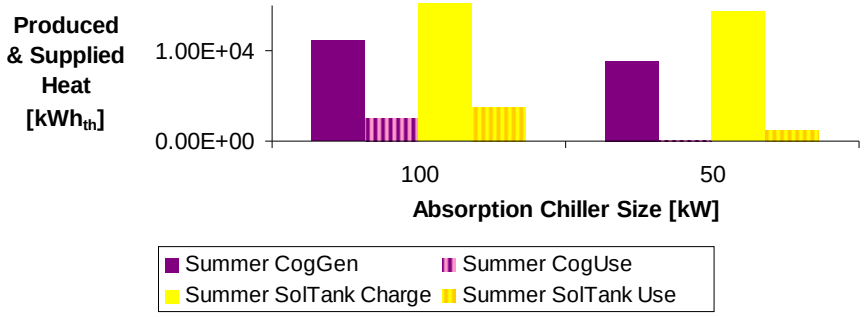

Figure 6.8 Comparison between the heat produced by the cogenerator Summer CogGen) and solar colelctors (Summer SolTank Charge) and the heat leaked out of the both hot tank (respectively Summer CogUse and Summer SolTank Use) for 100 kW and 50 kW absorption chiller.

As the size of the absorption chiller is reduced, its heat demand decreases faster than it does under the “Abs. Priority” control strategy (Figure 6.9). In fact, as the absorption chiller is secondly used, the cooling rate to be matched rapidly decreases with the reduction of the absorption chiller size. From the point of view of the heat demand, as the absorption chiller is used few times and requires small amounts of heat, solar fraction amounts to 54%.

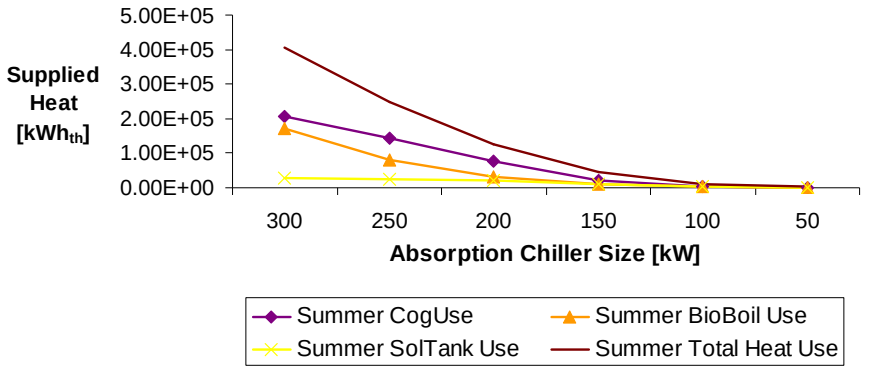

Figure 6.9 Total heat demand of the absorption chiller and contribution from each heat generator under the "Compr. Priority"

Concerning the PEC analysis, still the PECsaved is negative, as shown in Table 6.7, except in the 3rd parametric run (200 kW absorption chiller) when the cogenerated heat represents 61% of the demand of the absorption chiller, the solar fraction amounts to 15% and the biomass boiler contribution is 24%. Table 6.7 also shows that in correspondence to the smallest use of absorption chiller, the PECs of the examined and reference system are really similar.

Table 6.7 PEC comparisons between the examined and the reference system under the "Compr. Priority" strategy

Simulations	PEC [kWhth]		
	Examined System	Reference System	PECsaved
1st Run	6.35E+05	5.85E+05	-5.04E+04
2nd Run	5.02E+05	4.92E+05	-9.62E+03
3rd Run	3.91E+05	3.93E+05	1.88E+03
4th Run	3.18E+05	3.16E+05	-2.45E+03
5th Run	2.98E+05	2.93E+05	-4.56E+03
6th Run	2.95E+05	2.91E+05	-4.43E+03

The CO_2saved, is reported in Table 6.9 under the CO_2 neutral approach. It results always positive except in the last case when the examined system acts similarly to the reference one but with a further fuel consumption due to the

charging of the tanks [14] (Figure 6.13). Anyway, under this approach, the maximum CO_2saved corresponds to the largest use of absorption chiller, i.e. when its size is 300 kW.

Table 6.8 CO_2 comparisons between the examined and the reference system under the "Compr. Priority" strategy and null emissions from the biomass

Simulations	CO2 [kg]		
	Examined System	Reference System	CO2 saved
1st Run	7.67E+04	1.10E+05	3.32E+04
2nd Run	7.35E+04	9.25E+04	1.90E+04
3rd Run	6.50E+04	7.38E+04	8.76E+03
4th Run	5.66E+04	5.94E+04	2.81E+03
5th Run	5.51E+04	5.51E+04	6.51E+01
6th Run	5.51E+04	5.47E+04	-4.75E+02

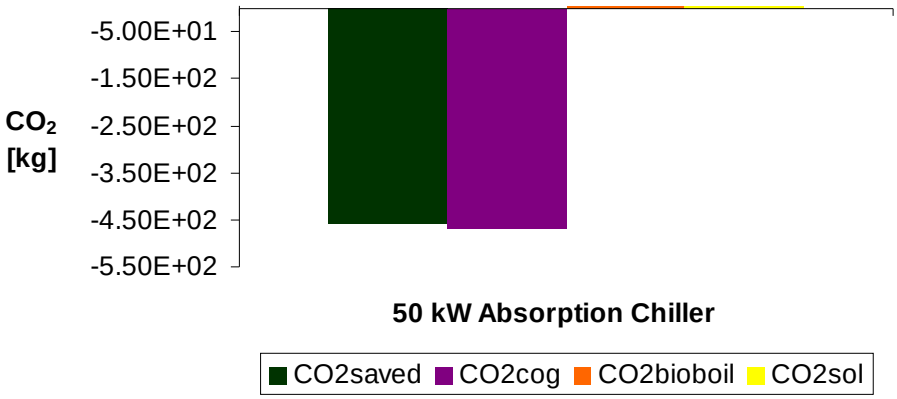

Figure 6.10 Total CO_2saved and contribution from each heat generator with 50 kW absorption chiller. In this case the cogeneration unit gives a engative contribution due to the fact that it is used more to heat up its tank than to provide the absorption chiller.

Considering a not null CO_2 emissions rate for the biomass, still the CO_2 emitted by the examined systems are higher than the ones by the reference system (Table 6.9) for the same reasons above explained. Still the maximum CO_2 saved occurs for the minimum use of the biomass boiler even if the negative saving

[14] The reference system produses as much cooling as the one transferred by the examined facility to the distribution system.

are more effected by the cogeneration unit (Figure 6.11) because of the tank charging (read footnote 14).

Table 6.9 CO_2 comparisons between the examined and the reference system under the "Compr. Priority" strategy and not null emissions from the biomass

Simulations	CO2 [kg]		
	Examined System	Reference System	CO2 saved
1st Run	1.85E+05	1.10E+05	-7.53E+04
2nd Run	1.24E+05	9.25E+04	-3.14E+04
3rd Run	8.42E+04	7.38E+04	-1.04E+04
4th Run	6.42E+04	5.94E+04	-4.87E+03
5th Run	5.71E+04	5.51E+04	-1.99E+03
6th Run	5.52E+04	5.47E+04	-5.23E+02

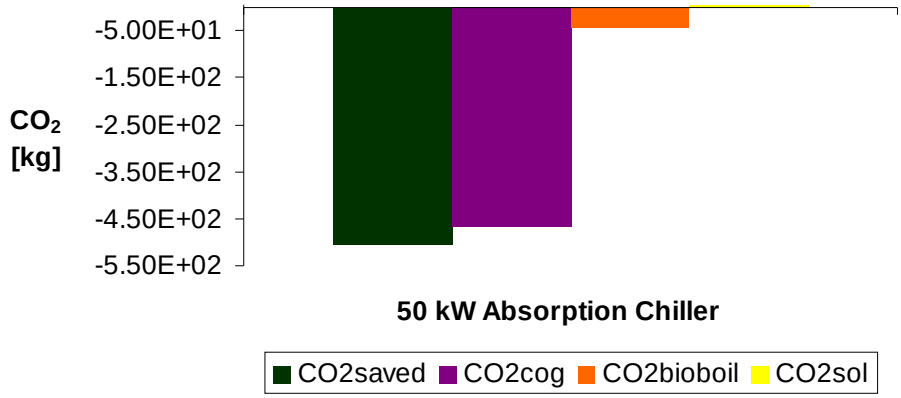

Figure 6.11 Total CO_2saved and contribution from each heat generator. for 50 kW absorption chiller. In this case the cogeneration unit gives a engative contribution too due to the fact that it is used more to heat up its tank than to feed into the absorption chiller

Likewise under the "Abs. Priority" strategy, also in this case the maximum OC_{saved} corresponds to the maximum electricity production from the cogeneration unit, which corresponds to the first parametric run (see also Figure 6.9 at 300 kW absorption chiller size).

The influence of each heat generator on the PEC_{saved} shows an interesting peculiarity: as it can be seen in Figure 6.10, the positive effect due to the cogeneration unit and to the solar collectors are practically the same. This is

mainly due to the poor exploitation of the cogeneration unit related to the few operation hours of the absorption chiller which supplies with 25% of the total cooling demand.

Table 6.10 OC comparisons between the examined and the reference system under the ”Compr. Priority” strategy

Simulations	OC [€]		
	Examined System	Reference System	OCsaved
1st Run	2.08E+04	3.48E+04	1.40E+04
2nd Run	1.98E+04	2.93E+04	9.48E+03
3rd Run	1.84E+04	2.34E+04	5.01E+03
4th Run	1.72E+04	1.88E+04	1.60E+03
5th Run	1.72E+04	1.75E+04	2.98E+02
6th Run	1.68E+04	1.73E+04	1.05E+02

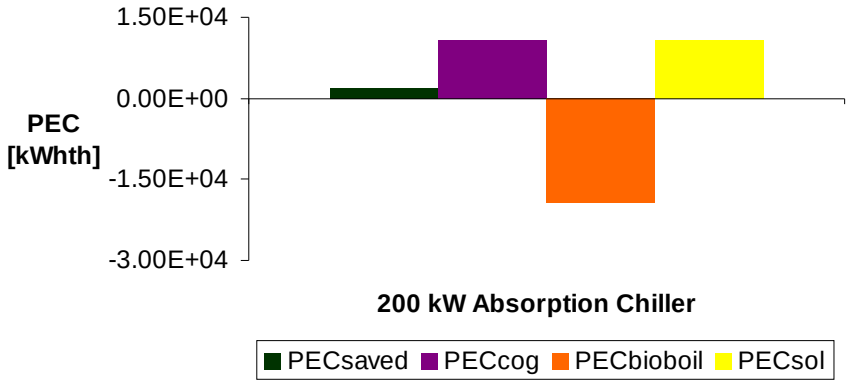

Figure 6.12 Total PECsaved with 300 kW absorption chiller and PECsaved rate due to each heat generator under ”Compr Priority” strategy

Looking at the influence of each heat generator on the OCsaved in Figure 6.13, the cogeneration unit still represents the major positive factor because of the electricity production.

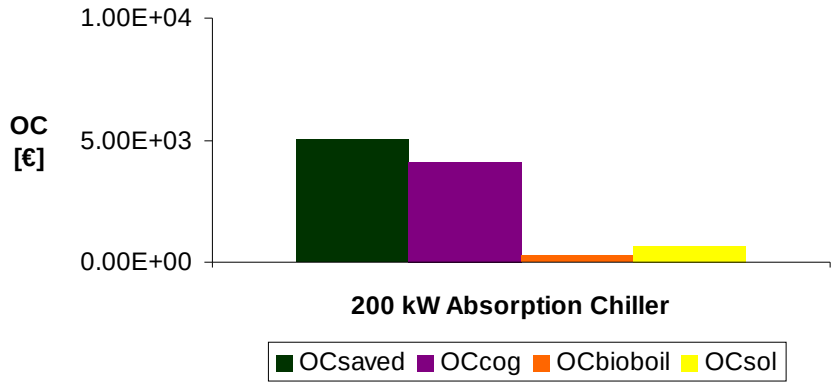

Figure 6.13 Total OCsaved with 300 kW absorption chiller and rate of the OCsaved due to each heat generator under "Compr Priority" strategy

6.3.3 "Abs/Compr Threshold" control strategy

To select the parametric runs under this control strategy, it has been checked that the minimum cooling demand is guaranteed in each combination without over sizing the compression chiller. The selected parametric runs are below reported.

Table 6.11 Sizes of the absorption and compression chiller per simulation under the "Compr/Abs threshold" strategy

Simulations	Qevanom [kW]	QcomprNom [kW]
1st Run	250	77
2nd Run	200	128
3rd Run	150	178
4th Run	100	228
5th Run	50	279

The simulations have shown results very similar to the "Abs. Control Stragegy" (see Figure 6.14 and Figure 6.15). As always, decreasing the absorption chiller size leads to a reduced heat demand and the cogenerator contribution depends on the range the heat demand is included in, i.e. if it is included in its range of capacity or not. So likewise the "Abs. Priority", for 50kW absorption chiller size, the cogeneration unit is not well exploited and the boiler supplies most of the heat demand, whereas the solar fraction amounts to 14%.

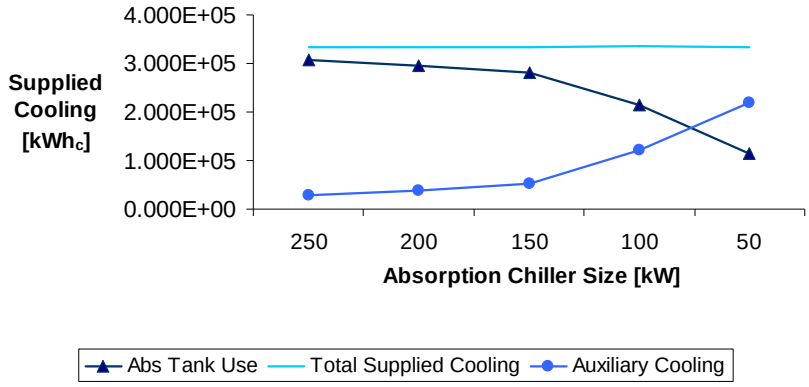

Figure 6.14 Total cooling supply and cooling supplyed by each chiller under the "Compr/Abs threshold" strategy

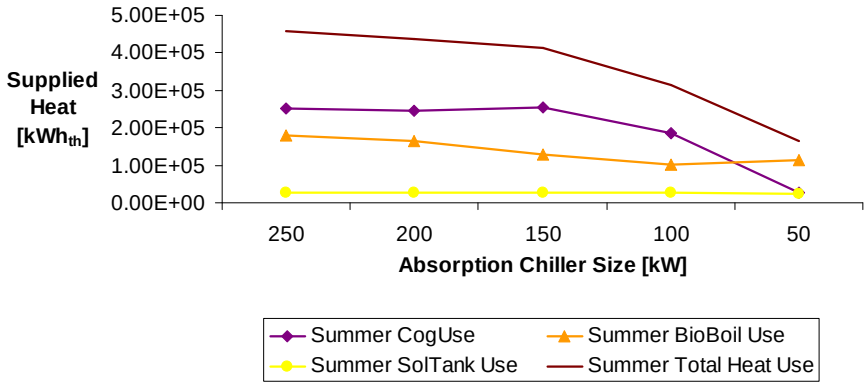

Figure 6.15 Total heat demand of the absorption chiller and contribution from each heat generator under the "Compr/Abs threshold" strategy

Just like in the "Abs. Priority", the maximum PEC_{saved} (Table 6.12) corresponds to 100 kW absorption chiller size because of the largest heat demand slice covered by the cogeneration unit; whereas the maximum OC_{saved} (Table 6.9) corresponds to 250 kW absorption chiller size because of the maximum exploitation of the cogeneration unit, thus the maximum electricity production (see also Figure 6.15). From the point of view of the CO_2 emissions, to the maximum CO_2saved is achieved at the highest size under the CO_2 neutral scenario, whereas at 100 kW absorption chiller under a not null emissions rate of the biomass boiler as under the "Abs. Priority" strategy.

Table 6.12 PEC comparisons between the examined and the reference system under the ”Compr/Abs threshold” strategy

Simulations	PEC [kWhth]		
	Examined System	Reference System	PECsaved
1st Run	7.02E+05	6.56E+05	-4.65E+04
2nd Run	6.76E+05	6.27E+05	-4.90E+04
3rd Run	6.55E+05	6.24E+05	-3.11E+04
4th Run	5.67E+05	5.38E+05	-2.98E+04
5th Run	3.85E+05	3.26E+05	-5.93E+04

Table 6.13 OC comparisons between the examined and the reference system under the ”Compr/Abs threshold” strategy

Simulations	OC [€]		
	Examined System	Reference System	OCsaved
1st Run	2.25E+04	3.91E+04	1.65E+04
2nd Run	2.21E+04	3.74E+04	1.53E+04
3rd Run	2.22E+04	3.72E+04	1.49E+04
4th Run	2.09E+04	3.20E+04	1.11E+04
5th Run	1.61E+04	1.94E+04	3.37E+03

6.3.4 Comparisons within “Abs. Priority”, “Compr. Priority” and “Abs/Compr threshold” control strategies

Figure 6.16 and Figure 6.17 resume the PECsaved and OCsaved under each control strategy examined.
As far the PEC savings are concerned, the “Compr. Priority” control strategy is the most advantageous one, as it leads to a short use of the heat generators for the absorption chiller. In particular, the following sizes selection has resulted to lead to a positive, thus the maximum, PEC_{saved}:

- 130 kW for the compression chiller;
- 200 kW for the absorption chiller.

Even if such a selection lead to the maximum PEC_{saved}, it could not represent an interesting investment as the absorption chiller only supplies 25% of the cooling demand although its relatively high nominal cooling capacity.

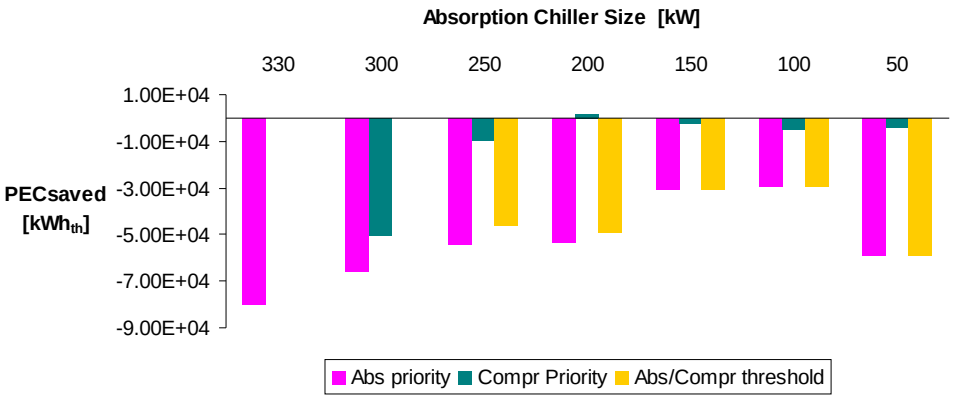

Figure 6.16 PECsaved comparisons between the three different control strategy for cooling mode

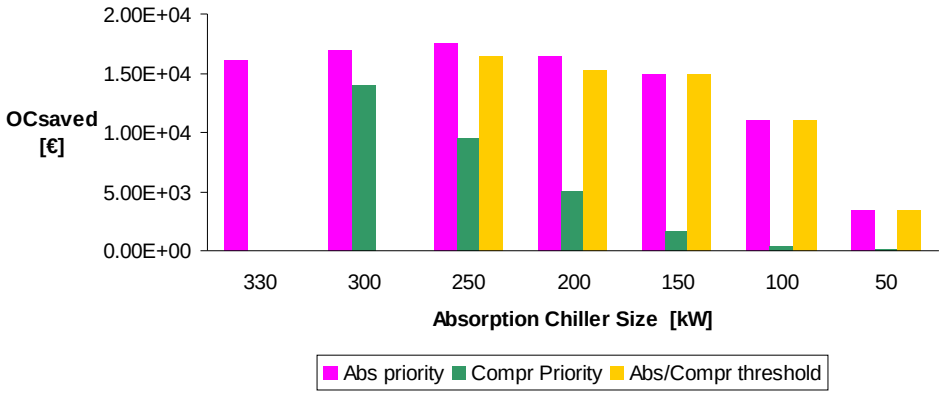

Figure 6.17 OCsaved comparisons between the three different control strategy for cooling mode

The advantageous scenario from the financial point of view occurs under the "Abs. Priority". In fact, in this case, the absorption chiller being preferred, the cogeneration works longer, thus produces the largest amount of electricity and saves much money in comparison with the reference system. Under such control strategy, the sizes selection with the highest OC_{saved} is:

- 250 kW for the absorption chiller;
- 78 kW for the compression chiller.

It has to be noticed that the "Abs./Compr. Threshold" scenario is not really far from the best case under the "Abs. Priority" strategy as it leads to very similar results. In fact, also for this scenario, the optimal size selection from the point of view of the financial saving coincides with 250 kW absorption chiller.

As far as the emissions are concerned, considering the biomass CO_2 neutral, the best selection is 330 kW absorption chiller under the "Abs Priority" (Figure 6.18), otherwise the optimal size selection is 50 kW absorption chiller under the "Compr. Priority" (Figure 6.19). However, such sizes selection will not be further investigated as on one hand they lead to the absorption machine work mostly at partial load, on the other hand because to large losses from the hot and cold tanks according to sub-chapter 6.3.2.

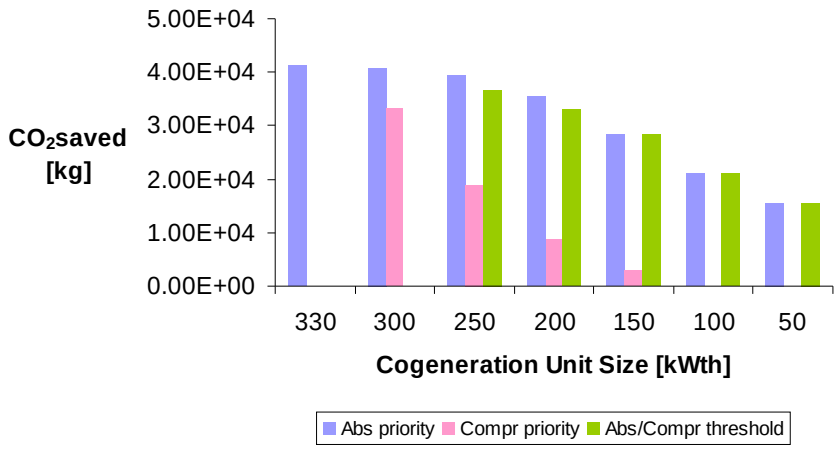

Figure 6.18 CO_2saved comparisons between the three different control strategy for cooling mode under the CO2 neutral biomass hypothesys

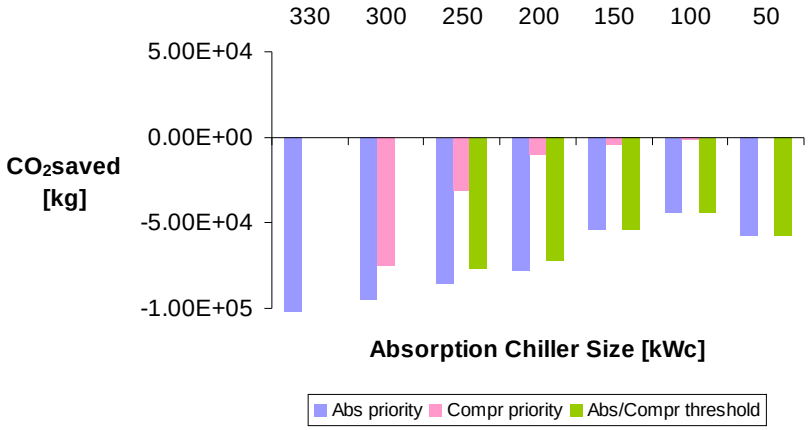

Figure 6.19 CO_2saved comparisons between the three different control strategy for cooling mode

6.4 Optimization of the Cogenerator Size

In the previous subchapters it has been shown that the PEC_{saved} and OC_{saved} are strongly influenced by the cogeneration unit. That is the reason why it has been decided to go more in detail with this component by running further simulations with different cogenerator sizes.
The sizes with the maximum PEC_{saved} and OC_{saved} selected in subchapter 6.3.4 are here used.
Table 6.14 shows the selected parametric runs per summer control strategy. The maximum size has been selected on the basis of the results obtained in winter and summer time. Figure 6.20 shows that in winter the amounts of heat produced at 400 kW and 450 kW cogeneration unit are similar. This means that the maximum possible exploitation of the engine has been reached.

Table 6.14 Sizes of the cogeneration and biomass boiler per simulation under the ”Abs. Priority” and ”Compr. Priority” strategies

Simulations	Abs. Priority		Compr. Priority	
	PthCog [kW]	PthBio [kW]	PthCog [kW]	PthBio [kW]
1st Run	400	279	-	-
2nd Run	350	329	350	329
3rd Run	300	379	300	379
4th Run	250	429	250	429
5th Run	200	479	200	479
6th Run	150	529	150	529
7th Run	100	579	100	579

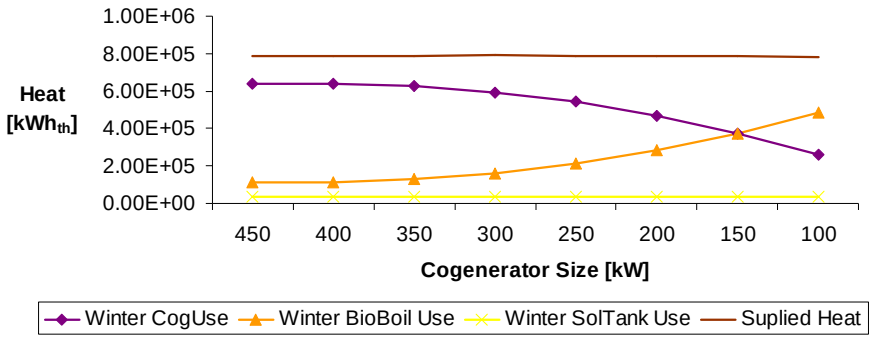

Figure 6.20 Total winter heat supply and contribution from each heat generator per simulation.

In summer, with 250 kW absorption chiller under the “Abs. Priority.”, the amount produced at 450 kW is really slightly higher than the one for 400 (see Figure 6.21), whereas, with 200 kW absorption chiller under the “Compr. Priority” strategy, the maximum use of the cogeneration unit occurs per 350 kW (see Figure 6.22). This is due to the fact that in the second case the heat demand is lower than in the first case, so the maximum contribution from the cogeneration unit is reached earlier.

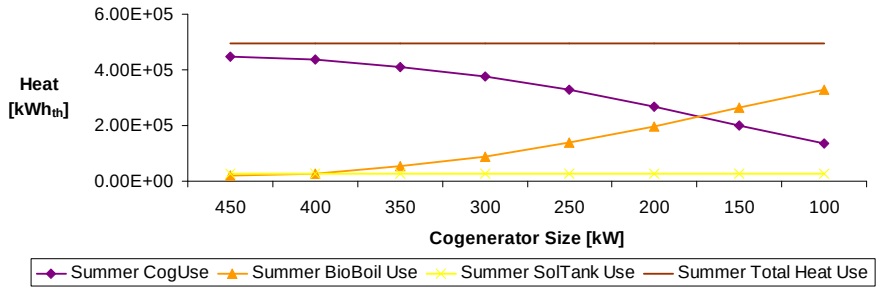

Figure 6.21 Total heat demand of the absorption chiller and contribution from each heat generator per simulation with 250 kW absorption chiller under the ”Abs.Priority” strategy

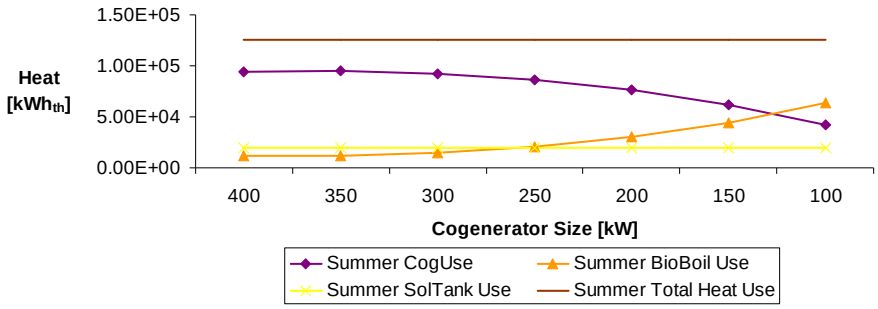

Figure 6.22 Total heat demand of the absorption chiller and contribution from each heat generator per simulation with 200 kW absorption chiller under the "Compr.Priority" strategy

Although it is clear that increasing the cogeneration size does lead to PEC and OC savings, the next subchapters will quantify these amounts and will focus on the differences in summer time due to the application of different control strategies.

6.4.1 Optimization of the cogenerator size with 200 kW absorption chiller under the "Compr.Priority" control strategy

Because EURAC case present a heating demand really higher than the cooling demand, the selection of the cogeneration size mostly affects the heating mode operation from the PEC point of view as shown in Table 6.15. In fact, as the cogenerator size is increased, a reduction occurs in both the winter and summer PEC, but in winter it amounts to 22% whereas in summer it amounts to 10%. Similarly, the advantage of the examined system in comparison with the conventional one is more evident in winter than in summer. Actually, in the last two parametric runs the summer PEC of the examined system is even higher than in the reference system, thus leading to a negative PEC_{saved}. The PEC_{saved} becomes positive with 200 kW_{th} cogeneration unit, when this latter supplies 61% of the heat demand of the absorption chiller and the solar fraction amounts to 15% (as already shown in subchapter 6.2.2). It means that with a biomass boiler contribution less than 24% of the heat demand, the examined system also leads to a positive PEC_{saved} in summer time.

Table 6.15 PEC comparisons between the examined and the reference system with 200 kW absorption chiller under the "Compr. Priority" strategy

Simulations	Examined System		Reference System	
	Winter PEC [kWhth]	Summer PEC [kWhth]	Winter PEC [kWhth]	Summer PEC [kWhth]
1st Run	-	-	-	-
2nd Run	1.29E+06	4.05E+05	1.82E+06	4.17E+05
3rd Run	1.28E+06	4.02E+05	1.78E+06	4.13E+05
4th Run	1.24E+06	3.97E+05	1.70E+06	4.04E+05
5th Run	1.19E+06	3.91E+05	1.59E+06	3.93E+05
6th Run	1.14E+06	3.80E+05	1.45E+06	3.72E+05
7th Run	1.06E+06	3.67E+05	1.28E+06	3.43E+05

From the point of view of CO_2 emissions, considering the biomass CO_2 neutral, it is interesting to highlight that the CO_2saved increase by reducing the cogeneration unit (Table 6.16). In fact, the reduction of the cogenerator size coincides with an increase of the biomass boiler size. On the contrary, considering 1.8 $kgCO_2$/kgBiomass, the results are inverted: the higher the cogeneration unit size, the higher the saved emissions (Table 6.19). In the latter case, the biomass boiler negatively influences the CO_2 saved not only in summer but also in winter because of its larger Carbon content [24] (Figure 6.23).

Table 6.16 Yearly CO_2 comparisons between the examined and the reference system with 200 kW absorption chiller under the ”Compr. Priority” strategy considering the biomass CO_2 neutral

Simulations	CO2 [kg]		
	Examined System	Reference System	CO2 saved
1st Run	-	-	-
2nd Run	2.76E+05	4.21E+05	1.45E+05
3rd Run	2.64E+05	4.12E+05	1.48E+05
4th Run	2.45E+05	3.96E+05	1.51E+05
5th Run	2.18E+05	3.72E+05	1.54E+05
6th Run	1.83E+05	3.41E+05	1.58E+05
7th Run	1.40E+05	3.02E+05	1.61E+05

Table 6.17 Yearly CO_2 comparisons between the examined and the reference system with 200 kW absorption chiller under the ”Compr. Priority” strategy not considering the biomass CO_2 neutral

Simulations	CO2 [kg]		
	Examined System	Reference System	CO_2 saved
1st Run	-	-	-
2nd Run	3.89E+05	4.10E+05	2.08E+04
3rd Run	3.98E+05	4.02E+05	4.18E+03
4th Run	4.09E+05	3.86E+05	-2.23E+04
5th Run	4.24E+05	3.63E+05	-6.13E+04
6th Run	4.42E+05	3.33E+05	-1.09E+05
7th Run	4.63E+05	2.96E+05	-1.67E+05

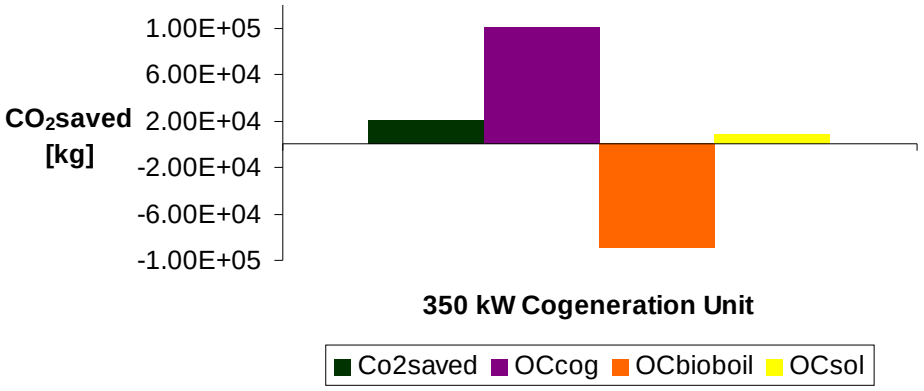

Figure 6.23 Winter total CO_2saved and contribution from each heat generator

From the financial point of view (Table 6.18), the maximum size of the cogenerator is always the most advantageous because of the electricity production in situ. Also from this perspective, the financial saving affect more the heating mode then the cooling mode compared to the reference system: in fact, even in the worst case (100 kW cogeneration unit size), the winter financial saving amounts to nearly 48% of the costs of the reference system, whereas the summer financial saving are approximately 18%.

Table 6.18 OC comparisons between the examined and the reference system with 200 kW absorption chiller under the "Compr. Priority" strategy

Simulations	Reference System		Conventional System	
	Winter OC [€]	Summer OC [€]	Winter OC [€]	Summer OC [€]
1st Run	-	-	-	-
2nd Run	4.43E+04	1.93E+04	8.76E+04	2.49E+04
3rd Run	4.31E+04	1.91E+04	8.52E+04	2.46E+04
4th Run	4.09E+04	1.88E+04	8.07E+04	2.41E+04
5th Run	3.78E+04	1.84E+04	7.40E+04	2.34E+04
6th Run	3.40E+04	1.78E+04	6.60E+04	2.22E+04
7th Run	2.93E+04	1.69E+04	5.58E+04	2.05E+04

Also in this parametric study, it is shown that the cogenerator is the major responsible of positive PEC_{saved} and OC_{saved} as shown in Figure 6.24 and Figure 6.25 for the optimal selection size, i.e. 350 kW cogeneration unit. It can also be observed that the PEC_{saved} due to the biomass boiler is still negative also in winter time. This is mainly related to its efficiency which is lower than the one of the gas boiler considered in the reference system. However, it has to be pointed out that in the simulations the biomass boiler always work at partial loads, so its efficiency hardly ever reaches its maximum, whereas the efficiency of the gas boiler in the reference system is constantly set at 90%.

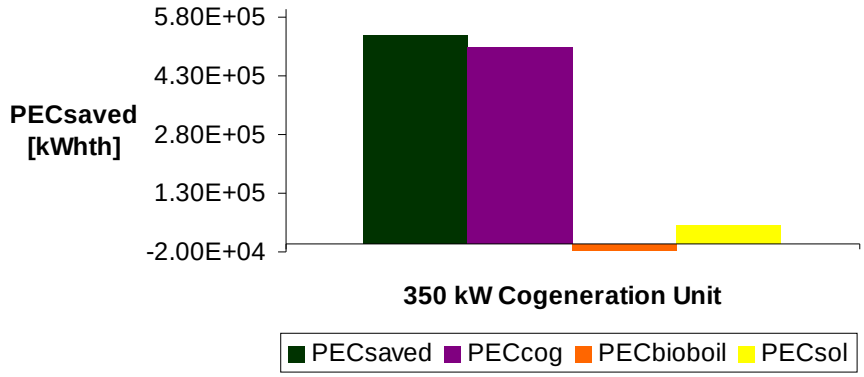

Figure 6.24 Yearly total PECsaved with 350 kWth cogeneration unit and PECsaved rate due to each heat generator under ”Compr Priority” strategy

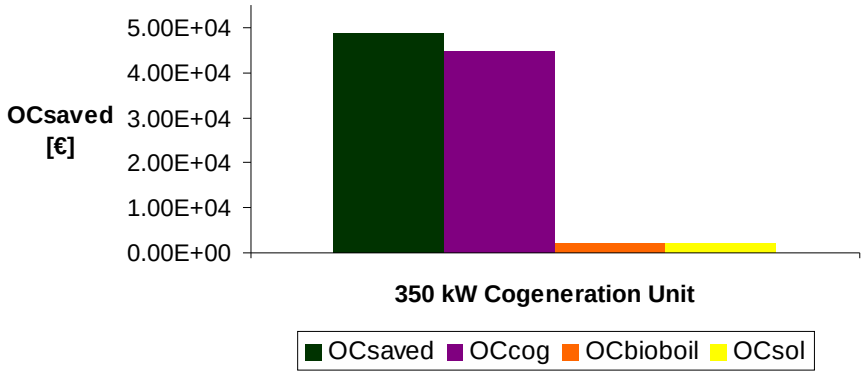

Figure 6.25 Yearly total OCsaved with 350 kWth cogeneration unit and PECsaved rate due to each heat generator under ”Compr Priority” strategy

6.4.2 Optimization of the cogenerator size with 250 kW absorption chiller under the "Abs.Priority" control strategy

This case is different from the previous one only in summer when a highest heat demand occurs due to a larger absorption chiller (250 kW instead 200 kW). Under this selection, the solar fraction only amounts to 6% of the heat demand of the absorption chiller. Consequently, to obtain the maximum PEC_{saved} it is needed to select big cogeneration unit sizes. In fact, as shown in Table 6.16, the summer PEC of the examined system is lower than in the reference system in the last 4 parametric runs. Under the analyzed sizes selections, the summer PEC_{saved} becomes positive with 300 kW cogeneration unit which supplies 76% of the heat demand. Such a high requirement is mainly due to the largest size selection of the absorption chiller and to the low solar fraction 6%. To sum up, positive summer PEC_{saved} are reached when the biomass boiler supply less than 18% of the heat demand.

Table 6.19 PEC comparisons between the examined and the reference system with 250 kW absorption chiller under the "Abs. Priority" strategy

Simulations	Reference System		Conventional System	
	Winter PEC [kWhth]	Summer PEC [kWhth]	Winter PEC [kWhth]	Summer PEC [kWhth]
1st Run	1.30E+06	8.20E+05	1.83E+06	8.75E+05
2nd Run	1.29E+06	8.09E+05	1.82E+06	8.52E+05
3rd Run	1.28E+06	7.93E+05	1.78E+06	8.19E+05
4th Run	1.24E+06	7.67E+05	1.70E+06	7.59E+05
5th Run	1.19E+06	7.30E+05	1.59E+06	6.75E+05
6th Run	1.14E+06	6.86E+05	1.45E+06	5.76E+05
7th Run	1.06E+06	6.46E+05	1.28E+06	4.80E+05

From the point of view of CO_2 emissions, the CO_2saved increases by reducing the cogeneration unit in a CO2 neutral scenario (Table 6.20), and decreases in a not null emissions from the biomass boiler (Table 6.21), as already explained in the previous subchapter.

Table 6.20 Yearly CO_2 comparisons between the examined and the reference system with 250 kW absorption chiller under the ”Abs. Priority” strategy with a CO2 neural biomass

Simulations	CO2 [kg]		
	Examined System	Reference System	CO2 saved
1st Run	3.46E+05	5.06E+05	1.60E+05
2nd Run	3.35E+05	5.00E+05	1.65E+05
3rd Run	3.14E+05	4.85E+05	1.72E+05
4th Run	2.82E+05	4.60E+05	1.77E+05
5th Run	2.39E+05	4.22E+05	1.83E+05
6th Run	1.87E+05	3.77E+05	1.89E+05
7th Run	1.30E+05	3.25E+05	1.95E+05

Table 6.21 Yearly CO_2 comparisons between the examined and the reference system with 250 kW absorption chiller under the ”Abs. Priority” strategy with emission from the biomass boiler

Simulations	CO2 [kg]		
	Examined System	Reference System	CO2 saved
1st Run	4.35E+05	4.98E+05	6.36E+04
2nd Run	4.49E+05	4.92E+05	4.34E+04
3rd Run	4.72E+05	4.78E+05	6.61E+03
4th Run	5.03E+05	4.53E+05	-5.01E+04
5th Run	5.43E+05	4.16E+05	-1.28E+05
6th Run	5.92E+05	3.72E+05	-2.20E+05
7th Run	6.48E+05	3.21E+05	-3.26E+05

From the financial point of view, this scenario is really attractive. The large use of the cogeneration unit allows large savings in the electricity costs, as it is shown in Table 6.22. Clearly, the maximum OC_{saved} occurs for the highest cogenerator size. It has to be pointed out that under the “Abs. Priority” cooling mode, the OC_{saved} in winter and in summer are more comparable than under the “Compr. Priority”cooling mode: respectively 49% and 44% of the OC of the reference system.

Table 6.22 OC comparisons between the examined and the reference system with 250 kW absorption chiller under the ”Abs. Priority” strategy

Simulations	Reference System		Conventional System	
	Winter OC [€]	Summer OC [€]	Winter OC [€]	Summer OC [€]
1st Run	4.48E+04	2.91E+04	8.82E+04	5.22E+04
2nd Run	4.43E+04	2.82E+04	8.76E+04	5.08E+04
3rd Run	4.31E+04	2.70E+04	8.52E+04	4.88E+04
4th Run	4.09E+04	2.51E+04	8.07E+04	4.53E+04
5th Run	3.78E+04	2.27E+04	7.40E+04	4.02E+04
6th Run	3.40E+04	1.99E+04	6.60E+04	3.44E+04
7th Run	2.93E+04	1.72E+04	5.58E+04	2.86E+04

6.4.3 Comparison within cogeneration sizes under the “Compr. Priority” and “Abs. Priority” control strategy

The PECsaved and OCsaved in winter time are the same in both the analyzed cases and are shown in Figure 6.26. It means that the selection of the optimal size is influenced by the summer operation which is described in Figure 6.27 and Figure 6.28 from both points of view: PECsaved and OCsaved.

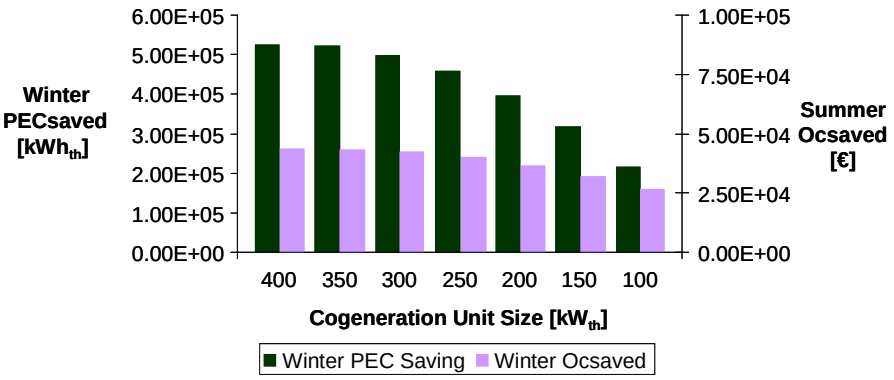

Figure 6.26 Winter PECsaved and OCsaved comparison at varying the cogeneration unit size under ”Abs.Priority” and ”Compr.Priority” cooling mode.

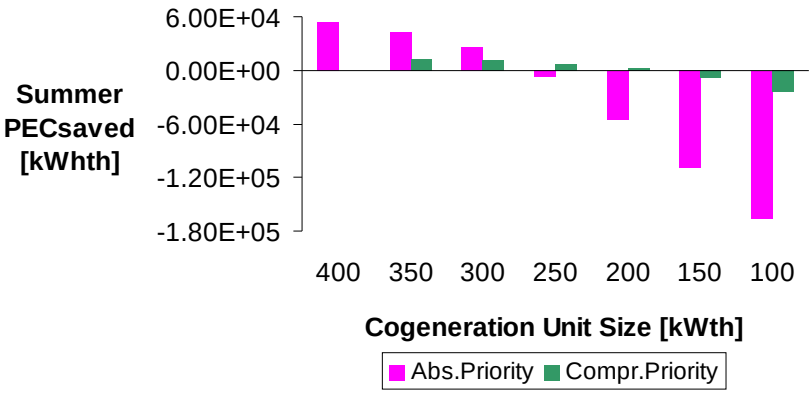

Figure 6.27 Summer PECsaved comparison at varying the cogeneration unit size under "Abs.Priority" and "Compr.Priority" cooling mode.

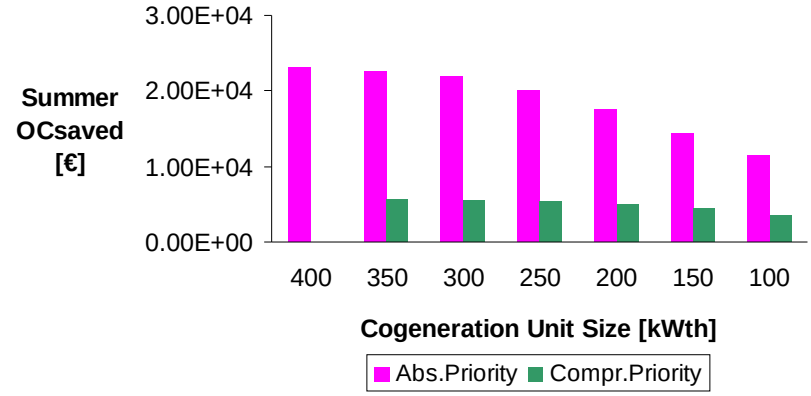

Figure 6.28 Summer OCsaved comparison at varying the cogeneration unit size under "Abs.Priority" and "Compr.Priority" cooling mode.

According to the results, the optimal size selection from both the points of view is 400 kW cogeneration unit under the Abs.Priority, even if the gap between this choice and the closest one (350 kW) is really small. Such remark suggests that in the sizes selection one more factor has to be accounted for, i.e. the discounted pay back period. In fact the optimal sizing should consider the increase of the investment cost compared to the achieved benefits. Such analysis is developed in the next subchapter.

From the point of view of the CO_2 emissions, as the cogenerator size decreases, the CO_2saved increases under the both summer strategies (Figure 6.29) and under the hypothesis of a CO_2 neutral biomass boiler. In this case, it would be

even advantageous not to include a cogeneration system in the designed plant at all. However, this would not be of interest in the present research work.

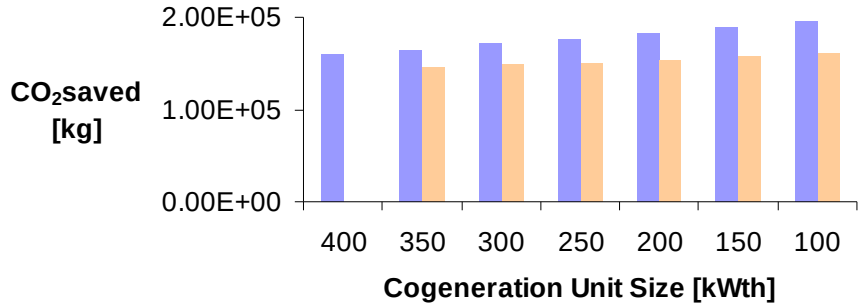

Figure 6.29 Yearly CO2saved comparison at varying the cogeneration unit size under ”Abs.Priority” and ”Compr.Priority” cooling mode and under null emissions from the biomass

On the other hand, considering a not null emission rate for the boiler, the optimum corresponds to the largest thermal capacity of the cogeneration unit, under both the summer control strategy as shown in Figure 6.30.

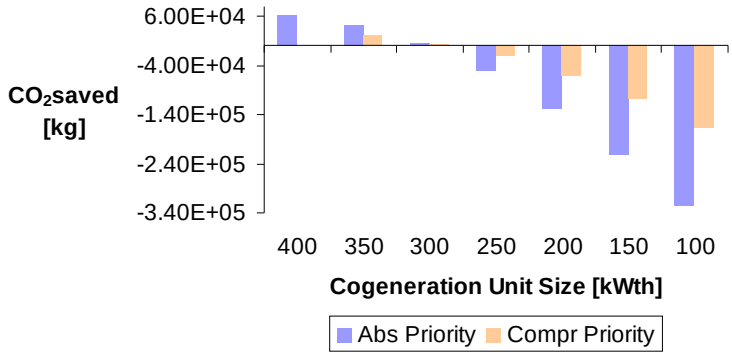

Figure 6.30 Yearly CO2saved comparison at varying the cogeneration unit size under ”Abs.Priority” and ”Compr.Priority” cooling mode and under not null emissions from the biomass

6.4.4 The investment costs and the Discounted Pay Back Period

This analysis considers on one hand the investment costs, on the other hand the yearly discounted cash flows due to the OC_{saved}. When the sum of the yearly discounted cash flows balances the investment costs, the discounted pay back

period (DPBP **Error! Bookmark not defined.**) is reached. From this point of view the best investment is the one with the minimum DPBP.
The DPBP is calculated as follows:

$$N: \sum_{k=1}^{N} \frac{C_k}{(1+i)^k} = C_0 \qquad 6.44$$

being

3. C_k, the yearly cash flow in the k-th year, i.e. the OC_{saved} in the k-th year
4. i, the discount rate[15]
5. C_0, the investment cost
6. N, the number of the years necessary to balance the investment costs.

To calculate the DPBP for each simulation under the "Abs. Priority" cooling mode, the operation costs of both the examined and the reference system are considered: in the first case the costs are related to the electricity, gas and biomass consumption, whereas, in the second case, the costs are only related to the electricity and gas consumption. Thereafter, the cash flow is calculated by subtracting the OC of the examined system from the OC of the reference system. This value coincides with the OC_{saved} for the first operation year. For the subsequent years, the OC_{saved} vary on the basis of the prices fluctuation. For this reason, 4 scenarios have been outlined which take into account different increase rates in the prices of each fuel:

- Scenario 1: +6% for electricity, +10% for gas and +10% for biomass
- Scenario 2: +6% for electricity, +10% for gas and +4% for biomass
- Scenario 3: +2.5% for electricity, +4% for gas and +4% for biomass
- Scenario 4: +2.5% for electricity, +4% for gas and+10% for biomass

In this analysis only the investment costs for the major components have been considered, i.e. the cogeneration unit, the biomass boiler, the absorption chiller and the compression chiller. Table 6.23 reports the costs of each configuration obtained by varying the cogeneration unit size with 250 kW absorption chiller under the "Abs. Priority" strategy. Such investment costs have been calculated with the single prices reported in Table 6.24.

[15] 5%

Table 6.23 Investment costs for each simulated configuration

Simulations	Investment Costs [€]
1st Run	456,393 €
2nd Run	436,403 €
3rd Run	416,474 €
4th Run	396,484 €
5th Run	376,494 €
6th Run	384,448 €
7th Run	455,236 €

Table 6.24 Specific costs for the major plant components

Components	Range	Specific Costs
Cogenerator [15]	[1,100] kW_{el}	1,300 €/kW_{el}
	[100,1000] kWel	1,000 €/kW_{el}
Biomass Boiler	[300,700]kW_{th}	215 €/ kW_{th}
Absorption Chiller [18]	[5,100] kW_c	4396.2* $(kW_c)^{-0.48}$
	>100 kW_c	500 €/ kW_c
Compression Chiller		300 €/ kW_c

The discounted bay back periods per each scenario and configuration are shown in Figure 6.31. According to the results, the most financially convenient size of the cogenerator is not the maximum size, as resulted in the previous sub chapter, but 300 kW_{th}.

According to Figure 6.31, this size is the most advantageous in all the scenarios and no large difference separates them. Nevertheless, the examined system would be more advantageous under the 2nd scenario in which the electricity and gas costs respectively increase 6% and 10%, whereas the biomass price increases 4%.

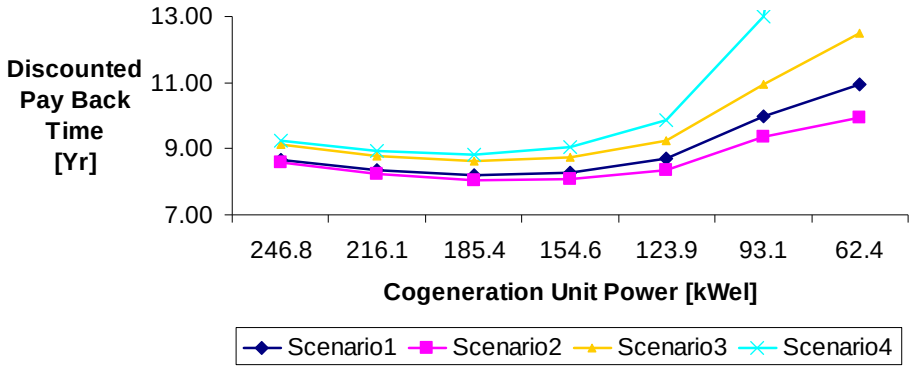

Figure 6.31 Discounted Payback Period per each configuration under 4 different fuel prices scenarios

Conclusions

In the present research work, a Combined Heating, Cooling and Power (CHCP) system combined with Evacuated Solar thermal Collectors (ETC) has been designed from three points of view: layout, control strategy and sizes. Afterwards, the project has been translated into a TRNSYS deck which is able to simulate the yearly operation of the entire plant at design and off-design conditions.
This simulation tool can be used to assist the design process itself, in particular the control strategy definition and the sizes selection. In fact, by simulating different components' sizes under different control strategies, it is possible to find out the configuration which can lead to the minimum primary energy consumption (PEC) or to the lowest operation costs (OC) or rather to the smallest amount of CO_2 emissions.
Such an approach has been applied to a real case, the EURAC building. So, given the EURAC heating and cooling demand, the following configuration has turned out to lead to the maximum PEC, OC and CO_2 savings with respect to a conventional system and under the efficiencies turned out of the simulations, the current fuel costs and the emissions rates listed in the literature (in particular 1.8 $kg_{CO2}/kg_{Biomass}$): 250 kW absorption chiller as the base cooling device and 400 kW thermal capacity of the cogeneration unit. With respect to a conventional system, the selected configuration leads to 21% PEC saving, 47% OC saving and 13% CO_2 saving.
The contribution of each heat generator to the overall PEC, OC and CO_2 savings has also been highlighted and the following general results have been output:

- In summer time, the examined system results in positive PEC savings only when the heat supply due to the cogeneration unit and the solar collectors accounts for over 76% of the heat required by the absorption chiller.
- The cogeneration unit and the solar collectors mostly lead to positive PEC savings but the first one often accounts for over 90%, above all thanks to its electricity production.
- All the heat generator lead to positive OC savings but the cogenerator often accounts for over 80%, above all thanks to its electricity production.
- The biomass boiler always lead to negative PEC savings, even in winter time as its off-design efficiency is lower than the gas boiler's one considered in the conventional system; on the other hand, thanks to a relatively low cost of the biomass, the boiler also accounts for c.a. 10% of the OC savings.

- CO_2 emissions savings are significantly influenced by the biomass boiler: if the biomass is supposed to be CO_2 neutral, using the biomass boiler instead of the cogenerator results to be more environmentally sustainable; on the contrary, given 1.8 $kgCO_2/kgBiomass$ emission rate for the biomass, the examined system is considerably less sustainable than the reference system.
- Solar thermal collectors always positively influences all the PEC, OC and CO_2 savings but its contribution can get significant only for relatively larger collectors surface.
- The selection of sizes with the maximum OC savings does not correspond to the minimum Discounted Pay Back Period (DPBP). For instance, the configuration which leads to the minimum DPBP includes 300 kW_{th} cogeneration unit instead of 400 kW_{th}, even under different assumptions on fuels price increases.

Research Limitations and Future Directions

The research work has been carried out under some significant hypotheses which of course influence and restrict the effectiveness of the obtained results. Nevertheless, such bounds can represent the starting point for future developments of the present work.

The major limitations concern the simulation of the absorption chiller. In the TRNSYS deck presented in Chapter 5, a model for the cooling tower which rejects the heat from the desorber and the condenser of the absorption chiller is missing and the chilling water temperature used to this end has been supposed to be constant. Such hypothesis is really far from the reality but it has been taken for two main reasons. On one hand, the cooling tower is not directly related to the cooling demand of the building but it can be considered as an auxiliary system which serves the operation of the absorption chiller. On the other hand a high effort would have been required to accurately simulate a cooling tower because of missing specifications. As such activity did not fall within the major goals of the present investigation, it was decided not to go more in detail with it.

Actually, not even the model of the absorption chiller used in the simulations was suitable to the purposes of the thesis as it did not take into account the regulation of the hot flow entering the absorber of the chiller depending on the chilled water temperature. In fact, this model was developed to react to hot inlet temperature and not to mass flow changes and a strong effort has been paid by adapting the model to this aim. Thereby, for a more reliable simulation of the absorption chiller it would be necessary to develop a new model for the chiller itself and to include in the deck a reliable model of the cooling tower which represents one of the most influencing aspects of the COP of the chiller.

Despite the mentioned restrictions, the simulation tool allows to gather many data for an in-depth understanding of CHCP plus ETC plants, in order to support the design of new plants or to optimize existing plants. Moreover, the output of the present research work can be the starting point not only for improvements but also for further developments. For instance, the biomass boiler could be replaced by a gas boiler, or the cogeneration unit could track the electricity and not the heat demand of the building, and so on.

References

[1] International Energy Agency, 2006. *Task 38 Solar Air-Conditioning and Refrigeration.* Resource available at: http://www.iea-shc.org/task38

[2] Sparber W., Napolitano A., Melograno P., 2007. *Overview on world wide installed solar cooling systems.* In: Otti, ed., 2007. 2nd International Conference on Solar Air Conditioning. Spain, October 2007.

[3] EURAC, 2002. *Una casa per l'Accademia Europea Bolzano. Architettura Storia Scienza* Resource available at: http://www.eurac.edu

[4] Reed Business Information, 2008. *CENTRO DI FORMAZIONE PROFESSIONALE "L. EINAUDI" Ottimizzazione dell'efficienza energetica con l'utilizzo di fonti rinnovabili.* Bolzano: Resource available at: http://www.infoimpianti.it [July, 2008]

[5] Climasol, 2004 *Guidelines for Solar Air Conditioning.* Resource available at: http://raee.org/climatisationsolaire/gb/documents.htm [February, 2009]]

[6] Peterson M., March 2008. *Energy Saving in the Municipality of Skive.* Warsaw. Resource available at: www.ambwarszawa.um.dk/NR/rdonlyres/17AA917E.../5_**Skive**_Kommune_Howtoarchive_**energy_savings**_in_Municipal_buildings.pdf [February 2009]

[7] Dorgan, C.B., Leight, S.P., Dorgan, C.E., 1995. Application Guide for Absorption Cooling/Refrigeration Using Recovered Heat. USA: ASHRAE.

[8] Napolitano A., Franchini G., Nurzia G., Sparber W., 2008 *Coupling Solar collectors and co-generation units in solar assisted heating and cooling systems.* EUROSUN 2008 – 1st International Conference on Solar Heating, Cooling and Buildings, Lisbon, October 2008

[9] Troi, A., Filippi, H., Sparber, W., 2005. *Practical Experience with Solar-Assisted Cooling in an Office and Educational Building in South Tyrol / Northern Italy*. In: Otti, ed., 2005. 1st International Conference on Solar Air Conditioning. Germany, October 2005.

[10] Mumelter, E., Carlini M., Progetto esecutivo impianti termoidraulici. Relazione tecnica, Bolzano, 08.05.1998

[11] [2] Mumelter, E.,"Voraussichtlicher Kostenaufwand für den Betrieb der Klima- und Sanitäranlagen im Neubau der NAG", Bozen, Italien, 27.03.2000

[12] Napolitano A., Troi A., Sparber W., 2007. *Monitoring activities for the optimization of a tri-generation plant including a solar heating and cooling system.* In: Otti, ed., 2007. 2nd International Conference on Solar Air Conditioning. Spain, October 2007.

[13] Avesani S., 2008 *Simulation of a combined heating and cooling energy system with solar integration and optimization of the solar collector's heat production.* Master thesis. University of Trento

[14] Petchers, N., edited by, 2003. Combined Heating, Cooling & Power Handbook: Technologies & Applications. Lilburn, GA: Fairmont Press.

[15] Macchi E., Campari S., Silva P., "La micro cogenerazione a gas naturale", Milano, Polipress, 2006

[16] Franchini G. ., 2006. *La certificazione energetica degli edifici ed il quadro normativo europeo.* Training Course on Energy efficiencyin the buildings. Bergamo: March, 2006

[17] Thermax. 2008 *Thermax Europe LTd catalogue* Resource available at: http://www.kellysearch.co.uk

[18] Nurzia G.,2008. *Design and simulation of solar absorption cooling systems.* PhD thesis in Energy and Enviromental Technologies, 2008 University of Bergamo

[19] TRNSYS 16 : a TRaNsient SYstem Simulation program Short Description", www.transsolar.com/__software/download/en/trnsys_shortinfo_en.pdf [July 2008]

[20] THERMOFLOW 17, 2007. Resource available at: http://www.thermoflow.com/Thermoflow_Overview.htm [February 2008]

[21] Institut für Solartechnik, 2007. *Collector* Tests Resource available at: http://www.solarenergy.ch

[22] Rossi, V., 2008. *La convenienza economica di produrre energia termica con il legno.* Arezzo, Marzo 2008

[23] Cf. Aube F. Guide for computing CO_2 emissions related to energy use, June, 2001.

[24] UCDAVIS Colleg of Engineering. *Biomass Properties, Characterization, and Analysis*. Resource available at: http://faculty.engineering.ucdavis.edu/

[25] Resource available at:, http://www.enel.it/attivita_en/ambiente/energiaelettrica/archivio/articolo.asp?page=/attivita/ambiente/energy/energia25_hp/energia25/index.asp [August 2008]

[26] The German Solar Energy Society, 2005. *Planning and Installing Solar Thermal Systems A guide for installers, architects and engineer*. James & James. UK, 2005